UNIVERSIDADE FEDERAL DO PARANÁ

FÁBIO BERTON

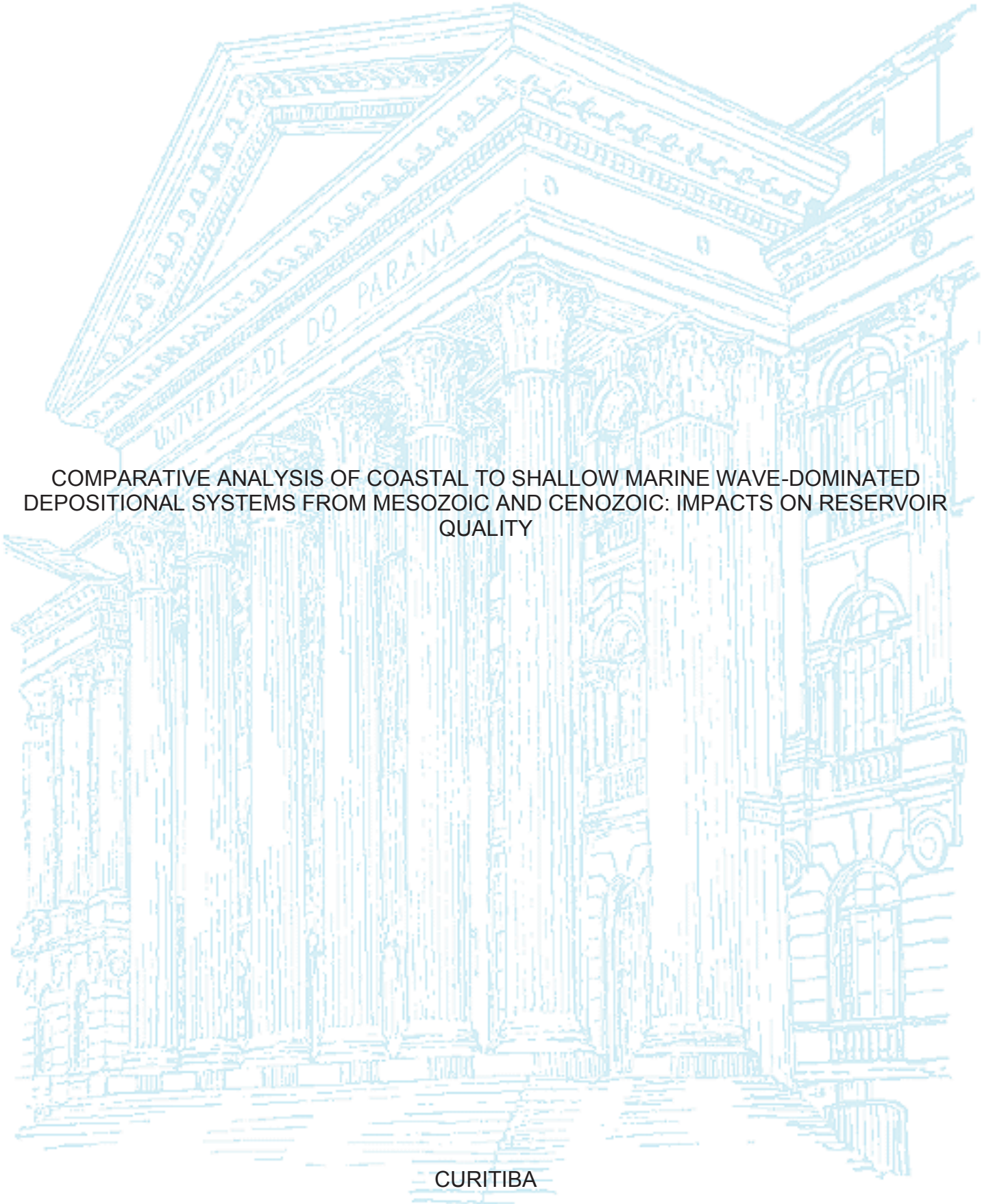

COMPARATIVE ANALYSIS OF COASTAL TO SHALLOW MARINE WAVE-DOMINATED DEPOSITIONAL SYSTEMS FROM MESOZOIC AND CENOZOIC: IMPACTS ON RESERVOIR QUALITY

CURITIBA

2020

FÁBIO BERTON

COMPARATIVE ANALYSIS OF COASTAL TO SHALLOW MARINE WAVE-DOMINATED DEPOSITIONAL SYSTEMS FROM MESOZOIC AND CENOZOIC: IMPACTS ON RESERVOIR QUALITY

Tese apresentada ao curso de Pós-Graduação em Geologia, Setor de Ciências da Terra, Universidade Federal do Paraná, como requisito parcial à obtenção do título de Doutor em Geologia

Orientador: Prof. Dr. Fernando Farias Vesely
Co-orientadores: Profa. Dra. Maria Cristina de Souza
Prof. Dr. Carlos Conforti Ferreira Guedes

CURITIBA

2020

CATALOGAÇÃO NA FONTE – SIBI/UFPR

B547c Berton, Fábio

Comparative analysis of coastal to shallow marine wave-dominated depositional systems from mesozoic and cenozoic: impacts on reservoir quality [recurso eletrônico]/ Fábio Berton. Curitiba, 2020.

Tese (Doutorado) - Programa de Pós-Graduação em Geologia, Setor de Ciências da Terra, da Universidade Federal do Paraná
Orientadores: Prof. Dr. Fernando Farias Vesely
Profa. Dra. Maria Cristina de Souza
Prof. Dr. Carlos Conforti Ferreira Guedes

1. Reservatórios. 2. Preservação – Bacia de Santos. I. Vesely, Fernando Farias. II. Souza, Maria Cristina de. III. Guedes, Carlos Conforti Ferreira. Título.

CDD 628.19

Bibliotecária: Vilma Machado CRB9/1563

MINISTÉRIO DA EDUCAÇÃO
SETOR DE CIENCIAS DA TERRA
UNIVERSIDADE FEDERAL DO PARANÁ
PRÓ-REITORIA DE PESQUISA E PÓS-GRADUAÇÃO
PROGRAMA DE PÓS-GRADUAÇÃO GEOLOGIA - 40001016028P5

TERMO DE APROVAÇÃO

Os membros da Banca Examinadora designada pelo Colegiado do Programa de Pós-Graduação em GEOLOGIA da Universidade Federal do Paraná foram convocados para realizar a arguição da tese de Doutorado de **FABIO BERTON** intitulada: **COMPARATIVE ANALYSIS OF COASTAL TO SHALLOW MARINE WAVE-DOMINATED DEPOSITIONAL SYSTEMS FROM MESOZOIC AND CENOZOIC: IMPACTS ON RESERVOIR QUALITY**, sob orientação do Prof. Dr. FERNANDO FARIAS VESELY, que após terem inquirido o aluno e realizada a avaliação do trabalho, são de parecer pela sua APROVAÇÃO no rito de defesa.
A outorga do título de doutor está sujeita à homologação pelo colegiado, ao atendimento de todas as indicações e correções solicitadas pela banca e ao pleno atendimento das demandas regimentais do Programa de Pós-Graduação.

CURITIBA, 02 de Março de 2020.

FERNANDO FARIAS VESELY
Presidente da Banca Examinadora

CAROLINA DANIELSKI AQUINO
Avaliador Interno (UNIVERSIDADE FEDERAL DO PARANÁ)

RODOLFO JOSÉ ANGULO
Avaliador Interno (UNIVERSIDADE FEDERAL DO PARANÁ)

SERGIO REBELLO DILLENBURG
Avaliador Externo (UNIVERSIDADE FEDERAL DO RIO GRANDE DO SUL)

PAULO CÉSAR FONSECA GIANNINI
Avaliador Externo (UNIVERSIDADE DE SÃO PAULO)

Dedico este trabalho aos colegas cientistas do Brasil.

Sem ciência e educação um país se torna um barco à deriva, impotente diante das intempéries. Quem paga o preço de um país que não valoriza seus cientistas e educadores é o povo, que assiste aos poucos desaparecer sua estabilidade social e econômica, sua liberdade, sua saúde e sua qualidade de vida.

Cientistas do Brasil, continuemos a usar o conhecimento para tornar nosso país mais justo e igualitário, mostrando a todo jovem que sonha em se tornar cientista que lutaremos para que o futuro lhe traga as mesmas oportunidades que nós tivemos.

Educação gratuita e de qualidade não é um luxo. É o único caminho para crescermos como povo e como nação.

AGRADECIMENTOS

São muitas as pessoas que me apoiaram nestes últimos anos, seja me auxiliando a ‘desatar os nós’ que se formam naturalmente em um trabalho científico, seja me incentivando nos momentos em que acreditava que não conseguiria concluir minha tese. A todas as pessoas, dedico minha eterna gratidão, e espero sinceramente poder um dia retribuir.

A começar por minha esposa, Renata Zanella, companheira de vida que faz com que momentos ruins se tornem bons, e que momentos bons se tornem perfeitos. Eu não teria conseguido sem você. Obrigado pelo apoio nos momentos de dúvida, pela compreensão pelas minhas longas ausências trabalhando sozinho, pela paciência me ouvindo divagar sobre problemas e hipóteses. Mais do que minha esposa, você é a minha melhor amiga, minha confidente, minha parceira intelectual com quem a cada dia aprendo algo novo. Só nós sabemos o que passamos nos últimos anos, e só nós sabemos como crescemos e como somos fortes juntos. Obrigado por ser meu Norte.

Agradeço também aos meus pais, Marcos e Carmen Berton, por sempre acreditarem em mim e pela confiança nas minhas decisões. Acima de tudo, obrigado pelas bases que me permitiram chegar até aqui. Obrigado por me apresentar a literatura, a música e a ciência, e por permitir que a minha mente voasse livremente. Me sinto um privilegiado em ter pais como vocês, pessoas das quais posso me orgulhar e que só me trouxeram alegrias. Desculpem pela distância que a vida às vezes nos impõe, mas saibam que não existe momento especial em que eu não sinta sua presença ao meu lado.

Obrigado minha irmã, Renata, por tudo que me ensinou e continua ensinando. Eu lhe admiro e sempre admirei, e desde cedo seguindo seus passos me tornei uma pessoa melhor. Continue sendo esse ser humano maravilhoso, que me dá esperança de que o mundo ainda possa se tornar um lugar melhor. Só uma pessoa boa como você poderia encontrar um companheiro igualmente bom. Obrigado Lorenzo, por todo o apoio que me deu ao longo destes anos. Me orgulho muito ao ver a família que vocês construíram e ao ver as crianças excepcionais que o Arthur e o Gabriel estão se tornando.

Agradeço pelo apoio dado por Lorenzo Santangelo, Amauri e Marilene Zanella ao longo destes anos. Desejo que as experiências passadas nos últimos tempos, nesta época de instabilidade e pandemia, lhes

abram os olhos para a importância da ciência desenvolvida nas Universidades públicas para o progresso do país. Não há dúvidas de que há muito a melhorar. Mas as mentes dispostas a realizar sacrifícios pessoais pelo avanço da pesquisa científica e do ensino nas Universidades são a grande maioria em todas as áreas.

Agradeço aos meus amigos por serem as pessoas incríveis que tornam a minha vida tão mais feliz. Leonardo Barão, Rafael Beruski, Bárbara Biasi, Aurora Garcia, Lucas Valore, William Peyerl, Fabiane Acordes, Lara Neves, Danielle Schemiko, Ismael Pereira, Tomás Chor e José Roberto, eu os admiro muito. Vocês não têm ideia da falta que fazem na minha vida. Eu tenho certeza de que o futuro lhes reserva apenas sucesso.

Agradeço aos meus orientadores, Fernando Vesely, Carlos Guedes e Maria Cristina de Souza, e aqui também incluo o mestre Rodolfo Angulo. O que aprendi com vocês sobre Geologia, ciência e vida não pode ser resumido em artigos ou livros, ou sequer descrito em palavras. Em um meio em que a relação entre orientador e orientado pode ser por vezes difícil, posso me considerar novamente um privilegiado. Sempre encontrei suas portas abertas para discussão e até mais apoio do que eu poderia esperar de orientadores, e por isso sou eternamente grato. Em especial, agradeço ao professor Fernando Vesely, orientador de graduação e pós-graduação, de vida profissional e pessoal. Que nossas parcerias científicas não acabem por aqui.

Agradeço aos meus colegas de Laboratório de Análise de Bacias (LABAP), pessoas com quem aprendi e aprendo muito. Fico feliz em ver suas vidas acadêmicas e profissionais decolando e vocês ganhando o mundo, pois conheço a capacidade e o potencial de cada um de vocês para se tornar a referência de suas áreas. Em especial, agradeço à Thammy Mottin, ao Bruno Merss, à Amanda Hammerschmidt, e ao Hugo Yamassaki pela ajuda que me deram e sempre estiveram dispostos a dar. Estendo este agradecimento aos meus colegas e amigos de Pós-Graduação, em especial Bruno Titon, Camila Silveira, Thailli Conte, Lara Lange e Mayara Santana.

Agradeço também a todos os professores do curso de Geologia e do Programa de Pós-Graduação em Geologia, em especial aos mestres Cristina Valle, Bárbara Trzaskos, Leonardo Cury, Fernando Mancini e Francisco Ferreira. Bons mestres marcam a vida de seus alunos, e para vocês dedico meu eterno

carinho e admiração. Também agradeço ao amigo Kazutoshi Matsugano, por tornar a vida dos pós-graduandos tão mais simples.

Meu profundo agradecimento aos colega e amigos da Equinor, por todo o incentivo dado na etapa final do meu doutorado. Apesar de terem entrado recentemente na minha vida, já guardo por vocês a mais profunda estima. Muito obrigado Mauro Ribeiro, Rafael Furuie, Marcelo Madeira, Gabriel Carneiro, Evelin Marquez, Paula Braga, Fabiana Chaves, Fabrício Filardi, Roelf Mulder, Luz Gomis e Marisa Makler. O que tenho aprendido com vocês vale por mais uma tese. Em especial, obrigado Marie Kjølleberg, por ter me dado a oportunidade de trabalhar com o que eu amo.

Esta tese foi sensivelmente melhorada após as correções, sugestões e observações da banca que avaliou meu trabalho e deu seu parecer favorável à aprovação. Por sua contribuição ao trabalho, agradeço aos membros da banca Sérgio Dillenburg e Paulo Giannini, que se deslocaram de suas cidades de residência para participar da avaliação em Curitiba, e à membro da banca representante da UFPR Carolina Aquino. Apesar de já terem sido citados anteriormente, também agradeço ao meu orientador Fernando Vesely e ao professor Rodolfo Angulo por sua contribuição e participação na banca de avaliação da tese.

O trabalho de pesquisa não seria viável sem a infraestrutura fornecida pelo LABAP e pelo Laboratório de Estudos Costeiros (LECOST). Também agradeço ao LECOST por diponibilizar o banco de dados de GPR do litoral paranaense, e aos professores Eduardo Barboza e Maria Luiza da Rosa e à Universidade Federal do Rio Grande do Sul pela aquisição dos dados e apoio em seu processamento. Agradeço à Agência Nacional do Petróleo, Gás Natural e Biocombustíveis (ANP) pela cessão de dados públicos de subsuperfície da Bacia de Santos. Agreadeço ao Conselho Nacional de Desenvolvimento Científico e Tecnológico (CNPq) pelo financiamento de projetos que custearam os trabalhos de campo, e à Coordenação de Aperfeiçoamento de Pessoal de Nível Superior (CAPES) pela concessão da bolsa de doutorado entre os anos de 2016 e 2018.

Por fim, obrigado ao governo brasileiro pela oportunidade de me formar profissional e cientista em uma Universidade pública de qualidade. Algumas das melhores lembranças que tenho são na Universidade Federal do Paraná, local de formação de muitas das mentes mais brilhantes que já tive o prazer de

conhecer. Lutarei como puder para que sua existência não seja ameaçada, e para que mais jovens possam encontrar em suas salas de aula e laboratórios o caminho para um futuro melhor.

RESUMO

Análogos de reservatórios são comumente utilizados na indústria do petróleo na predição da distribuição de heterogeneidades em escala de afloramento que afetam a qualidade dos reservatórios, mas não são capturadas por ferramentas de imageamento de subsuperfície. Os análogos são comumente sistemas deposicionais modernos, de acordo com uma visão atualística de interpretação estratigráfica. Entretanto, quando se considera o baixo potencial de prerservação do registro estratigráfico e a repetibilidade de processos de alta energia através do tempo geológico, análogos modernos podem não ser ideais para capturar a complexidade de depósitos mais antigos. O objetivo desta tese é avaliar a viabilidade do uso de análogos modernos na predição da qualidade de reservatórios, com base no estudo de sistemas costeiros dominados por ondas. Estes sistemas são reconhecidos como bons alvos e considerados reservatórios homogêneos e de padrão estratigráfico simples. Os controles deposicionais sobre a costa variam entre processos de ondas, fluviais e de maré, afetados por processos periódicos de energia anômala. A posição dos sistemas costeiros em porções rasas da bacia também resulta em baixo potencial de preservação durante os ciclos estratigráficos. As hipóteses da pesquisa são de que os produtos associados a processos de alta energia têm maior potencial de preservação que os relacionados a processos de energia 'normal', e de que consequentemente, análogos modernos são confiáveis apenas para o entendimento de elementos arquitetônicos dos depósitos, não para sua estruturação interna. Duas áreas foram escolhidas para a pesquisa. A primeira está localizada na porção offshore da Bacia de Santos, englobando sucessões marinhas rasas dos intervalos Campaniano e Eoceno. O banco de dados inclui linhas sísmicas 2D, volumes sísmicos 3D e poços, avaliados através de interpretação sísmica, correlação de poços e geomorfologia sísmica. A segunda área se localiza na coasta paranaense, onde sistemas costeiros do Quaternário da Bacia de Santos estão expostos em cavas de areia e imageados em linhas de Ground-Penetrating Radar (GPR). Os métodos incluíram análises sedimentológicas e estratigráficas e interpretação de GPR. Na área offshore, a análise sismo-geomorfológica resultou na definição de sistemas de planície costeira com cordões litorâneos formados durante regressões normais, sistemas costeiros parcialmente erodidos durante regressões forçadas, e sistemas de esporões e lagunas associados a transgressões. As planícies costeiras com cordões litorâneos apresentam maior homogeneidade e potencial para reservatórios, especialmente quando associadas a suprimento

sedimentar relativamente alto e baixa acomodação. Os resultados da costa paranaense mostram a interdigitação de depósitos de planícies costeira com cordões litorâneos, esporões e lagunas. Processos de alta energia foram responsáveis por erosão e deposição na costa e são considerados mecanismos importantes para a arquitetura deposicional, mas não processos dominantes. Este sistemas costeiro pode ser utilizado como análogo para um sistema de planície costeira com cordões litorâneos complexo, com barreiras expressivas na forma de depósitos lagunares lamosos, e diferentes unidades de fluxo associadas à planície costeira e aos esporões. Estas heterogeneidades seriam sub-sísmicas em um reservatório, e não previstas em modelos costeiros clássicos. Este sistema pode portanto ser utilizado como um caso pessimista para reservatórios costeiros como os do Cretáceo da Bacia de Santos.

Palavras-chave: análogos de reservatório, potencial de preservação, sistemas costeiros, Bacia de Santos

ABSTRACT

Reservoir analogs are commonly used in the petroleum industry to cover the gap between low resolution subsurface data and outcrop-scale heterogeneities that might affect reservoir quality. These analogs are commonly modern depositional systems, following an actualistic approach for stratigraphic interpretation. However, considering the low preservation potential of the rock record and repeatability of high-energy processes through the geological time, modern analogs might not be ideal to capture the complexity of past deposits. This thesis aims to evaluate the applicability of modern analogues to predict reservoir quality in subsurface, using wave-dominated nearshore systems as a base for the studies. Such systems are long recognized as good targets in the petroleum industry and often considered homogeneous sheet-like reservoirs. In terms of depositional controls, they are influenced by wave, tidal and fluvial mechanisms, affected by anomalous-energy processes that periodically reach the coast, and are located in shallow parts of the basin that are exposed to erosion during stratigraphic cycles. The hypotheses are that products related to anomalous-energy processes have a higher preservation potential than the ones related to 'normal' processes, and that as consequence, modern analogues can be used only to assess architectural elements, but not the internal character of nearshore systems. Two study areas were chosen for evaluation. The first area is in offshore Santos Basin, were nearshore successions were previously recognized in the Campanian and Eocene intervals. This area is covered by 2D and 3D seismic data and wells, and was studied through seismic interpretation, well log correlation and seismic geomorphology. The second area is in Quaternary Santos Basin, were nearshore systems are exposed in sand pits in the Paraná coast and imaged by Ground-Penetrating Radar (GPR). The methods included sedimentological and stratigraphic analysis and GPR interpretation. In offshore Santos Basin, seismic-geomorphologic interpretation leaded to the definition of strandplain systems related to periods of normal regression, partially-eroded systems associated with forced regressions, and spit-inlet and lagoon systems formed during transgressions. Strandplain systems are the most homogeneous and have best reservoir potential, especially the ones formed in periods of relatively low accommodation and high supply. The results from Quaternary Santos Basin show that the Paraná coastal plain is composed by the interdigitation of strandplain, spit-inlet and lagoon systems. High-energy processes caused both deposition and erosion of the coast and can be considered important mechanisms for the depositional architecture, but not the

dominant processes. This coast can serve as an analog for a complex strandplain system, with expressive flow barriers in the form of muddy lagoonal deposits, and different flow units associated with strandplain and spit deposits. These heterogeneities would be sub-seismic in a reservoir, differing from classic coastal models. This system could thus be used as a pessimistic case for strandplain reservoirs such as the ones from offshore Santos Basin.

Keywords: reservoir analog, preservation potential, coastal systems, Santos Basin

LIST OF FIGURES

LIST OF TABLES

SUMMARY

1. Introduction

The debate about the energy of depositional processes and the potential to preserve its products through the geological time is one of the most relevant in Earth sciences, as it affects the way geologists interpret past sedimentary systems and evaluate natural resource prospects. In the XIX century, it resulted in the clash of two opposing schools of thought: catastrophists influenced by creationist concepts, and uniformitarianists influenced by the ideas of James Hutton (Rudwick, 1967; Hooykaas, 1970; Baker, 1998; Romano, 2015). While catastrophism considered that the geological record was a result of anomalous events or even biblical catastrophes, uniformitarianism considered a timeless Earth, governed by 'normal', everyday processes with no changes of energy. With time both have proven to be wrong and dogmatic (e.g., Davis, 1926; Bretz et al., 1956; Rudwick, 1967; Hooykaas, 1970; Hsü, 1983; Baker, 1998), but both also interpreted correctly many aspects of the nature of the stratigraphic record. Uniformitarianism was gradually substituted by actualism, admitting the uniformity of processes and the variability of energy (Gould, 1967; Carneiro et al., 1994), while catastrophism proved to be right in what concerns to the importance of anomalous episodic processes in stratigraphy (Bretz et al., 1956; Bretz, 1969), supporting the bases of modern studies of episodic sedimentation (e.g., Miall, 2012, 2014). Considering that periods with absence of record are at least as expressive as the sedimentary record itself (Ager, 1993) the low potential of preservation of sedimentary products enhances the importance of this discussion (e.g., Sadler, 1999; Miall, 2000; Sommerfield, 2006; Smith et al., 2015).

This discussion has an economical impact in petroleum geology, where analogue outcrops and depositional systems are used as a base to understand and predict the distribution of reservoirs and heterogeneities in subsurface. Many facies models used as a base for reservoir modelling are actualistic (e.g., Galloway and Hobday, 1996; Clifton, 2006), considering that modern deposits can be used as analogues to understand the distribution of facies, heterogeneities and architecture of ancient deposits in subsurface (e.g., Grammer et al., 2004; Martinius and van den Berg, 2014; Nyberg and Howell, 2016). However, concepts of episodic sedimentation show that sedimentation rates in ancient deposits are generally higher than the ones from modern deposits, indicating that most of the sedimentary products preserved in the rock record are related to depositional processes of anomalous energy (Dott, 1983; Miall,

2012, 2014). This paradox in sedimentation rates in the past (Sadler, 1981) is compared by Ager (1993) with the life of a soldier, considering that the stratigraphical record consists of 'long periods of boredom and short periods of terror'. The dimensions and distribution of facies in modern and ancient deposits are therefore different, affecting reservoir modeling (Miall, 2016). The ideal analog would thus be a deposit formed in tectonic-sedimentary conditions similar to the depositional context of the reservoir rock (e.g., O'Byrne and Flint, 1993; Phelps et al., 2018).

Based in the discussions above, this thesis aims to use a multi-scale approach to compare a modern depositional system with its equivalent in subsurface, evaluating the preservation of sedimentary facies and the impacts on subsurface prediction and reservoir modelling. The research is focused on wave-dominated coastal systems, as they are dynamic environments where deposition and erosion are associated to the incidence of waves and wave currents, tidal currents, river discharges and storms (e.g., Heward, 1981; Niedoroda et al., 1984; Reinson, 1984; Hampson et al., 2008; Raynal et al., 2009; Souza et al., 2012). Deposits formed in this context tend to form laterally-continuous bodies with sand-rich composition, relatively homogeneous and with good permeability and porosity, often configuring prolific petroleum reservoirs (Galloway and Hobday, 1996; Higgs et al., 2010). Two areas were selected for investigation with a variety of methods that include outcrop studies, Ground-Penetrating Radar (GPR) interpretation, well logs, and 2D seismic and seismic geomorphology. In an offshore area in Santos Basin, Campanian shelfal successions that act as gas reservoir rocks in the Merluza Field and Eocene shoreface clinoforms are imaged by 2D and 3D seismics and intersected by wells. In the second area, the Quaternary coastal record of Santos Basin is exposed in sand pits and imaged by GPR along the coast of the Paraná State.

2. Structure of the Thesis

This thesis is divided in four main sections. The first section is dedicated to the introduction of the research, a detailed overview of the problems and hypotheses. The second part, exposed in the form of a scientific article, shows the result of interpretation of subsurface data in offshore Santos Basin, and discusses the architecture, reservoir potential, and relation with base level fluctuations of coastal deposits. The third part, also in the form of a scientific article, is focused in the results obtained in Quaternary Santos

Basin and in discussions of the use of modern analogues for reservoir modeling. The paper entitled 'Quaternary coastal plains as reservoir analogs: wave-dominated sand-body heterogeneity from outcrop and Ground-penetrating radar, central Santos Basin, southeast Brazil', was published in Sedimentary Geology and referenced as Berton et al. (2019). The fourth part of the thesis is dedicated to the integration and discussion of the results exposed in the articles, as well as to general conclusions of the research.

3. Analysis of the Problem

Preservation of sedimentary products through the geological time is one of the most debated matters in stratigraphy and sedimentology (e.g., Barrell, 1917; Passega, 1962; Dott, 1983; Miall, 2016), as it ultimately leads to a more precise interpretation of past depositional systems. In pioneer studies, Hutton (1788) (Fig. 1) defended that nature is governed by order rather than chaos, reflecting a vision of perfection and eternity of the planet (Baker, 1998). Lyell (1835; originally published in 1830) (Fig. 1) embraced the concepts previously exposed by Hutton (1788) and defended the idea that the sedimentary record is a result of depositional processes associated to conditions such as the ones observed in present-day systems, and that variations of energy were not admitted (Barrell, 1917; Hooykaas, 1970; Baker, 1998). This principle was called uniformitarianism by William Whewell in 1832 (Romano, 2015), and resulted in a clash of ideas from authors that used catastrophism to explain the evolution of the Earth (Lyell, 1835; Hughes, 1872). According to catastrophism and its variations, the rock record and surface landforms could not be explained exclusively by 'causes now in operation', but also by anomalous, maybe cataclysmic high-energy processes (Hooykaas, 1970). Although some catastrophists used a scientific approach in their studies (e.g., Conybeare, 1831) (Fig. 1), catastrophism was essentially creationist in its roots (Lyell, 1835), even considering the role of biblical events in the history of Earth. While for uniformitarianism Earth was old or even timeless (Rudwick, 1967; Hooykaas, 1970), for catastrophists Earth was only some thousands of years old and controlled by God-driven processes.

Catastrophist ideas gradually lost ground for uniformitarianism during the XIX century (Rudwick, 1967; Hooykaas, 1970; Baker, 1998, 2014). Uniformitarianism became the base of Geosciences in the beginning of the XX century, supported by the development of methods to estimate the age of rocks as million- or billion-years old, coherently with Hutton's and Lyell's ideas. In this context, the interpretation of an extreme-

energy process such as a gigantic flood to explain the anomalous landscape of the Scablands in the Washington State by Bretz (1923, 1925) (Fig. 1) was received with strong resistance and skepticism (Baker et al., 1993; Baker, 1998). The main problem was that Bretz's interpretation was too aligned with catastrophism, even though he never appealed to any divine or theological argument to defend his hypothesis (e.g., Bretz, 1923, 1925, 1969). Only after more than twenty years of Bretz's original research, complementary studies in the Scablands revealed that his hypothesis of catastrophic flood was not only coherent, but the only one fully capable to explain the features of the region (Bretz et al., 1956; Bretz, 1969). The role of high-energy events in depositional systems gradually became more accepted in the following years.

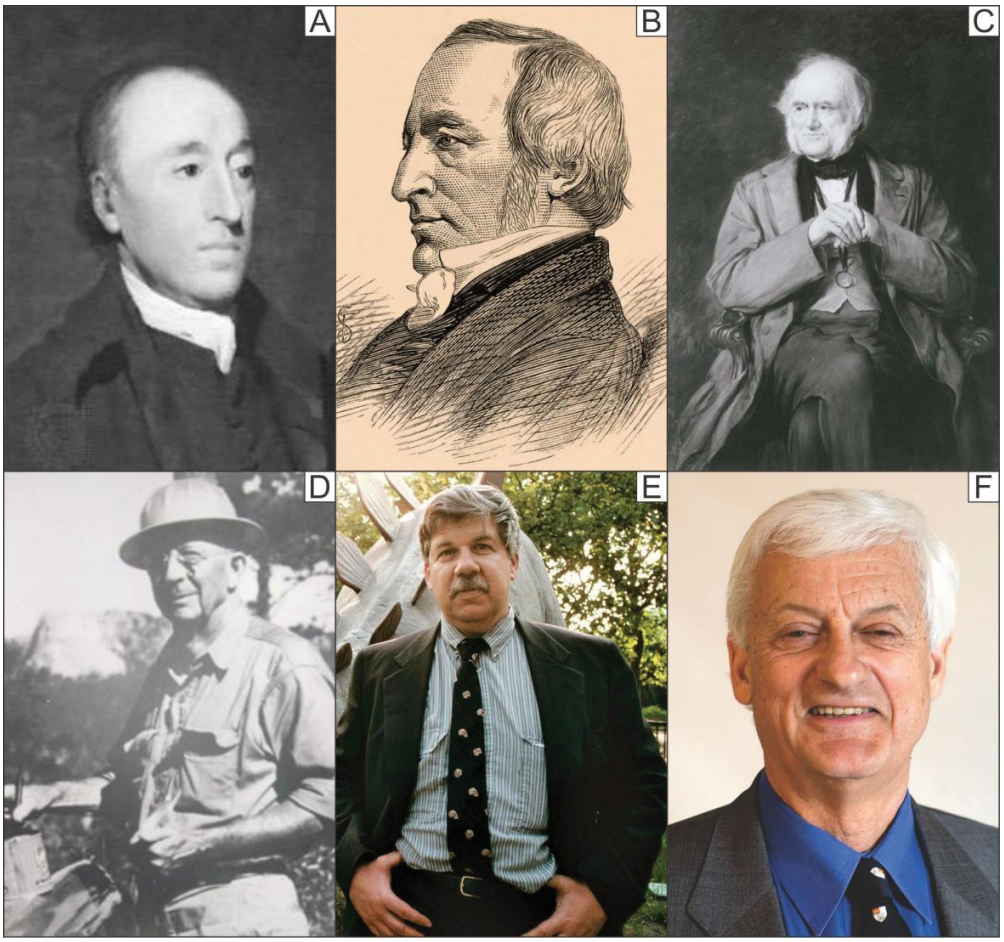

Figure 1: In (A), James Hutton (1726-1797), a pioneer Earth scientist that defended a very old planet Earth, in direct opposition to the theological dogmas that prevailed at the time. In (B), reverend William Conybeare (1787-1875), an affectionate for Geology and one of the most prominent voices in defense of catastrophism. In (C), Sir Charles Lyell (1797-1875), recognized as one of the most important scientists of all time, and the author of many concepts that served as base for uniformitarianism. In (D), J. Harlen Bretz (1882-1981), a former geography teacher that faced strong resistance to prove the importance of high-energy processes in the past. In (E), Stephen Jay Gould (1941-2002), a paleontologist that defended the principles of actualism, considering the uniformity of processes and variability of energy in nature. In (F) Andrew Miall (1944-), a geologist that established the principles of episodic sedimentation in the stratigraphic record. Images (A) to (E) are courtesy of Encyclopaedia Britannica; (F) is courtesy of the University of Toronto.

The acceptance of the natural occurrence of high-energy processes such as the megaflood proposed by Bretz was a turning point in Geology, exposing the fragility of uniformitarianism to explain Earth history. Mass extinctions, for instance, are hard to explain in a planet with permanent stable conditions (Hsü, 1983). The strong resistance faced by Bretz also revealed that uniformitarianism had become as dogmatic as the theological variations of catastrophism (Davis, 1926; Bretz et al., 1956; Rudwick, 1967; Hooykaas, 1970; Hsü, 1983; Baker, 1998). Early scientific catastrophist ideas accepting the variation of energy of geological processes (e.g., Conybeare, 1831) but maintaining part of the uniformitarianist principles were adapted into the actualism (e.g., Gould, 1967) (Fig. 1), admitting the uniformity of geological processes, but abandoning the idea of stable and immutable processes taking place in an infinite or quasi-infinite time (Carneiro et al., 1994). In other words, in actualism the present is the key to the past, but variations of energy may occur. Despite being more flexible than uniformitarianism, actualism was criticized for giving little attention to one of the most important components of the geological record: the absence of record.

The importance of erosive or non-depositional gaps in the stratigraphic record is long recognized (e.g., Blackwelder, 1909; Barrell, 1917; Sloss, 1963; Sadler, 1999; Miall, 2016), and Ager (1993) even defends the idea that most of the sedimentary history of a basin is represented by erosion or non-deposition (Fig. 2). These ‘empty’ intervals vary in scale from time breaks between the deposition of laminaes of sediment to expressive basinal unconformities related to global tectonic/eustatic shifts (Dott, 1983; Sadler, 1999; Miall, 2012, 2016) (Fig. 2). The sedimentary record is thus incomplete and the potential of preservation of a sedimentary product is generally low (Ager, 1993; Sommerfield, 2006; Miall, 2012, 2014; Smith et al., 2015). These assumptions leaded to the development of concepts of episodic sedimentation, considering that the duration of the gaps and the rates of sedimentation are fractal (Sadler, 1999; Bailey and Smith, 2005; Miall, 2014, 2016; Smith et al., 2015) (Fig. 2). Both sedimentary records and gaps could be divided in hierarchies that vary in scale and duration (Miall, 2012, 2014) (Fig. 2). When the gaps are considered for studies of sedimentation rates, it becomes evident that many sedimentary products previously related to normal-energy processes are, in fact, the result of relatively fast and episodic processes (Dott, 1983; Miall, 2012, 2014).

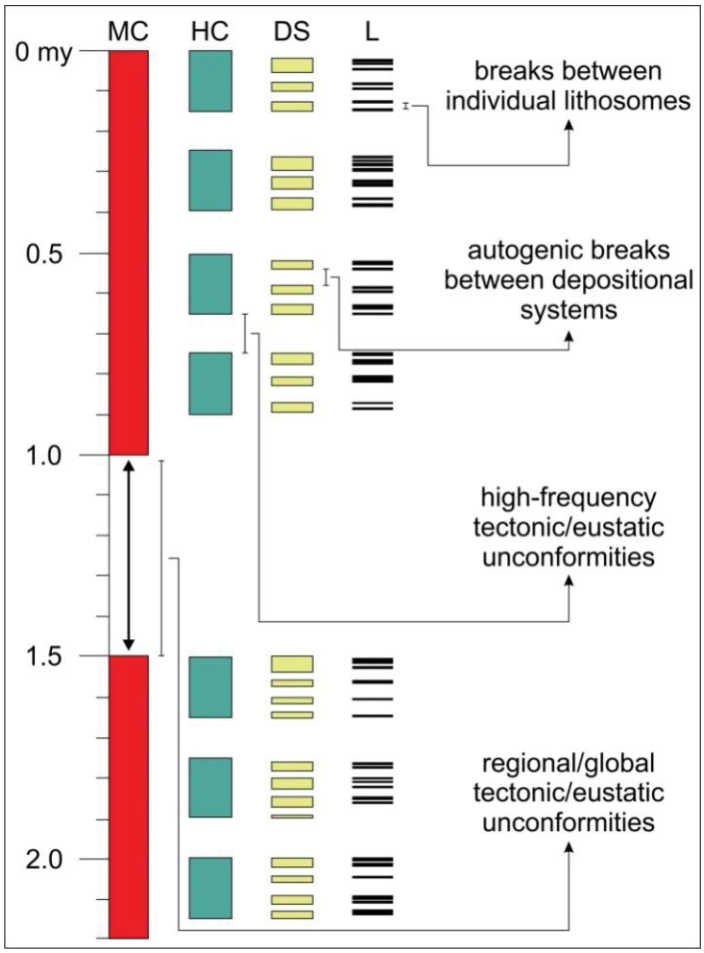

Figure 2: The stratigraphic record in multiple scales. MC: records with duration of millions of years, as depositional sequences; HC: records with duration of hundreds of thousands of years, as systems tracts and parasequences; DS: records with duration of tens of thousands of years, as depositional systems; L: records with duration of thousands of years, as bedsets and beds. Note the predominance of gaps representing the absence of record. Adapted from Miall (2014).

Coastal depositional deposits are probably the most indicated products to evaluate the importance and expressiveness of 'normal'- and 'abnormal'-energy processes in sedimentation, as they record the interaction of rivers, waves and tides (Heward, 1981; Niedoroda et al., 1984; Reinson, 1984; Raynal et al., 2009), and are susceptible to the incidence of episodic processes such as storms (e.g., Hampson et al., 2008; Souza et al., 2012; Gosling and Clemmensen, 2017) or tsunamis (e.g., Dawson et al., 1996; Bondevik et al., 1997; Paris et al., 2007) (Fig. 3). For example, during the Atlantic storm season in 2017 at least six major hurricanes reached the Caribbean countries, affecting mainly the coast (e.g., 2017 Atlantic Hurricane Season, 2018). Did they eroded previously-deposited fair-weather bedforms and subsequently formed high-energy bedforms? What is the preservation potential of storm-related bedforms during the following fair-weather period and consequent re-establishment of the coastal profile? Considering the everyday frequency of fair weather processes and the historical frequency of decades to

centuries of incidence of hurricanes in the Caribbean Sea (e.g., Elsner et al., 2000; Malaizé et al., 2011), which are the most important processes for the depositional architecture and facies distribution? Although this example refers to a carbonatic environment, these same questions can be applied to any siliciclastic coastal succession from the present and past.

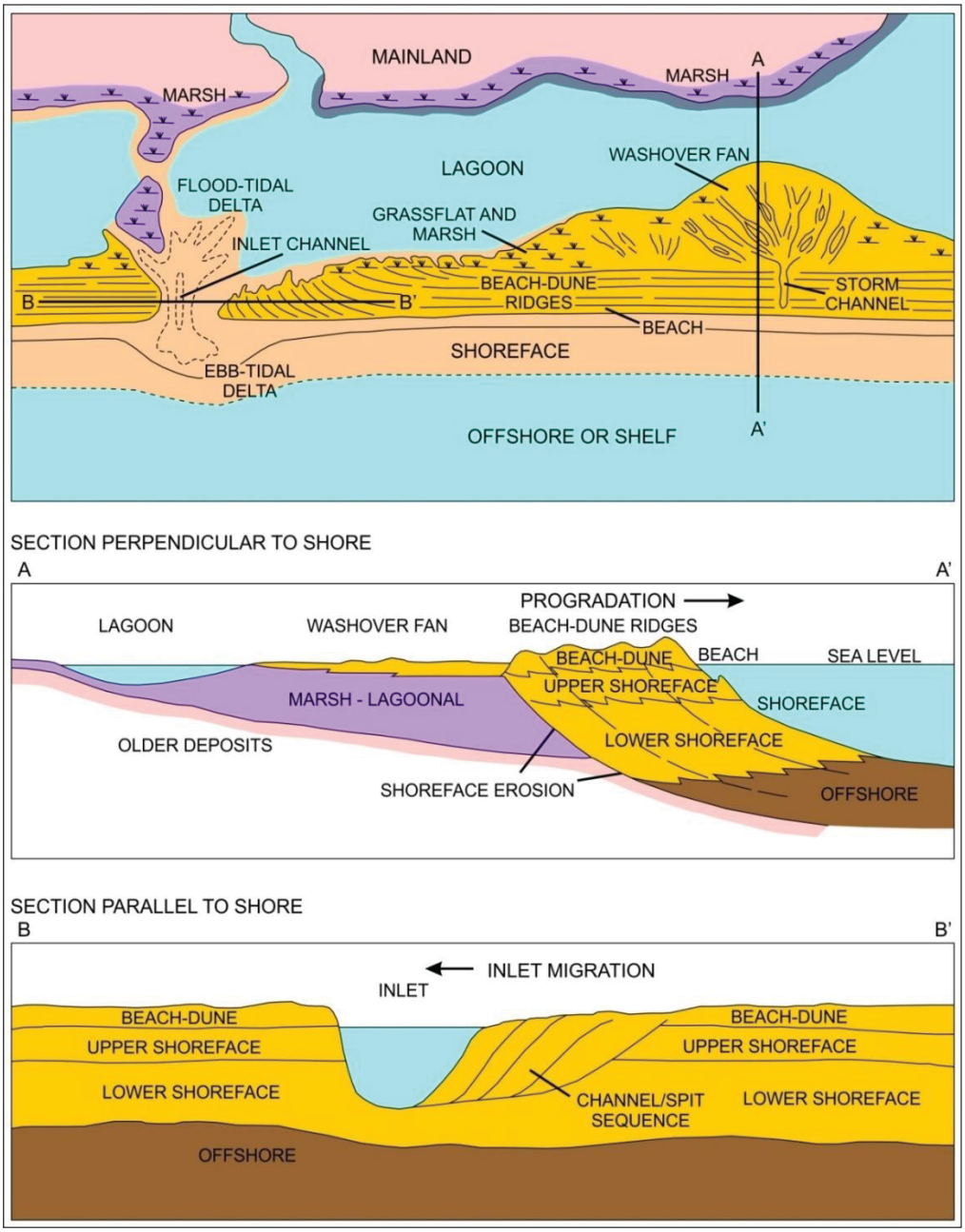

Figure 3: Architecture and compartmentalization of coastal and shallow marine wave-dominated systems. Note the lateral continuity and sand-rich composition of the deposits (depicted in yellow), important characteristics for petroleum reservoirs. Adapted from McCubbin (1982).

As previously mentioned, coastal deposits are often considered as good reservoirs in petroleum geology (Galloway and Hobday, 1996; Sech et al., 2009; Higgs et al., 2010; Nyberg and Howell, 2016) (Fig. 3). Heterogeneities within the reservoir are used to populate conceptual models that feed reservoir

models, which aim to predict reservoir behavior during production and establish a drainage strategy (e.g., Sech et al., 2009) (Fig. 4). Present-day analogues are usually the base to determine facies distribution and architecture in a conceptual model, following an actualistic approach (e.g., Grammer et al., 2004; Martinius and van den Berg, 2014; Nyberg and Howell, 2016) (e.g., Fig. 3). However, if the periodic and repetitive incidence of high-energy processes and episodic sedimentation are considered, both internal and external characteristics of past deposits might differ from modern analogues, affecting the reliability of the reservoir model.

A comparative analysis involving a coastal petroleum reservoir and a modern coastal succession is proposed to evaluate the applicability of modern analogues for reservoir modelling, considering characteristics such as internal heterogeneities, stacking patterns and architecture of the deposits (e.g., Fig. 4). Two hypotheses were formulated for investigation. The first hypothesis considers that only a fraction of the structures generated in a depositional system is preserved in the stratigraphic record, especially in a dynamic context such as a coastal zone submitted to the destructive influence of wave- and tide-related processes. Preservation would be conditioned to moments of interruption of the high energy erosive/depositional processes and re-establishment of the 'normal' conditions of the system, resulting in an increased potential for facies related to episodic events with abnormal energy when compared to the regular low-magnitude processes.

The second hypothesis is that modern deposits are not good analogues for subsurface reservoirs in a detailed scale. They can be correlated with past deposits when only the depositional architecture is considered (e.g., Nyberg and Howell, 2016), but the limited resolution of subsurface methods result in high uncertainties for the prediction of internal heterogeneities (e.g., Martinius and van den Berg, 2014) (Fig.4). In this case, the comparative analysis is mostly determined by the availability and distribution of subsurface data. When a high density of subsurface data is available, subtle heterogeneities within individual parasequences might be recognizable (e.g., Sech et al., 2009). When such volume of subsurface data is not available, uncertainties are too high for a precise interpretation, and only the general architecture and stacking patterns can be inferred.

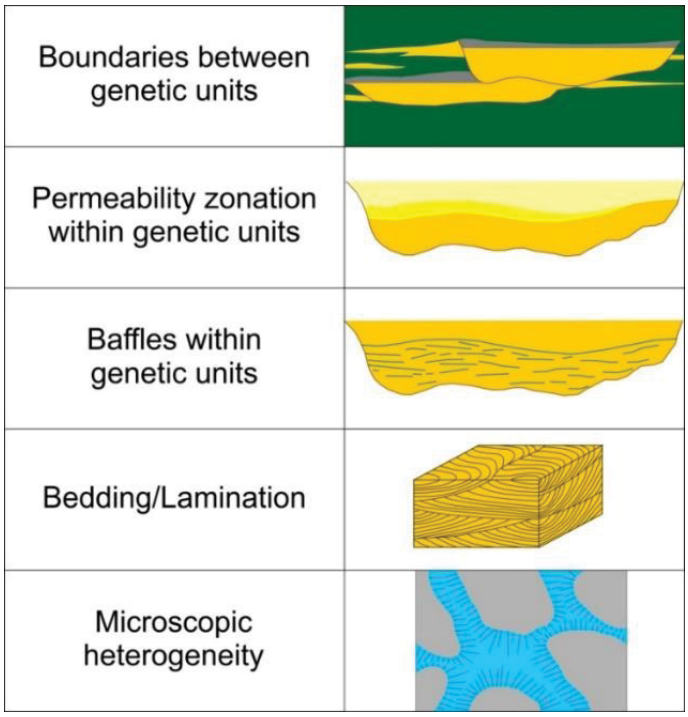

Figure 4: Types of reservoir heterogeneities, from the megascale (reservoir architecture) to the microscale (thin section). Reservoir modelling aims to realistically distribute such heterogeneities in reservoir systems. Adapted from Slatt (2006).

4. Objectives

The scope of the research is the evaluation of the viability of use of modern deposits as analogues for subsurface reservoirs, with focus on wave-dominated coastal systems. Specific objectives were also established, including:

- evaluation of the influence of high-energy processes in the coastal depositional record;
- determination of radarfacies from coastal successions and interpretation of their internal and external character through the correlation with sedimentary facies;
- determination of seismic facies and stacking patterns of subsurface coastal successions from offshore Santos Basin;
- determination of the depositional architecture of coastal successions in subsurface using seismic geomorphology, and comparison with modern examples;
- prediction of internal heterogeneities of coastal reservoirs from the comparison of the architecture and facies of modern and ancient coastal successions.

5. Study Areas

Two study areas were chosen for investigation in the south-southeastern region of Brazil (Fig. 5). Area 1 is in offshore Santos Basin, approximately 190 km distant from the city of Santos (São Paulo), covered by public 2D and 3D seismics and wells provided by the Brazilian Agency of Petroleum, Natural Gas and Biofuels (BDEP-ANP) (Fig. 5). Area 2 is in the Quaternary Paraná coastal plain, distant approximately 100 km from the city of Curitiba. The deposits are exposed in sand pits and imaged by GPR lines acquired in previous researches (e.g., Souza et al., 2012) (Fig. 5).

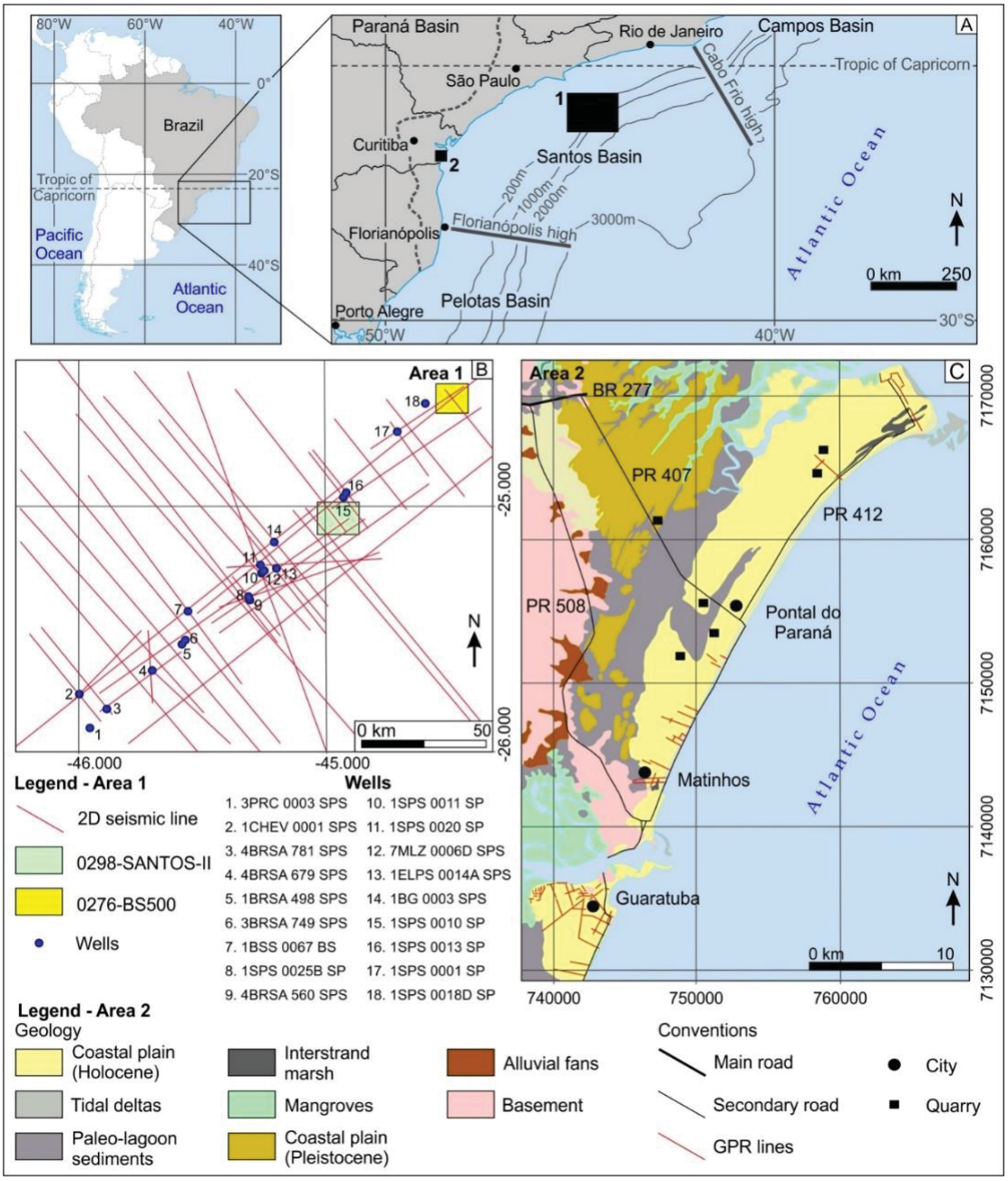

Figure 5: Location of the study areas in Santos Basin (A). Area 1, offshore, is imaged by 2D and 3D seismic and wells (B). Area 2, in the coast of Paraná, is exposed in sand pits and imaged by GPR (C).

6. Database and Methods

The two study areas selected for investigation demand different methods of analysis due to their individual characteristics (Fig. 6). Area 1 (Fig. 5) was studied through the interpretation of subsurface data such as 2D and 3D seismics and wells. In area 2 (Fig. 5), sedimentary analysis was complemented with GPR interpretation. These methods of outcrop, shallow and deep subsurface analysis have different resolutions and scales of visualization, but can be complementary (Fig. 6). Deep subsurface methods (i.e. seismics and wells) are useful for the interpretation of general depositional trends and depositional architecture in a scale that goes from tens of kilometers to hundreds of meters (Fig. 6). Shallow subsurface methods (i.e. GPR) are more detailed, ideal for the imaging of depositional elements and interpretation of depositional systems and their architecture. The scale of visualization goes from several kilometers to less than 1 m (Fig. 6). The highest resolution is achieved in outcrops, whose visualization varies from tens of meters to several millimeters, ideal for the interpretation of facies, internal heterogeneities and depositional elements (Fig. 6). All techniques have a superposition of scales that allows a comparative approach.

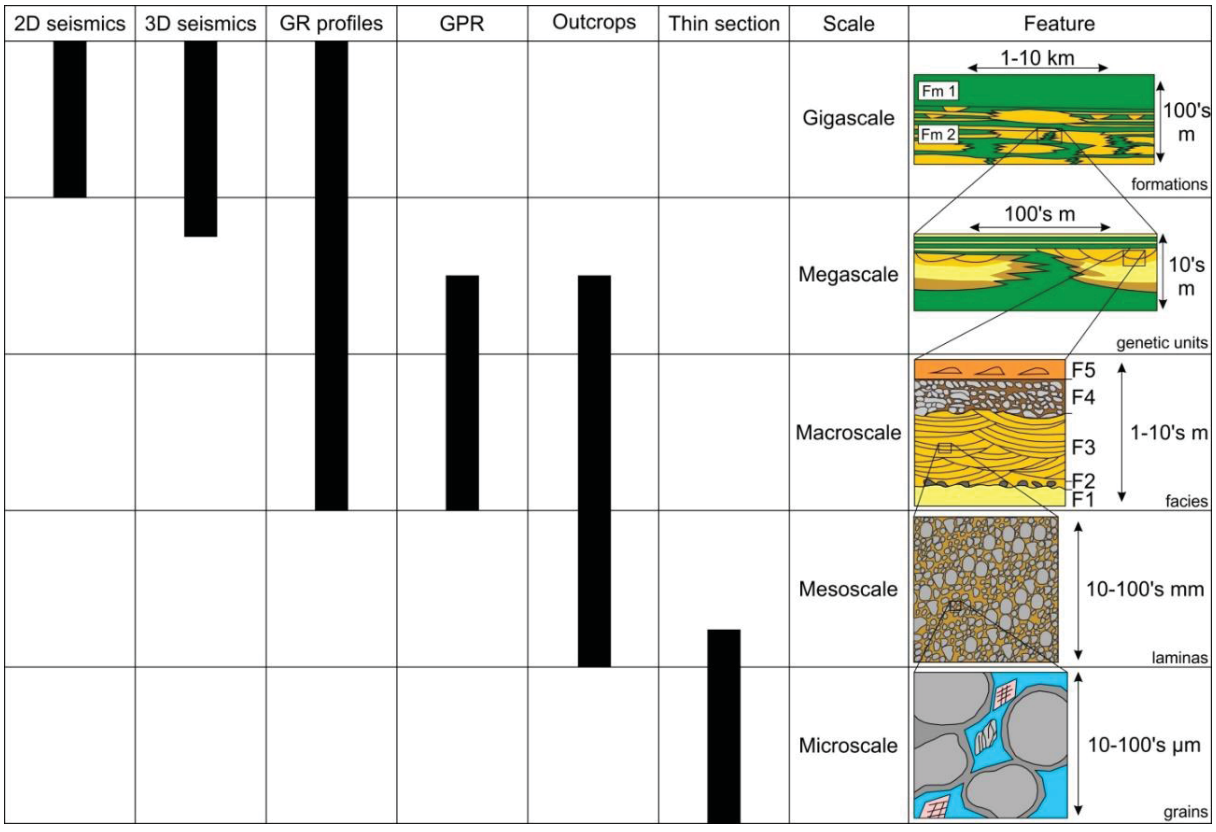

Figure 6: Relation of methods commonly used in the petroleum industry, from tools ideally used in the gigascale to tools ideally used in the microscale. Observe the superposition of scales between the methods, allowing a comparative approach. In the present research, the focus is given in the tools that range from the giga (seismics) to the mesoscale (outcrops). Modified from Dreyer (1992).

7. Subsurface architecture of wave-dominated nearshore deposits: contrasting styles of reservoir heterogeneity in response to shoreline trajectory

7.1 Introduction

Wave-dominated nearshore deposits have long been considered attractive targets for the petroleum industry, as they often configure good reservoirs in subsurface (e.g., Hamilton, 1995; Jennette and Riley, 1996; Cook et al., 1999; Jackson et al., 2009; Higgs et al., 2012; Raef et al., 2015; Olsen et al., 2017; Phelps et al., 2018; Niazi et al., 2019) or, more recently, sites for storage of carbon dioxide (e.g., Sundal et al., 2016). This potential is associated to their sandy composition and consequent high net to gross, good lateral continuity along strike, relative internal homogeneity, and overall high permeability and porosity (e.g., Galloway and Hobday, 1996; Ainsworth, 2005; Sech et al., 2009; Nyberg and Howell, 2016; Ainsworth et al., 2016; Olsen et al., 2017). However, the distribution of sand and the architecture of coastal systems might differ from classic depositional models, influenced by variations in accommodation and supply, changes in the dominant energy regime, and to the interplay of different depositional processes (i.e., wave, tidal and fluvial) (e.g., Ainsworth et al., 2011; Ainsworth et al., 2016). These variables are controlled by both autogenic and allogenic factors, which impact on the distribution of non-reservoir facies, internal heterogeneities and compartmentalization, resulting in reservoirs that are often more complex than classic coastal models.

Studies of nearshore deposits in subsurface are commonly based on the interpretation of parasequences and/or transgressive-regressive cycles (T-R cycles), which represent relatively short-term stratigraphic cycles in the order of m- to tens of m-thick and extending for several kms along dip to tens of km along basin strike (e.g. Cook et al., 1999; Hampson and Storms, 2003; Jackson et al., 2009; Ainsworth, 2010). These 4^{th} to 5^{th} order units are the building blocks of longer-term intervals related to basinal fluctuations in accommodation and sedimentation controlled by allogenic factors (Catuneanu and Zecchin, 2013; Colombera et al., 2016). The allogenic controls can be estimated from classic sequence stratigraphy using seismic and well log interpretation (e.g., Vail et al. 1977), but autogenic controls that also affect the characteristics of the deposits and sand/shale distribution (Catuneanu et al., 2009; 2011; Ainsworth et al. 2011; Catuneanu and Zecchin, 2013) are harder to predict due to limitations of resolution and areal cover

of subsurface data. Seismic geomorphology can thus be used to estimate the effects of autogenic processes in buried coastal systems by the correlation of architectural elements identified in seismic horizons with modern analogs (e.g., Jackson et al., 2010; Ainsworth et al., 2016).

The present paper aims to evaluate the relation of architecture, dimension and distribution of heterogeneities of nearshore systems in subsurface with short-term stratigraphic trends (*sensu* Catuneanu and Zecchin, 2013) and autogenic controls on the coastal domain. Two shelfal intervals within 3rd order sequences were chosen for evaluation in the Santos Basin, offshore SE Brazil. In the central part of the basin, the target is a Campanian depositional sequence composed mainly of normal-regressive, highstand shelfal deposits with internal coastal successions that act as reservoirs in the Merluza field (Sombra et al., 1990; Anjos et al., 2003; Assine et al., 2008). In the northern part of the basin, the targets are Eocene depositional sequences that record long-term forced regressions and shorter-term transgressions and normal regressions, marking a period of intensive shelf erosion (Moreira et al., 2001; Berton and Vesely, 2016a, b). Each interval depicts shorter-term cycles within the topset domains (paleoshelf), recording transgressive, normal- and forced-regressive trends assessed from topset subparallel reflectors to delta-scale clinoforms. The methods of investigation include the mapping of overall shoreline trajectories from seismic combined with higher resolution, parasequence-scale stacking patterns in well logs, and the interpretation of depositional systems from seismic geomorphology and modern analogues (e.g., Jackson et al., 2010; Raef et al., 2015; Eluwa et al., 2017).

7.2 Regional Setting

Santos Basin, located in the Brazilian southeastern margin, is limited in the north by the Cabo Frio high and in the south by the Florianópolis high (Fig. 7). Its evolution is associated to the opening of the South Atlantic Ocean during Cretaceous, comprising a Barremian to Early Aptian rift phase, an Aptian to Early Albian transitional evaporitic phase, and a divergent open marine phase from Albian to present (Modica and Brush, 2004; Moreira et al., 2007). During Turonian, regional tectonic adjustments resulted in an increase of sediment supply and in a long-term progradation that persisted until late Eocene (Jureia progradation) (Macedo, 1989; Mohriak and Magalhães, 1993) (Fig. 7). Sediment load associated to this

phase contributed to trigger halokinesis and the consequent generation of structural highs, mini-basins, arching and salt-related faulting (Sombra et al., 1990; Chang et al., 2008; Contreras et al., 2010).

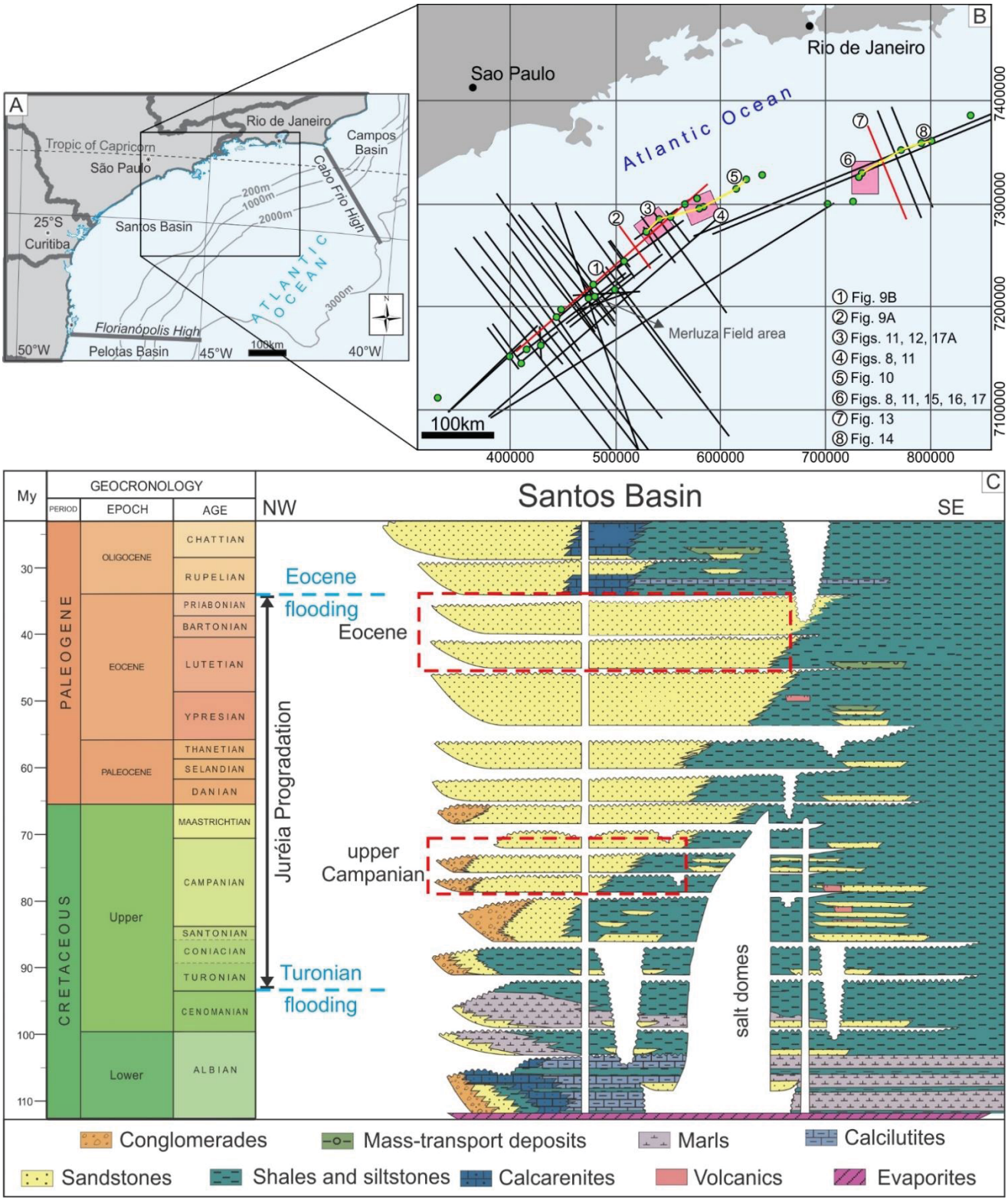

Figure 7: Santos Basin is located in the Brazilian southeastern continental margin (A). The study area is in the central-north part of the basin (B). Seismic sections are in red, seismic volumes correspond to pink rectangles, and wells are depicted as green dots. Data used in the figures are highlighted. The Campanian and Eocene intervals, focus of this study (highlighted in the red dashed rectangles), record part of the Jureia Progradation (C) (adapted from Moreira et al., 2007).

The Upper Campanian interval in central Santos Basin is characterized by a progradational wedge associated with a highstand normal-regressive trend (Assine et al., 2008). Topset reflectors from this interval are interpreted as sand-rich coastal systems from the Jureia Fm., which act as gas reservoirs in the Merluza petroleum field (Sombra et al., 1990; Anjos et al., 2003) (Fig. 7). Sedimentary facies described in well cores from the reservoir section include fine- to medium-grained sigmoidal cross-stratified sandstone, coarse-grained bioclastic massive sandstone, conglomerate with mud intraclasts, and very fine sandstone with bioturbation (Sombra et al., 1990). This facies association is attributed to complexes of barrier islands with influence of storms (Sombra et al., 1990; Anjos et al., 2003). The sand-rich reservoir units are commonly cemented by quartz, calcite or dolomite, with mean porosity of approximately 12% (Sombra et al., 1990). The top of the Campanian interval is limited by a regional Maastrichtian unconformity (Assine et al., 2008).

The Eocene interval in north Santos Basin represents the last stages of the Jureia progradation (Fig. 7), marking the gradual migration of the paleodrainage systems that controlled sedimentation towards the north, while the south-central parts of the basin became sediment-starved (Assine et al., 2008). It is characterized by a progradational wedge that records several third-order depositional sequences with a predominant forced-regressive character, intercalated with normal regressions and punctuated by short-term transgressions (Moreira et al., 2001; Berton and Vesely, 2016a). In seismic data, the topset domain depicts small-sized clinoforms with high amplitude and linear geometry in plan view that are interpreted as sandy shoreface progradations (Berton and Vesely, 2016a, b). Tectonic and climatic changes in the end of the Eocene resulted in an early Oligocene transgression that marks the interruption of the Jureia progradational trend (Moreira et al., 2001; Berton and Vesely, 2016a, b; 2018).

7.3 Dataset and Methods

The study area is located at offshore central-north Santos Basin, covering an area of approximately 7000 km² (Fig. 7). Dataset comprises three volumes extracted from two 3D post-stack depth-migrated seismic surveys in the central (survey 0298-SANTOS-II) and northern (survey 0276-BS500) parts of the basin, 45 2D post-stack time-migrated seismic sections, and composite logs from 30 wells provided by the Brazilian National Agency of Petroleum, Natural Gas and Biofuels (ANP). As part of the Campanian interval

and the whole Eocene interval are relatively shallow, the only log present in all wells is gamma-ray, altogether with lithologic interpretation data. Density, neutron porosity, sonic and caliper logs are available only in part of the wells intersecting the Campanian interval. Methods included mapping of onlaps and shoreline trajectories (e.g., Vail et al. 1977; Steel and Olsen, 2002; Helland-Hansen and Hampson, 2009; Henriksen et al., 2011; Berton and Vesely, 2016a) in order to address general trends of accommodation vs. sedimentation such as normal/forced regressive and transgressive patterns. These trends were the base for selecting reflectors to be picked for seismic geomorphological analysis. The interpretations of 3rd-order depositional sequences in the studied intervals are from previous works (Moreira et al., 2001; Assine et al., 2008; Berton and Vesely, 2016a).

7.3.1 Trends of shoreline migration

Delta-scale clinoforms in the topset domain of continental-margin clinoforms (*sensu* Patruno and Helland-Hansen, 2018) can be interpreted as shoreface or deltaic clinoforms that mark the migration of shoreline through time (e.g., Bourget et al., 2014; Berton and Vesely, 2016a). The trajectories of the rollover of such clinoforms (i.e. the point of inflexion between topset and foreset) can thus be used as a proxy for shoreline trajectories and to assess short-term regressive and transgressive patterns in seismic scale (e.g. Steel and Olsen, 2002; Hampson and Storms, 2003; Steel et al., 2008; Helland-Hansen and Hampson, 2009; Henriksen et al., 2011; Patruno and Helland-Hansen, 2018). Sub-horizontal, linear trajectories correspond to progradations in normal-regressive contexts with quasi-stable base level, with absent or below seismic resolution aggradation (Fig. 8a). The resultant shelfal horizon represents thus a toplap surface comprising several clinoforms, assuming a relative continuity along dip and representing more than one stage of progradation. Ascending trajectories basinward are also associated to normal regressions, but with considerable aggradation (Fig. 8a). Landward ascending trajectories are associated to transgressions, while descending trajectories are associated to forced regressions that result in degradational topsets (Fig. 8a).

7.3.2 Seismic geomorphology

Depositional and erosive geomorphic features were analyzed using concepts and techniques of seismic geomorphology, through the mapping of horizons in three-dimensional seismic volumes (e.g. Posamentier

et al., 2007). The mapping started with the selection of a seismic reflector representing a time line, based on a previous 2D interpretation and geological criteria. In the present study, the focus was given on topset reflectors with strong negative amplitudes and small scale clinoforms. The reflectors were picked using a semi-automatic approach along crosslines and inlines in the seismic volume using a regular spacing of 8x8 (approximately 240x240 m). The semi-automatic method was chosen to speed up interpretation where confidence was high (continuous reflector with low changes in seismic amplitudes), while a manual interpretation was carried out were confidence was low (i.e., faults zones or areas with dimmed amplitudes). After the whole reflector was covered in the seismic volume using the regular grid, it was interpolated to generate a seismic horizon. Errors in interpolation were corrected manually, and a gridding process using triangulation around interpolation gaps was used to cover “blank” areas. Such blank areas were generally associated to faults, zones with low amplitudes and gas chimneys. The process of manually correcting wrong interpolations and applying a gridding process to correct gaps was repeated until a full horizon was generated.

Sixteen horizons were mapped in the Campanian intervals and nine in the Eocene interval, using the software OpendTect from DGb Earth Sciences. After picking and mapping horizons, seismic attributes were applied for the enhancement of specific properties that allow a more clear and detailed view of the characteristics of geomorphic features. The amplitude RMS (Energy attribute) reflects the distribution and intensity of seismic amplitudes and can thus be used as a lithology proxy (e.g. Zhu et al., 2017; Eluwa et al., 2017). Instantaneous amplitude attribute enhances instantaneous variations of acoustic impedance within a horizon and can also be applied as a proxy for lithologic variations such as the contact between sandy and muddy units (e.g. Zhu et al., 2017). Similarity is a coherency attribute used to determine the similarity or dis-similarity of trace segments in relation to the dip in the horizon, being useful for the identification and mapping of faults, ridges, troughs, mounds etc. (e.g. Peyton et al., 1998; Raef et al., 2015; Berton and Vesely, 2018). Spectral decomposition reflects the amplitude spectrum of a horizon, based on the constructive interference of reflections from overlying and underlying layers. It can be used for the enhancement of relatively small-size features in the limit of seismic resolution, such as incisions or small sand bodies (e.g., Peyton et al., 1998; Partyka et al., 1999; Tayyab and Asim, 2017; Eluwa et al., 2017; Berton and Vesely, 2018). The application of different attributes allowed for the definition of seismic-

geomorphological features (GFs) that were interpreted in terms of paleoenvironments by means of comparison with modern analogs (e.g. Hampson et al., 2008).

7.3.3 Well-log interpretation

Well correlation was based on indications in composite logs provided by ANP and regional markers, such as a Maastrichtian regressive surface and the Oligocene transgressive surface. Gamma-ray logs were used for the interpretation of T-R sequences (van Wagoner et al., 1988, 1990; Embry and Johannessen, 1992; Catuneanu and Zecchin, 2013) and stratigraphic surfaces such as maximum regressive and maximum flooding surfaces. In a more detailed analysis, log-facies from gamma-ray logs were interpreted as irregular, funnel, bell, cylindrical (or blocky) and symmetrical patterns (Rider, 1996) (Fig. 8b). These log motifs were used to interpret fining/coarsening up trends and to support the interpretation of depositional features identified through seismic geomorphology. API values in gamma ray logs were also used as indirect indicators of sand/shale composition, considering low values (below 30 API) for clean sand units, and high values (more than 50 API) for shaly units (e.g., Rider and Kennedy, 2011; Corina, 2016). When available, interpretations from gamma ray logs were confronted with lithotype information from composite logs, considering the limitations of the use of gamma ray for lithology interpretation (Rider and Kennedy, 2011). Density-neutron logs were cross-plotted and also used as a proxy for the interpretation of sand and shale.

7.4 Results

7.4.1 Campanian interval

The Campanian interval is composed of sigmoidal continental-margin clinoforms with reliefs up to 1200 ms TWT (approx. 1500 m), recording a total progradation that exceeds 20 km. In the topset domain the reflectors configure a subparallel and subhorizontal pattern (when undeformed) with moderate to high amplitudes (Fig. 9). This group of topset reflectors is up to 500 ms TWT thick (approx. 625 m). Topset Campanian reflectors are often deformed by the underlying salt domes, in the form of arching and faulting (Fig. 9). The high concentration of faults above salt domes commonly imprints a complex arrangement of

disrupted reflectors, resulting in a chaotic pattern that difficult the interpretation of high-frequency stacking trends exclusively by seismics.

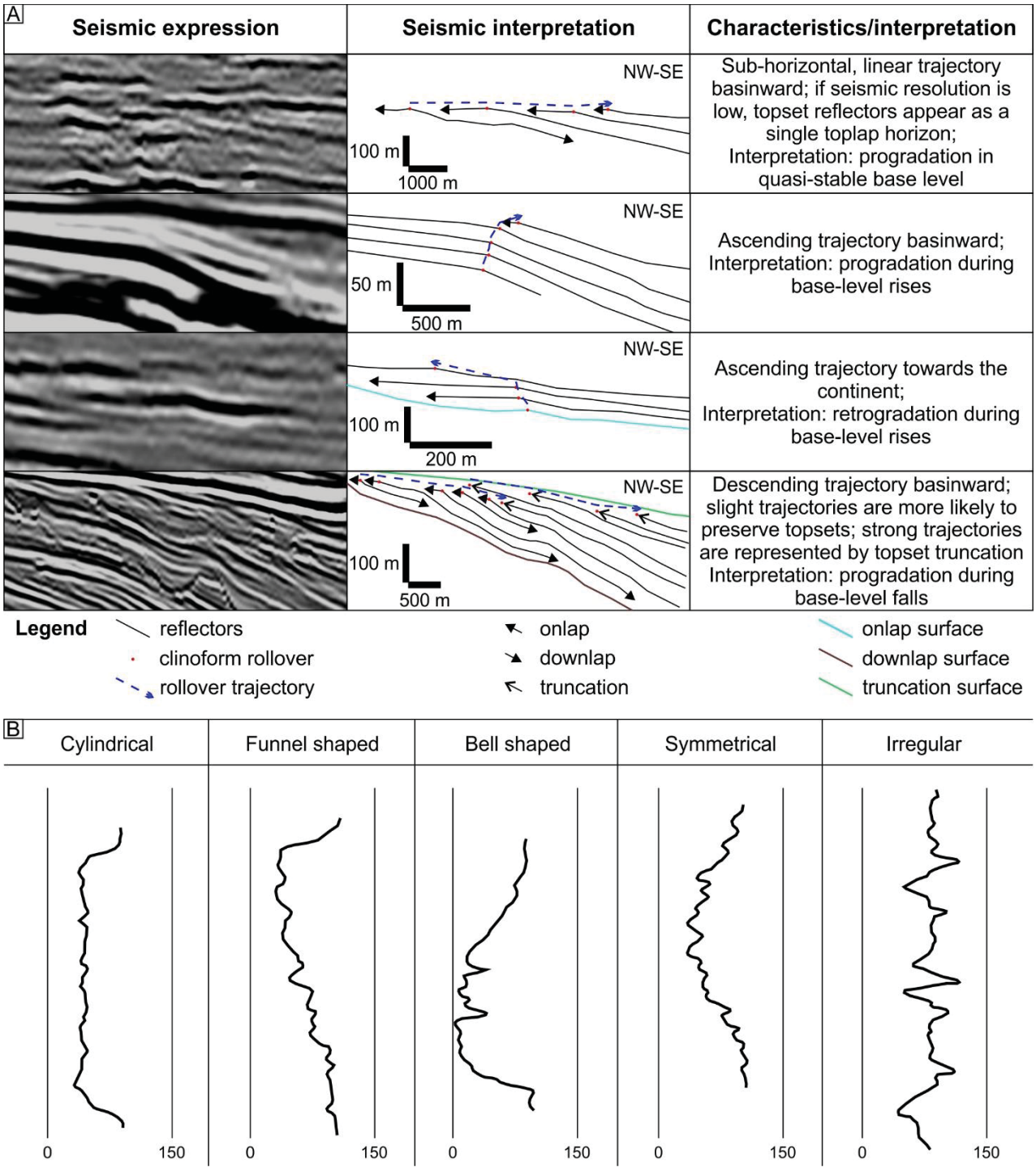

Figure 8: Seismic stratigraphy in topset successions from continental margin-scale clinoforms was based on the interpretation of trends of delta-scale clinoform rollover trajectory, mapping the displacement of the point of inflexion between topset and foreset of the small-sized topset clinoforms (A). In gamma ray logs, relatively short-term stratigraphic trends were interpreted from log facies (B) (adapted from Corina, 2016).

Although amplitudes are predominantly moderate, topset reflectors are punctuated by zones of anomalous high amplitude. These zones extend from 1 to 7 km along dip and up to 30 km along strike,

indicating an elongated geometry parallel to the basin strike (Fig. 9). The topset domain is locally represented by small-sized (delta-scale *sensu* Patruno and Helland-Hansen, 2018) tangential clinoforms with extensions along dip varying from 1.6 to 3.8 km, and reliefs up to 45 ms TWT (approx. 56 m). When seen in plan view, such clinoforms have low sinuosity and strong NE-SW orientation parallel to the basin strike. The mapping of trajectories of the rollovers of the clinoforms indicates an ascending basinward migration trend, coherent with overall normal-regressive conditions. Quasi-linear trajectories are also observed, with distances of progradation from 1 to 6.5 km.

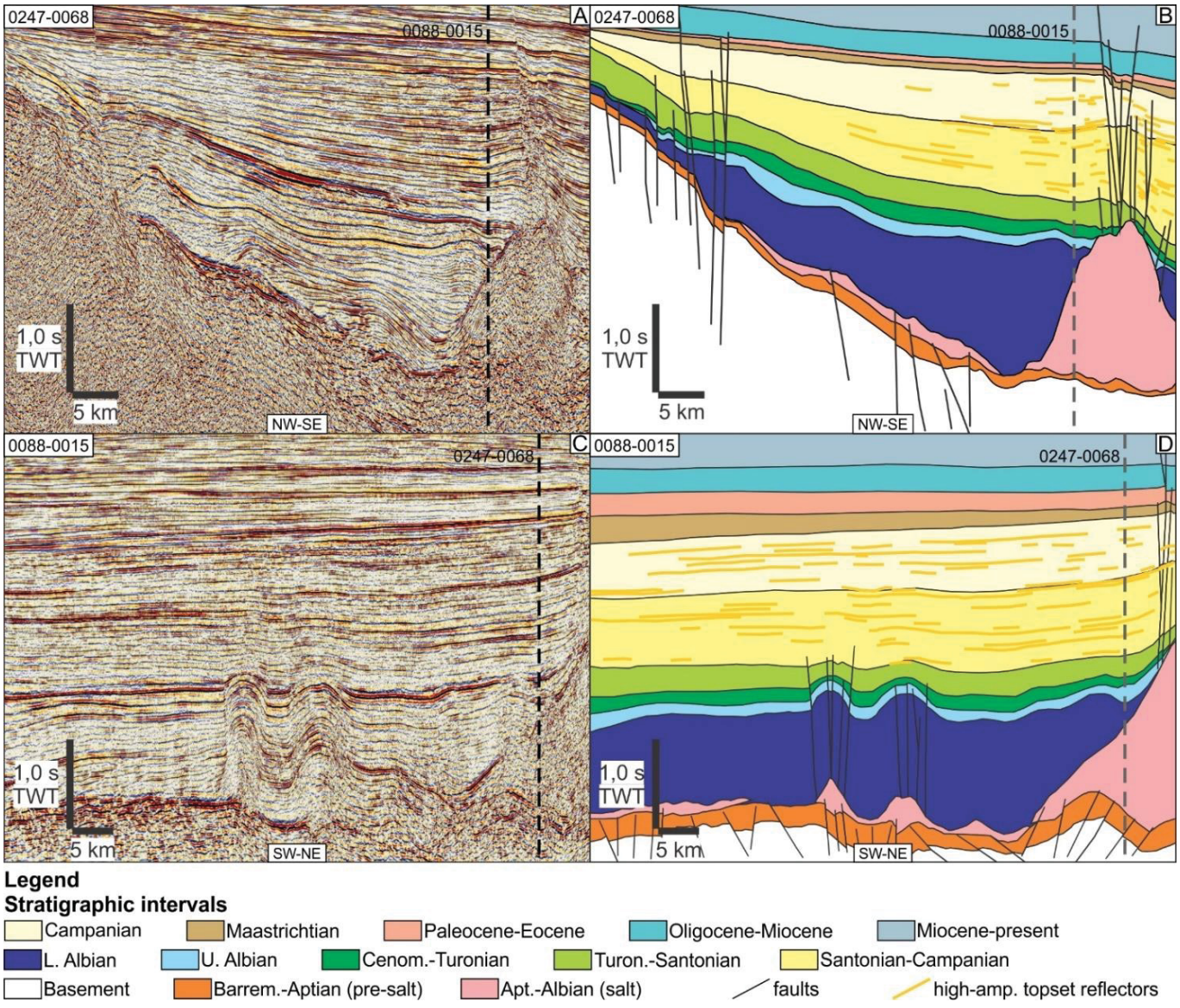

Figure 9: Part of a dip seismic section covering the topset domain of Campanian continental margin-scale clinoforms from central Santos Basin (A) and its interpretation (B). The targets for seismic geomorphology are the high-amplitude sub-horizontal topset reflectors interpreted as nearshore successions. In a strike section (C), these high-amplitude topset reflectors are elongated along strike (D). These reflectors are partially deformed and intersected by faults associated with the underlying salt. Regional stratigraphic interpretation is based in Assine et al. (2008).

Lithologic interpretations and the cross-plotting of density (RHOB) and neutron-porosity logs (NPHI) indicate an overall sand-rich composition in the Campanian interval, with thinner successions of clay and/or siltic nature (Fig. 10). Although these logs show the occurrence of continuous sand intervals up to 30 m thick, gamma-ray logs indicate that they correspond in fact to sand-rich intervals with bell, funnel or cylindrical log patterns, and each log facies is commonly less than 10 m thick (Fig. 10). T-R sequence interpretation shows that internally the Campanian interval is composed of at least four sequences, but the low amplitude of gamma-ray variation indicates predominant aggrading conditions (Fig. 10). The only expressive changes in logs within the interval correspond to peaks in gamma ray in the base and top of the Campanian interval.

7.4.1.1 Seismic geomorphology

The seismic-geomorphologic interpretation was concentrated on high-amplitude topset reflectors and individual small-sized clinoforms. Most of the interpreted horizons are discontinuous and strongly affected by salt-related faulting and arching, but it is still possible to recognize patterns of depositional/erosive features (Fig. 11; Tab. 1). The strongest negative-amplitude zones in Campanian horizons correspond to elongated features in Energy attribute maps, oriented in a NE-SW trend (shore-parallel) (Fig. 12). These zones extend from 1.5 to 7 km along dip and exceed the size of the seismic volumes along strike (>20 km). Attribute maps highlight the occurrence of internal geomorphic features that are predominantly subparallel to oblique, and of geomorphic features located landward in relation to the negative-amplitude zones.

The most expressive internal geomorphic signatures configure sets of subparallel to oblique linear features with high negative amplitudes and a transverse morphology of elongated ridges and valleys (GF1) (Fig. 11). Highs/depths of the ridges and valleys are not measurable due to limitations of seismic resolution, and the surface morphology is only visible in Similarity maps. The external limits of GF1 tend to be linear and well-defined, marked by the variation of angles of the ridges and valleys. The composition of the zones is dominantly sandy as indicated by attribute maps and gamma-ray logs. GF1 depicts a cylindrical gamma ray log pattern and low API values in well 3-BRSA-347-SPS (Fig. 12). The cylindrical interval is more than 100 m thick, only interrupted by local, abrupt increases in API values.

Shoreline-parallel zones of positive moderate to high amplitudes and with irregular distribution and undefined limits (GF2) intercalate with GF1 in Instantaneous maps (Fig. 12). Some of these elongated zones depict internal shoreline-parallel, sinuous features as discontinuous positive high-amplitude elements up to 50 m wide (Fig. 11). Similar patterns are observed landward in relation to the negative-amplitude zones, as shoreline-transverse linear features with predominant moderate amplitudes (GF3). These features configure sinuous valleys up to 0.5 km wide in Similarity maps (Fig. 12). Positive high-amplitude zones (GF4) might also occur landward in relation to the negative-amplitude zones. They are oblique to the shoreline and have irregular external limits, with a rugose character in Similarity maps and a muddy composition in well logs (Fig. 12). GF4 was intersected by well 3-BRSA-242A-SPS, showing high API values and log motifs that alternate between irregular and funnel (Fig. 12). This pattern occurs only locally in the study area, and in well 3-BRSA-347-SPS the correspondent interval is covered by an interval with cylindrical gamma ray log patterns and low API values.

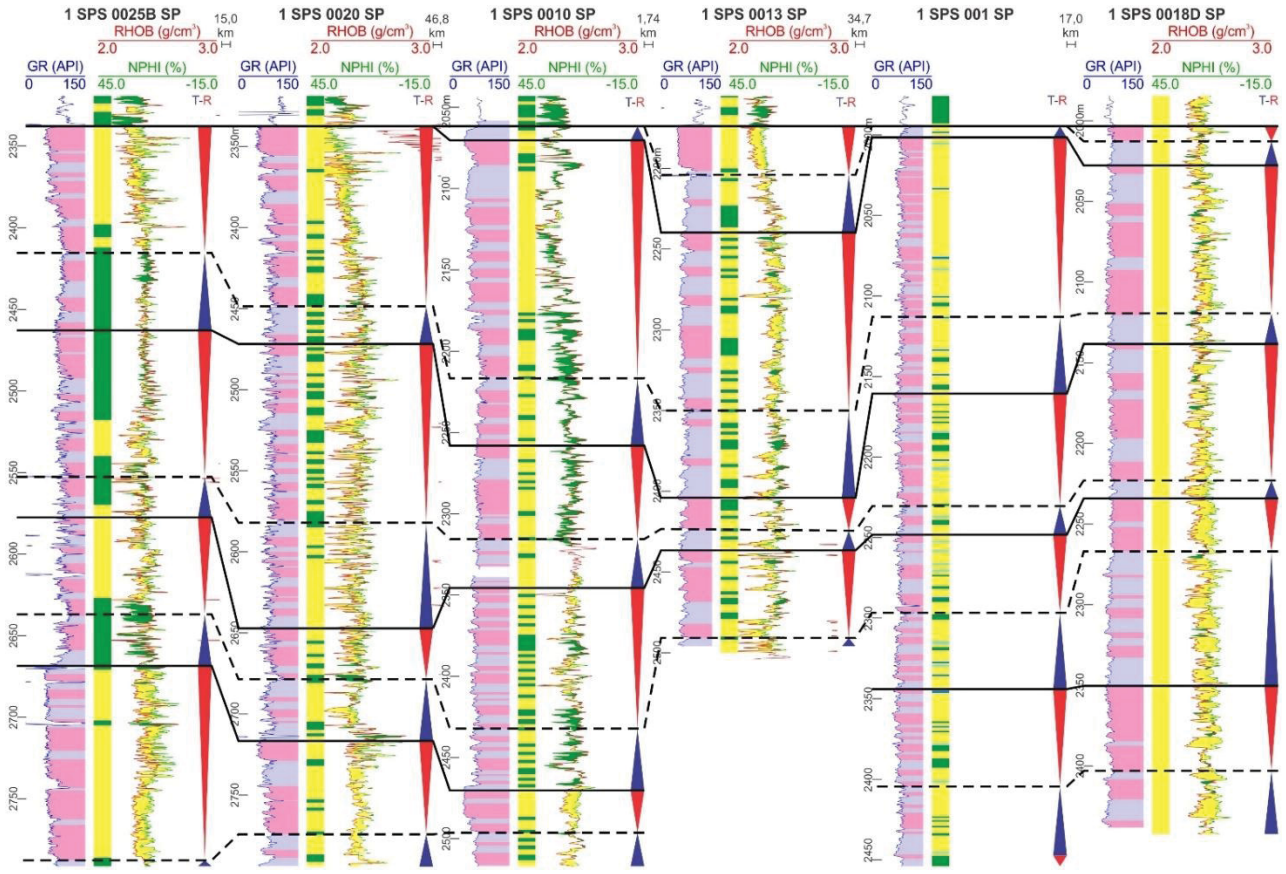

Figure 10: SW-NE well correlation of the Upper Campanian interval, using a Maastrichtian unconformity as top datum. Coloring on the right side of the gamma ray logs indicates relatively short-term fining- (blue) and coarsening-up (pink) trends within T-R cycles. Each of these short-term intervals might also include internal parasequences, but their correlation is uncertain due to the distance between wells (up to 47 km). T-R cycles are clearer in the SW wells, while towards NE log patterns indicate aggrading conditions that difficult the correlation. Dashed lines represent maximum flooding surfaces, while solid lines represent maximum regression surfaces (T-R sequence boundaries).

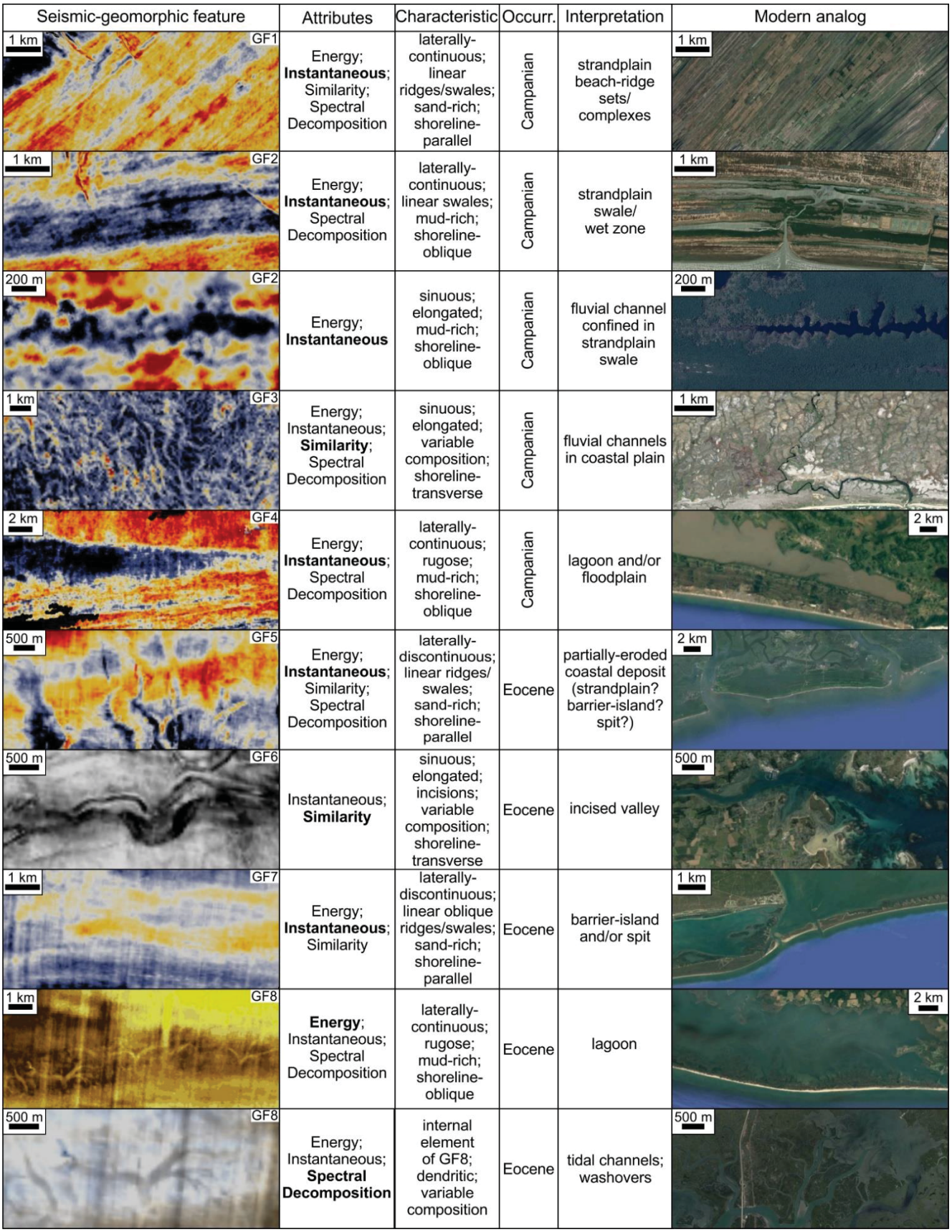

Figure 11: Correlation between seismic-geomorphologic features and elements in modern coasts, based on architecture, size and interpreted composition. Beach-ridge sets/complexes and swale deposits are from the coast of Nayarit, Mexico. Confined fluvial channel and backbarrier lagoon are from the coast of Rio Grande do Sul, Brazil. Partially-eroded coastal deposits and incised valley are from the coast of Brittany, France. Barrier-island deposits are from the coast of Texas, while lagoon and tidal channels are from the coast of New Jersey, USA.

7.4.1.2 Interpretation

High-amplitude reflectors from the topset domain of the Campanian interval are interpreted as sandy nearshore systems (Tab. 1), based on the combination of high negative amplitudes that sometimes configure ‘bright spots’ in seismic (Fig. 9), the occurrence of delta-scale clinoforms elongated along strike, the predominant shoreline-parallel to shoreline-oblique seismic-geomorphologic geometries in attribute maps, and the sand-rich composition in well logs. The dominant geometries in attribute maps corresponds to GF1, composed by sand-rich, laterally elongated deposits with surface morphology of small ridges and valleys, intercalated with elongated zones with a muddier composition (Fig. 12). The architecture, composition, internal and surface character of GF1 are comparable to strandplain beach-ridge sets/complexes (*sensu* Nyberg and Howell, 2016; e.g., Hampson et al., 2008; Jackson et al., 2010; Klausen et al., 2016; Eluwa et al., 2017), resultant from the progradation of barred wave-dominated coastal systems that form an intercalation of ridges and swales (e.g., Jackson et al., 2010; Eluwa et al., 2017) (Fig. 11).

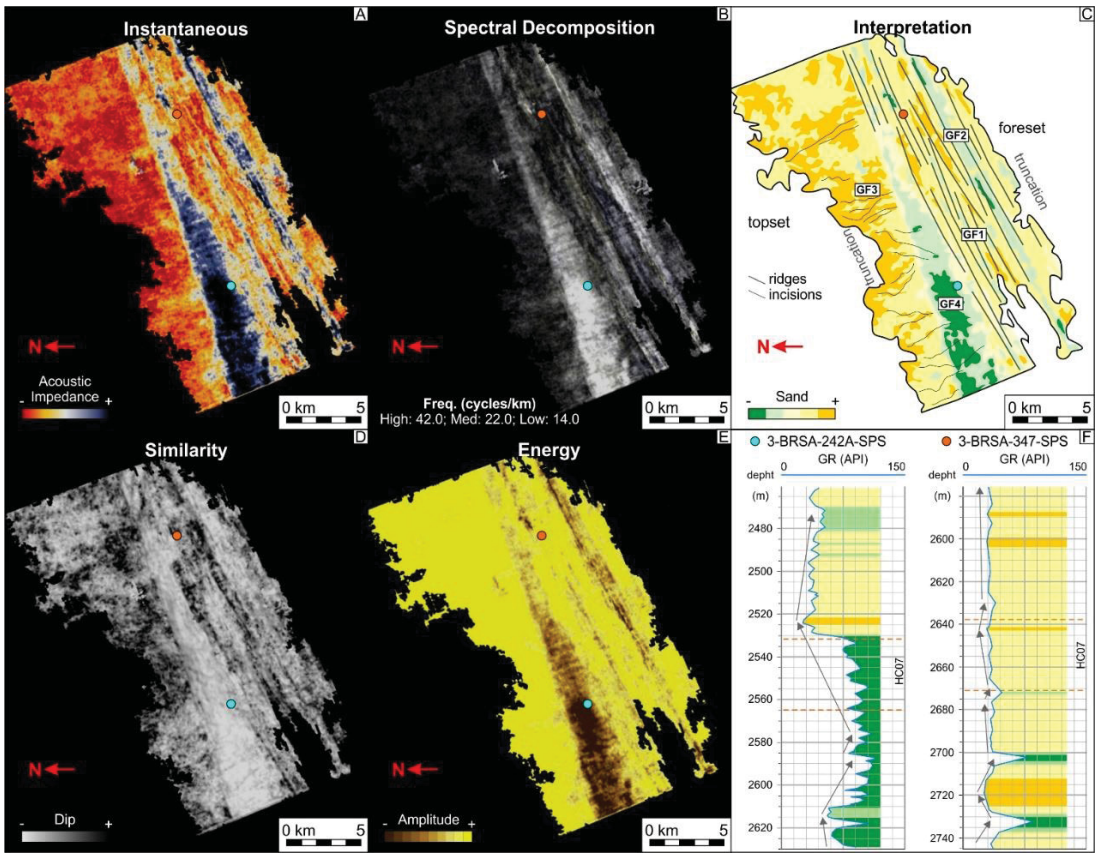

Figure 12: Seismic horizon HC05, interpreted in the topset domain of the Campanian interval. Note the high negative-amplitude shoreline-parallel linear bodies (A, E), with a surface morphology of ridges and valleys (D), interpreted as GF1, intercalated along dip with GF2. Landward in relation to GF1, shoreline-transverse linear features (GF3) and zones with positive amplitude (GF4) can be seen in both amplitude maps (A, E) and in spectral decomposition (B). The interpretation of the horizon is depicted in (C). In gamma-ray logs (F), GF4 is attributed to an interval with high API values, while GF1 is attributed to a zone with low API values and cylindrical log facies.

Table 1: Summary of the geomorphic features and its internal elements interpreted through seismic geomorphology. These features were grouped in three genetic associations, namely strandplain, partially-eroded coast, and spit-inlet and lagoon.

Context	Geomorphic Feature	Amplitude	Geometry	Size	Internal Elements	Surface Morphology	Composition	Interpretation	Association
Topset subparallel reflectors (mainly) or delta-scale clinoforms; basinward flat to ascending trajectories	GF1	moderate to high negative	shoreline-parallel, elongated, linear to slightly lobate	up to 7 km along dip; >20 km along strike	linear subparallel features	ridges and valleys	sandy (from well logs + seismic attributes)	beach-ridge set/complex	Strandplain
	GF2	moderate to high positive	shoreline-parallel, irregular	up to 1.5 km along dip, up to 15 km along strike	channelized sinuous features	rugose	muddy (from seismic attributes)	swale/interstrand marsh	
	GF3	moderate positive to negative	shoreline-transverse, channelized sinuous	>10 km along dip, up to 0.5 km along strike	-	undefined	variable (from seismic attributes)	fluvial channels	
	GF4	high positive	shoreline-parallel, elongated	up to 5 km along dip, >15 km along strike	-	rugose	muddy (from well logs + seismic attributes)	lagoon/coastal plain	
Delta-scale clinoforms; basinward slightly descending trajectories	GF5	low to moderate negative	shoreline-parallel, elongated	up to 0.7 km along dip, >10 km along strike	linear subparallel features (subtle)	ridges and valleys (subtle)	sandy (from well logs + seismic attributes)	beach-ridge set/complex	Partially-eroded coast
	GF6	moderate to high positive	shoreline-transverse, elongated	up to 6.5 km along dip, up to 0.6 km along strike	channelized sinuous features	valleys (up to 50 m deep)	variable (from seismic attributes)	incised valleys	
Topset subparallel reflectors; landward ascending trajectories	GF7	low to moderate negative	shoreline-parallel, elongated	up to 3 km along dip, up to 10 km along strike	linear oblique features (subtle)	ridges and valleys (subtle)	sandy (from seismic attributes)	spit	Spit-inlet and lagoon
	GF8	low positive	shoreline-oblique, elongated	up to 6 km along dip, >15 km along strike	channelized dendritic	rugose with internal channels	muddy with sandier channels (from well logs + seismic attributes)	lagoon	

GF2 has a muddier composition and intercalates along dip with the sandy beach-ridge deposits from GF1 (Fig. 12). In the context of a coastal system composed by beach-ridge deposits, GF2 can be correlated with muddy interstrand marshes that accommodate on the surface swales formed by progradation of the barrier system (e.g., Jackson et al., 2010; Eluwa et al., 2017) (Fig. 11). The internal strike-oriented meandering forms are thus interpreted as coast-parallel restrict fluvial courses that flow within the confined swales (e.g. Eluwa et al., 2017) (Fig. 11) with a mud- and organic-rich composition (e.g., Otvos, 2000, 2012). The shoreline-transverse meandering forms (GF3) that occur exclusively landward in relation to GF1 have variable impedances and amplitudes (Fig. 12) and are interpreted as fluvial deposits with variable sediment composition (e.g., Eluwa et al., 2017; Tayyab and Asim, 2017) (Fig. 5). In attribute maps there are no evidence that these fluvial systems cut GF1 and associated features, and therefore they can be attributed to a fully backbarrier context. The low amplitude zones labeled as GF4 are interpreted as muddy backbarrier lagoons from the coastal plain (e.g., Jackson et al., 2010; Steel and Milliken, 2013) (Fig. 5). The association of GF1, GF2 and GF4 in horizons attributed to a nearshore context is attributed to strandplain systems (e.g., Hampson et al., 2008; Ainsworth et al., 2011).

7.4.2 Eocene interval

The Eocene interval in north Santos Basin is composed of prisms of sigmoidal and tangential continental-margin clinoforms with reliefs up to 700 ms TWT (approx. 870 m), recording a total progradation of 35 km (Fig. 13). The topset domain is up to 480 ms TWT thick (approx. 600 m) and composed mainly of subparallel and subhorizontal reflectors truncated basinward by slump scars. Among these, some sets of reflectors depict an ascending landward trajectory of rollovers, coherently with transgressive settings. This interpretation is reinforced by thinning-up trends in gamma-ray logs (Fig. 14). Intra shelf delta-scale clinoforms were identified locally, with progradation distances of up to 7 km, and up to 80 ms TWT thick (approx. 100 m) (Fig. 13). Trajectory of the rollovers of these clinoforms is predominantly quasi-linear, varying from slightly ascending to slightly descending. Locally, a strong descending trajectory is imposed by prominent truncation surfaces, and topsets are not preserved. These topset clinoforms can be the result of progradation of shoreface deposits and/or shelf-margin deltas. Gamma-ray logs indicate the variability of thinning- and coarsening-up intervals that are internal to the dominant forced-regressive intervals interpreted from seismic (Fig. 14). At least two T-R cycles can be

interpreted from well logs, with a predominance of regressive conditions (Fig. 14). The top of the Eocene interval is represented by a marine flooding surface.

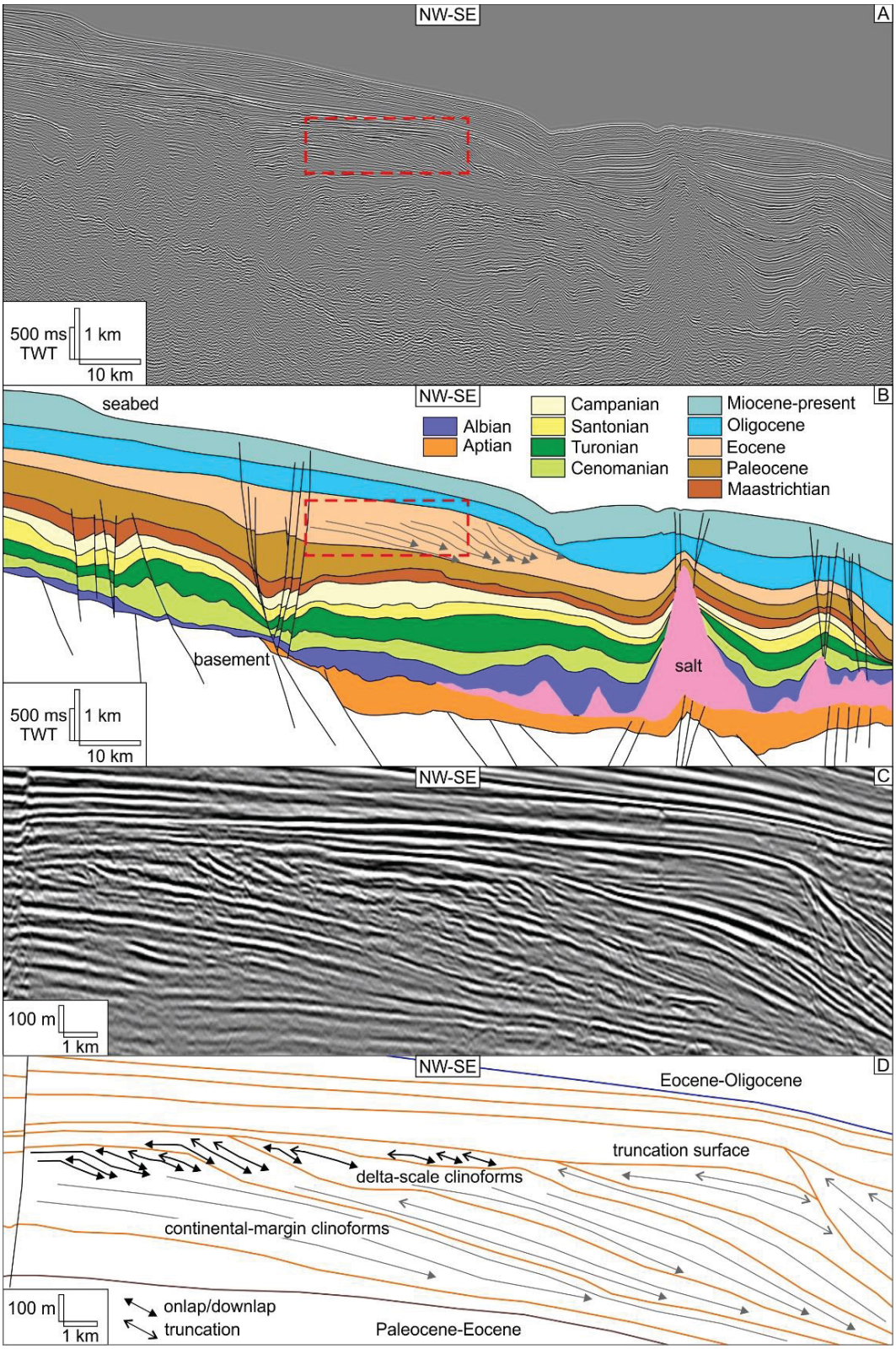

Figure 13: Regional dip seismic section from north Santos Basin (A), with interpretation of the main seismic-stratigraphic intervals (B). Note the presence of continental-margin scale clinoforms in the Eocene interval. A detailed view of the proximal part of the Eocene interval (C) shows the presence of delta-scale clinoforms in the topset domain of continental-margin clinoforms (D).

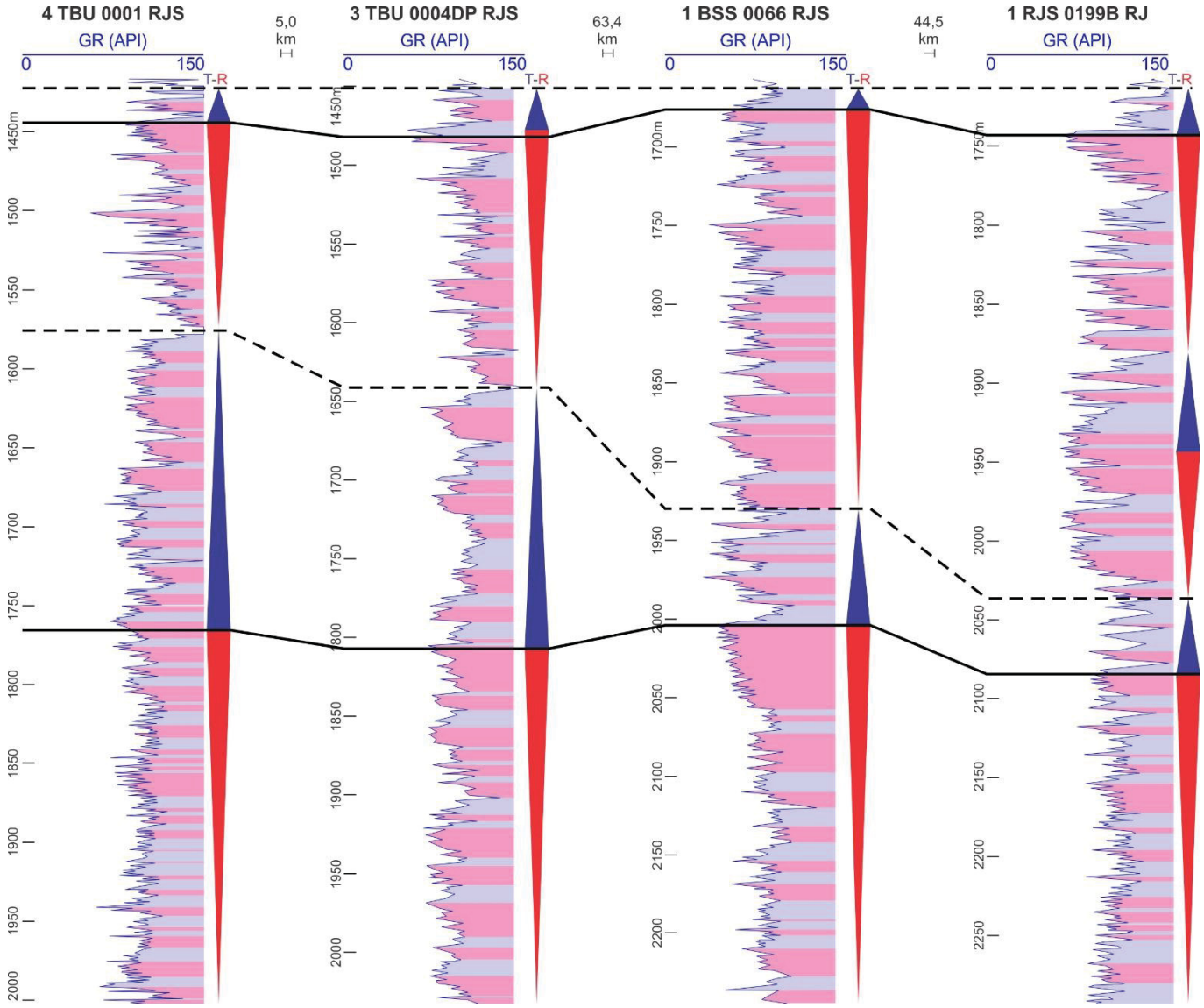

Figure 14: Well correlation of the Eocene interval (SW-NE), using the top Eocene limit as datum. Colors on the right side of the gamma ray logs indicate relatively short-term fining- (blue) and coarsening-up (pink) trends within T-R cycles. Each short-term interval might also include internal parasequences. T-R cycles have lower frequency than in the Campanian interval. Dashed lines represent maximum flooding surfaces, while full lines represent maximum regression surfaces (T-R sequence boundaries).

7.4.2.1 Seismic geomorphology

Three different seismic-geomorphologic configurations were assessed in Eocene horizons. The first type of configuration is correspondent to the extensive truncation surfaces that impose a strongly descending trajectory for delta-scale topset clinoforms. These horizons have an irregular pattern of zones with low to moderate amplitudes, and no specific and/or well-defined geometry was identified. The second type of configuration is associated with less extensive truncation surfaces that impose a more subtle descending trajectory for the underlying delta-scale clinoforms (Fig. 15). In these cases, the shelfal domain is mostly represented by irregular NE-SW zones (shoreline-parallel) with low- to moderate-amplitude

negative acoustic impedances (GF5), with lateral extensions of up to 10 km (locally exceeds the seismic volume) and up to 0.7 km along dip (Fig. 11). Similarity maps show the occurrence of very subtle linear features aligned following the NE-SW trend. The geometry, dimensions and surface morphology of GF5 are similar to GF1, although it is more discontinuous along strike.

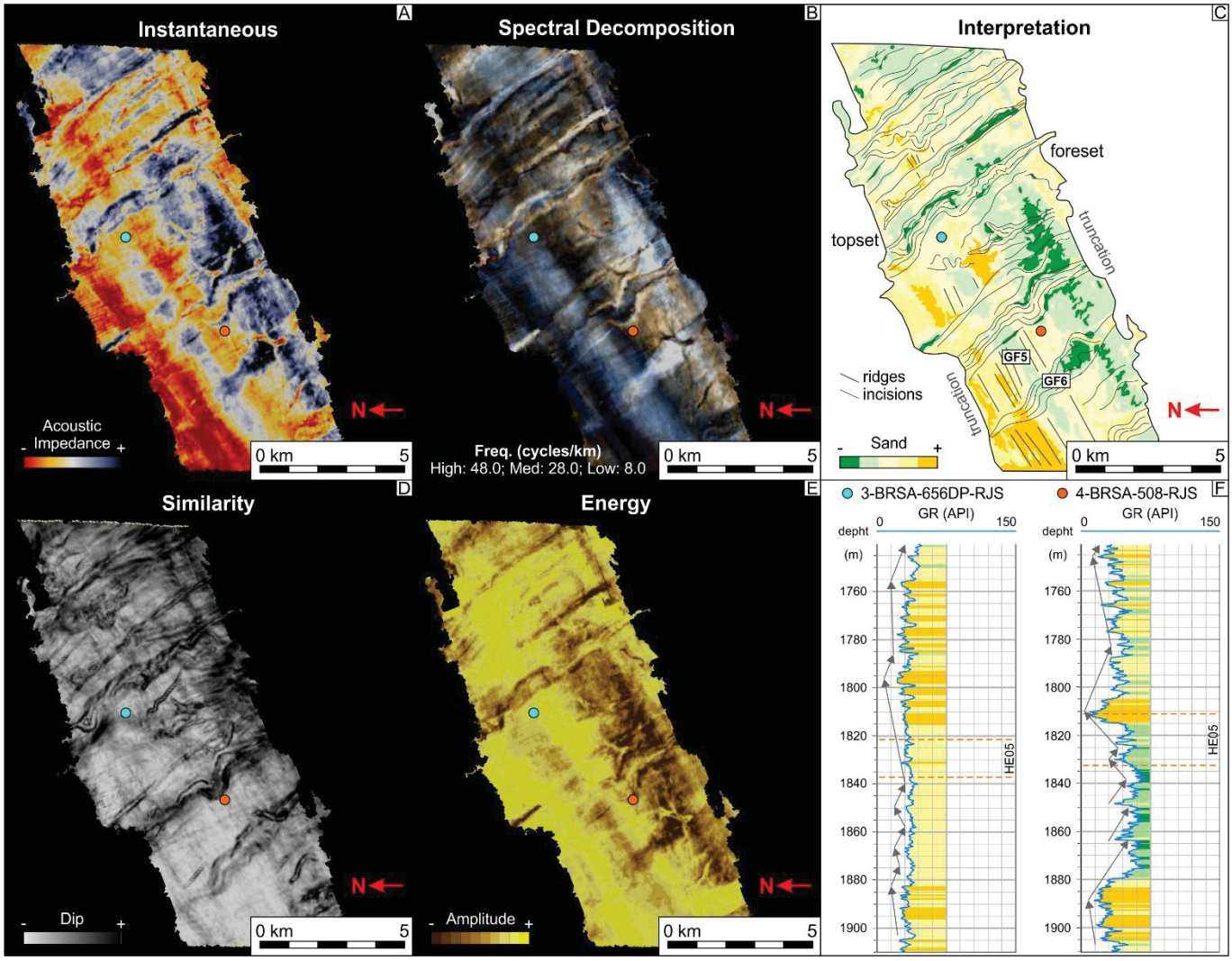

Figure 15: Seismic horizon HE05, from the Eocene interval. High amplitude shoreline-parallel zones (GF5) are cut by shoreline-transverse features (GF6) in Instantaneous amplitude (A) and Energy maps (E). Similarity attribute (D) shows that GF6 corresponds to valleys with internal linear sinuous elements (B). In wells, GF5 corresponds to coarsening-up deposits with predominantly low API values (F). This seismic-geomorphologic configuration is thus interpreted as strike-parallel sand-rich deposits cut by dip-oriented narrow valleys (C).

In well 3-BRSA-656DP-RJS, GF5 (identified in horizon HE05) presents low API values in gamma-ray log, coherent with an overall sandy composition (Fig. 15). The base of the horizon depicts a 9 m thick funnel motif, followed by a 5 m thick cylindrical pattern in the top. These log facies are the base of a 40 m-thick interval with a general decrease in API values (funnel shape), with irregular to funnel patterns in the base, and cylindrical patterns in the top, interpreted as stacked parasequences. In well 4-BRSA-508-RJS,

intersecting a zone with lower amplitude of GF5, API values in gamma ray logs are more varied. In the base of the horizon, a 5 m thick interval records a progressive increase in API values, resulting in a bell pattern. Above, a 14 m thick interval shows a general decrease of API values, resulting in a funnel shape. Therefore, this well shows the transition from a finning-up to a coarsening-up pattern (Fig. 15).

The zones attributed to GF5 are highly disrupted, intersected by shoreline-transverse valleys (NW-SE) that extend from the shelf to the upper slope (GF6) (Fig. 11). In plan view, these valleys have a linear to slightly sinuous geometry, with extensions varying from 2 to 6.5 km, and up to 600 m wide (Fig. 15). In the 3D view, the wider valleys tend to be U-shaped, while narrower valleys are V-shaped. Depth of the valleys gradually increases basinward, reaching 50 m in the shelf break. Internally, they are represented predominantly by positive moderate to high amplitude reflections (Fig. 15). In strike-parallel sections, internal reflectors onlap against the valley walls and dip towards the center of the features. Similarity maps show that locally the internal part of the valleys is composed of several sinuous channels up to 130 m wide, forming a slightly sinuous to meandering pattern (Fig. 15).

The third horizon configuration is associated with ascending landward trajectories (transgressive trend) (Fig. 16). Low to moderate amplitudes are predominant, mainly associated with zones with positive acoustic impedance contrasts. Zones with negative impedance contrasts and moderate to high amplitude configure features with strike-oriented elongated geometry (GF7) (Fig. 16). Maximum extension exceeds 10 km, while dip extensions reach 3 km. These features are distinguished in 2D seismic sections as discontinuous high amplitude zones in both strike and dip, with a character similar to GF1 but with smaller dimensions (Fig. 16). The similarity attribute highlights the occurrence of linear, discontinuous ridges and valleys oriented internally in GF7.

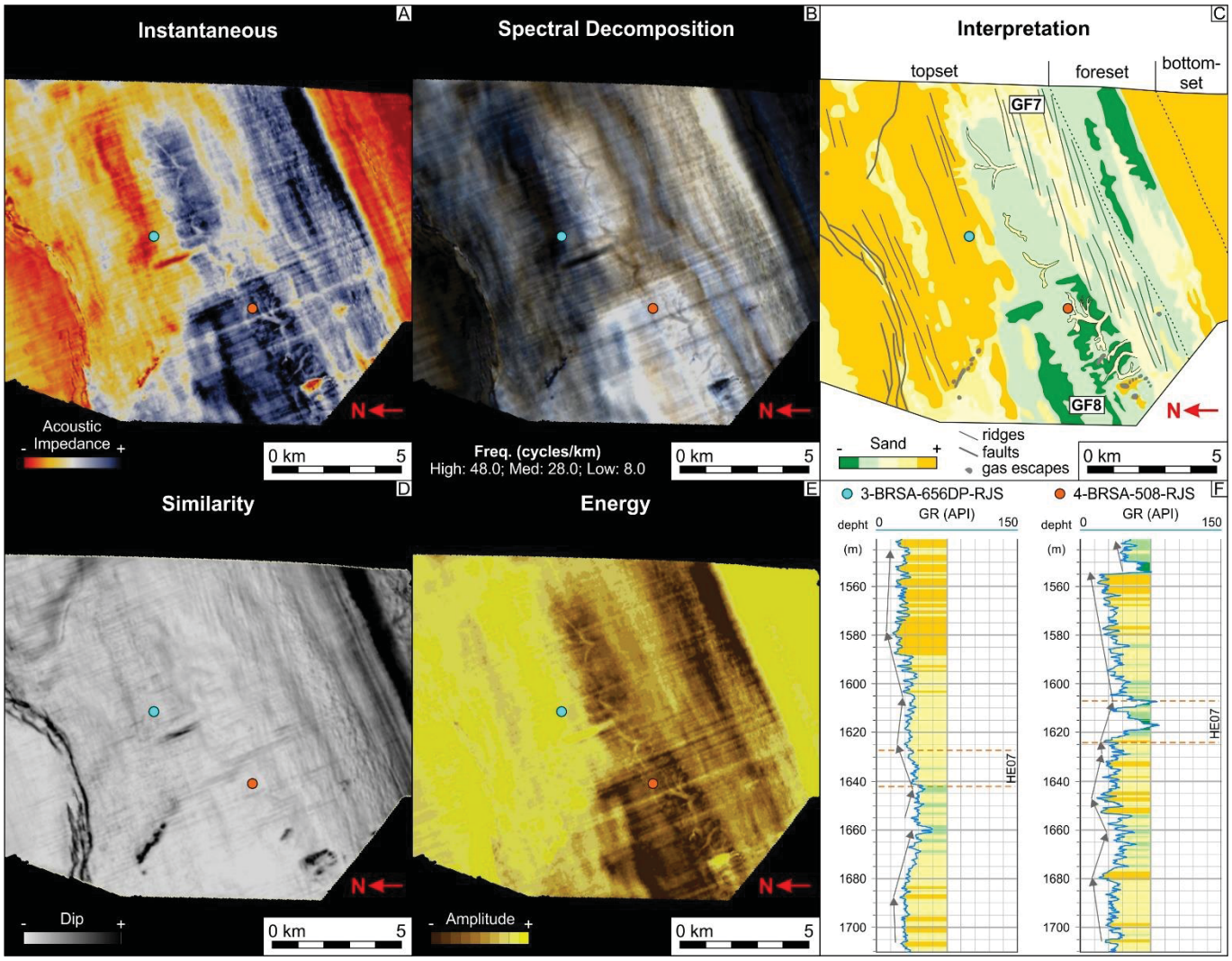

Figure 16: Seismic horizon HE07, from the Eocene interval. Instantaneous amplitude (A) and Energy attributes (E) show the occurrence of wide shoreline-parallel to oblique positive amplitude zones (GF8), limited basinward by discontinuous zones with negative amplitude (GF7). Channelized elements with a dendritic pattern are located within GF8 and are enhanced in Spectral Decomposition map (B). In Similarity map (D), GF7 has a surface morphology of shoreline-oblique linear ridges. Well data from GF8 (F) shows high API values within a fining-up trend. An interpretation considering the results from all the attribute maps and wells is shown in (C).

GF8 occurs landward in relation to GF7, in the form of zones with predominant positive low amplitudes, elongated obliquely to the shoreline and with irregular boundaries (Fig. 16). Minimum extension along strike reaches 15 km (exceeds the limit of the seismic volumes), while dip extensions vary from 1.4 to 6 km. It depicts a predominance of positive impedance contrasts in maps of acoustic impedance (Instantaneous attribute), and a smooth surface morphology punctuated by several subtle channelized features in Similarity maps (Fig. 16). These channelized features compose systems of channels with a dendritic pattern in Spectral Decomposition maps, following a general shoreline-transverse trend (NW-SE) normal to the direction of GF8 (Fig. 16).

The extension of individual channels varies from 0.4 to 2.5 km, while widths vary from less than 50 m to more than 200 m (Fig. 11). They have negative amplitudes in Instantaneous maps that contrast with the positive amplitude of GF8 (Fig. 16). These internal features were not identified in 2D seismic, probably due to their subtle character and small vertical dimensions. The systems of channels have an external fan geometry, with a wider main channel ramifying landward to the inner portion of the positive-impedance zones from GF8 (Fig. 11). The size and geometry of the dendritic systems is variable, from 1.2 to 1.8 km along dip and 0.6 to 3.1 km along strike. In well logs GF8 depicts a bell pattern in the base with a strong increase in API values, covered by an interval with decrease of API values (Fig. 16). It is therefore dominated by finning-up patterns and relatively high API values. The zone landward to GF8 have predominantly low API values with a basal irregular log pattern and towards the top a funnel pattern, corresponding to the base of an interval with funnel pattern and internal parasequences (Fig. 16).

7.4.2.2 Interpretation

Topset horizons within delta-scale clinoforms with descending trajectories depict narrow valleys (GF6) that cut underlying reflectors and have internal reflectors onlapping against its walls, being interpreted as the result of shelf erosion and generation of shoreline-transverse incised valleys (e.g., Peyton et al., 1998; Higgs et al., 2012) (Tab. 1). Their internal composition is heterogeneous as indicated by seismic attribute maps, but sinuous features within the valleys can be interpreted as fluvial channel systems (e.g., Peyton et al., 1998; Raef et al., 2015; Tayyab and Asim, 2017). In attribute maps these valleys cut through GF5 (Fig. 15). GF5 corresponds to shoreline-parallel elongated sand bodies with coarsening-up trend in gamma-ray logs, pointing to the interpretation of coastal and/or shallow marine detached prograding systems (Posamentier and Morris, 2000) (Fig. 15). The transition of funnel gamma-ray patterns in the base of the regressive succession to cylindrical motifs in the top is coherent with the transition of shoreface to beach deposits during a progradation. GF5 is thus interpreted to be initially laterally-continuous, and later cut by canyon incision.

Horizons associated with landward ascending trajectories of clinoform rollovers in the Eocene interval correspond to transgressive intervals marked by the association of GF7 and GF8 (Tab. 1). The strike-elongated, laterally-discontinuous zones of negative amplitudes (GF7) are interpreted as sandy coastal

deposits with more heterogeneous composition and smaller dimensions than beach-ridge systems. These characteristics, coupled with the discontinuity along strike, are coherent with coastal deposits such as barrier islands or coastal spits (e.g., Dreyer et al., 2005; Sundal et al., 2016) (Fig. 11). Shoreline-oblique ridges seen on Similarity maps may thus indicate oblique rather than frontal accretion of the systems, with a migration from NE to SW. The shoreline-oblique zones with positive impedance contrasts from GF8 have predominantly high API values in gamma ray logs (Fig. 16), being interpreted as muddy backbarrier lagoons (e.g., Eluwa et al., 2017) (Fig. 11). In this context, the internal fan-shaped systems of distributary channels have dimensions, geometry and composition comparable to washover fans or flood tidal deltas (Fig. 11). They are probably heterogeneous deposits as indicated by impedance contrasts and amplitudes, and by sudden decreases in API values in gamma-ray logs from GF8 (Fig. 16). The API values are coherent with a silty to sandy composition, such as in fine-grained flood tidal delta deposits (e.g., Heward, 1981).

7.5 Discussion

The topset high-amplitude reflections in both Campanian and Eocene intervals (Figs. 9 and 13) have been interpreted as coastal to shallow marine deposits (Assine et al., 2008; Berton and Vesely, 2016a). The delta-scale topset clinoforms can be attributed to shoreline clinoforms based on their position, sand-rich composition, dimensions and elongated geometry along strike with high linearity (e.g. Bourget et al., 2014; Cross et al., 2015; Graham et al., 2015; Berton and Vesely 2016a, b; Klausen et al., 2016; Sundal et al., 2016). A transitional zonation is expected within such clinoforms, with parallic deposits in the topsets grading to shallow marine (inner shelf/offshore) deposits in the foresets (Patruno and Helland-Hansen, 2018). Although delta-scale clinoforms were identified only locally and predominantly in the Eocene interval (Fig. 13), where seismic resolution is higher, it is reasonable to consider that topset subhorizontal reflectors with strong linear strike-elongated negative amplitude peaks from the Campanian interval also correspond to shoreline successions. In these cases, relatively small dimensions incompatible with seismic resolution prevented their visualization as individual clinoforms, but as subparallel reflectors that record a quasi-linear shoreline trajectory.

The shoreline successions are mainly sandy as indicated by well logs, with predominant cylindrical gamma ray log motifs showing intermediate to high API values that are coherent with shallow marine, nearshore deposits, and funnel patterns associated with low API values that can be attributed do coastal parasequences (e.g., Jennette and Riley, 1996; Cook et al., 1999; Eluwa et al., 2017) (Figs. 10 and 14). Bell-shaped log motifs were identified locally in the Campanian interval, and they may correspond to fining-upward coastal and/or fluvial deposits. The seismic-geomorphologic features identified in the horizons are concentrated in the topsets of shoreline clinoforms and in peaks of amplitude in subhorizontal topset reflectors. These geomorphic features are distinguished by specific characteristics in attribute maps that allow a comparison with analog present-day coastal systems (e.g. Jackson et al., 2010; Nyberg and Howell, 2016) (Fig. 11), especially when well logs are also present. They were grouped into three main associations: strandplain, eroded coast (or degraded shelf), and spit-inlet and lagoon (Tab. 1).

The strandplain association is predominantly sandy, with a surface morphology of linear ridges and swales formed as result of progradation of the barred coast (Heward, 1981). An analog for these deposits occurs in the modern coast of Rio Grande do Sul (Brasil) (Fig. 17). The fluvial deposits from GF3 are not considered here as part of the strandplain association, as they occur landward in relation to GF1 and do not appear to affect or cut through other geomorphic features. Lagoonal deposits (GE5) are not common in strandplain systems but can occur as relicts of older stages of coast evolution with different depositional conditions, prior to the development of the strandplain (e.g., Berton et al., 2019). Coasts intersected by incised valleys are more heterogeneous than the strandplain systems, due to both erosion of previous deposits and to patterns of infilling of the valleys (e.g., Peyton et al., 1998; Higgs et al., 2012).

Analogues of incised valleys can be seen in the modern French coast (Fig. 11), but an example of modern incised fluvial systems cutting through older coastal to shallow marine regressive intervals can be seen in the modern coast of Somalia (Fig. 17). Although this example does not show the development of incised valleys, it can be used to illustrate the lateral compartmentalization of strike-elongated coastal deposits representing potential reservoirs by dip-oriented erosive features. Spit-inlet systems and their associated backbarrier lagoons also represent relatively heterogeneous nearshore systems. The dimensions and net sand content of barrier-island/spit associations and associated deposits are smaller than strandplain systems, and backbarrier lagoonal muddy deposits tend to be more expressive in area

than sandy barrier deposits (Fig. 17). An analogue for such systems can be seen in the modern coast of New Jersey (USA). The geomorphic features that compose the three associations represent internal architectural units that compartment the deposits and affect their reservoir quality.

The architectural units identified through seismic geomorphology can be classified in hierarchical terms, following the scheme proposed by Vakarelov and Ainsworth (2013). Each horizon is part of a higher hierarchical level (short-term stratigraphic cycle, such as a parasequence or T-R cycle) and includes one or more Element Complex Assemblage or Element Complex Assemblage Set. This could be represented, for instance, by a strandplain association in a Campanian topset reflector. The geomorphic features described in the horizons (GFs) correspond to Element Complexes, such as the beach-ridge sets that compose most of the strandplain systems. Internal features in the limit of seismic resolution are thus interpreted as Elements, representing the lower hierarchical level. This is the case of linear beach ridges or interstrand meandering channels. The Elements and Element Complexes potentially affect fluid flow in a reservoir but might be hard to recognize in subsurface data (Vakarelov and Ainsworth, 2013). The understanding of the controls on its distribution therefore leads to the prediction of heterogeneities that affect reservoir quality.

7.5.1 Autogenic and allogenic controls on reservoir architecture

Short-term, high order stratigraphic cycles (4th order or higher) are often associated with allogenic controls that result in variations in the accommodation/supply ratio and in the formation of parasequences or T-R cycles (van Wagoner et al., 1988; Catuneanu, 2002; Catuneanu et al., 2009; 2011; Catuneanu and Zecchin, 2013; Zecchin and Catuneanu, 2013), affecting sediment distribution in the shallow marine to coastal domain (e.g. Hampson et al., 2008; Catuneanu et al., 2009; Ainsworth et al., 2011; Phelps et al., 2018). The thickness of those cycles is in the order of m to tens of m, and they usually extend for several kms along dip to tens of km along strike, making them the optimal units to be identified in both seismic and well data (e.g. Cook et al., 1999; Hampson and Storms, 2003; Jackson et al., 2009; Ainsworth, 2010). These dimensions are also ideal to serve as inputs for static reservoir models in the petroleum industry (e.g., Kjønsvik et al., 1994; Ciammetti et al., 1995; Ainsworth, 2005; Graham et al., 2015; Adelu et al.,

2019). The short-term stratigraphic cycles are therefore the basic units for studies of buried nearshore deposits (e.g., Cook et al., 1999; Hampson and Storms, 2003; Ainsworth, 2010).

Such short-term cycles can be interpreted in subsurface through detailed seismic analysis and well correlation (e.g., Jennette and Riley, 1996; Cook et al., 1999; Hampson and Storms, 2003; Jackson et al., 2009; Olsen et al., 2017; Niazi et al., 2019), and used to predict the type of coastal deposit and its stacking patterns (e.g., Boyd et al., 1992; Posamentier and Morris, 2000; Catuneanu et al., 2011; Steel and Milliken, 2013). However, the interplay between autogenic controls such as wave, tidal and fluvial processes influences depositional architectures in coastal successions (Heward, 1981; Reinson, 1984; Ainsworth et al., 2011), and cannot be assessed in conventional 2D seismic and well log analyses. Such variability of controls on nearshore deposition often results in compartmentalization by both inter-parasequence heterogeneities (*sensu* Ainsworth, 2010) such as marine flood-related continuous shales, and intra-parasequence heterogeneities (inter-sand body; *sensu* Ainsworth, 2010) such as confined interstrand muddy sediments or coal deposits (e.g., Hampson et al., 2008; Jackson et al., 2010; Berton et al., 2019). These heterogeneities affect fluid flow and increase the uncertainty regarding the connectivity of sand bodies below seismic resolution (e.g., Jennette and Riley, 1996; Cook et al., 1999; Jackson et al., 2009; Phelps et al., 2018).

A combination of studies of clinoform rollover migration trends, well log interpretation, and the comparison between geomorphic features identified through seismic geomorphology and the architecture of present-day coastal analogues can, in the other hand, be useful for evaluating the influence of both allogenic and autogenic controls on nearshore deposition, and their consequences for coastal deposit architecture in subsurface (e.g., Jackson et al., 2010; Ainsworth et al., 2011; Hampson et al., 2018). This was the base for the assessment of the depositional context and main autogenic controls that affected deposition in the studied intervals in Santos Basin. The coastal deposits identified in seismic horizons were classified based on the scheme proposed by Ainsworth et al. (2011) to assess autogenic controls on nearshore successions, and on the classification proposed by Vakarelov and Ainsworth (2013) for the architectural hierarchies in coastal systems.

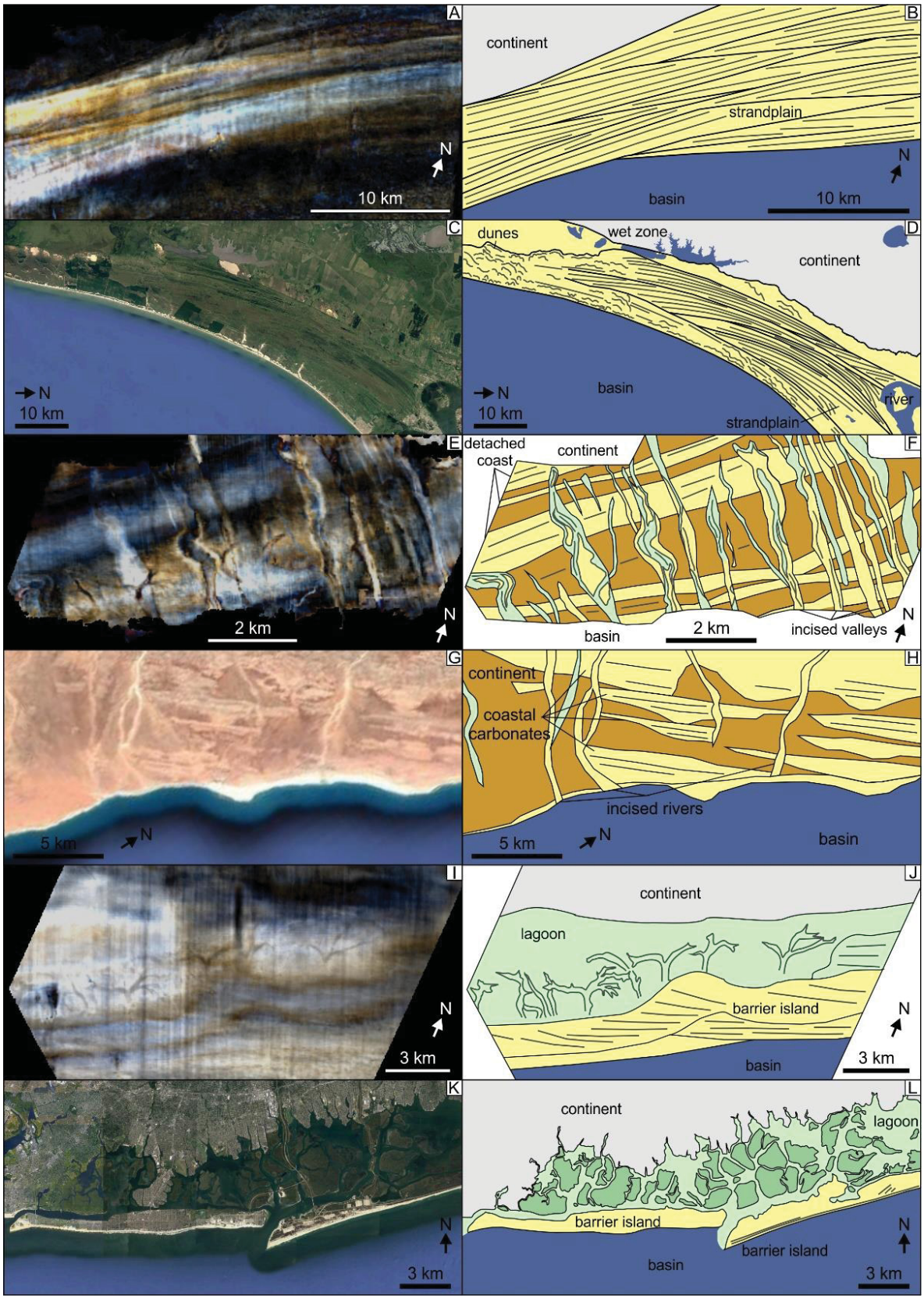

Figure 17: Comparison between nearshore deposits interpreted through seismic geomorphology (spectrally-decomposed horizons) and modern coastal systems. The geometry and composition of a strandplain interpreted in horizon HC01 (A/B) is comparable to a strandplain system in the coast of Rio Grande do Sul, Brazil (C/D). Incised valleys cutting through older coastal deposits in horizon HE09 (E/F) are comparable in terms of geometry and distribution of potential reservoir bodies with modern fluvial incisions cutting through Pleistocene coastal deposits in the coast of Eyl, Somalia (G/H). A transgressive coastal system with backbarrier lagoon interpreted in horizon HE05 (I/J) is compared with modern barrier-island and lagoon system in the coast of New Jersey, USA (K/L).

7.5.1.1 Normal-regressive deposits in the Campanian interval

The Campanian interval depicts the predominance of ascending to slightly ascending sub-horizontal delta-scale clinoform trajectories, coherently with a period of nearshore progradation associated with normal regressions. This trend was also observed in well logs, as the most common log facies are cylindrical and bell, indicating progradational to aggradational sets (Fig. 10, 14). Some of the horizons with patterns interpreted as strandplains are associated with shoreline clinoforms, and the most continuous along dip are the ones associated with predominantly flat trajectories of delta-scale clinoform rollovers. These flat trajectories result in relatively continuous topset reflectors that record progradation of the strandplain for up to 7 km, while in predominantly ascending trajectories the strandplains are considerably smaller (up to 3.5 km along dip).

The predominantly flat trajectories are related to periods of low accommodation/supply ratio, and strandplains are expected to be sandier and more homogeneous than the ones associated with ascending trajectories, which can be capped by muddy offshore deposits from the next parasequence (Ainsworth, 2010; Ainsworth et al., 2011). The extension along dip is also higher than in strandplain systems associated with ascending trajectories, resulting in larger deposits encompassing several amalgamated beach-ridge sets/complexes (e.g., Reynolds, 1999; Jackson et al., 2010). Although these differences might be caused by the proximity of source areas such as deltas controlling the intensity of progradation (Catuneanu et al., 2009; Catuneanu and Zecchin, 2013), no evidence of sediment input points was found in the study area, and the controls on the stacking patterns and dip extension of such intervals are therefore interpreted as allogenic.

Despite the differences in size from strandplains associated with predominantly flat and predominantly ascending trajectories, the geomorphic features identified in the two contexts are essentially the same (GF1, GF2 and GF4). Their geometry and distribution along strike indicate a major control of longshore wave processes in the formation of linear to slightly lobate shorelines (e.g., Hampson et al., 2008; Ainsworth et al., 2011; Nyberg and Howell, 2016) (Fig. 17). The combination of positive sediment budget during the regression and wave-dominated conditions is favorable for the development of strandplains (Boyd et al., 1992), and a single strandplain may be composed of several progradation stages that result

in a patchwork of strike-oriented linear sandy beach ridges with different directions (e.g. Jackson et al., 2010) (Fig. 17). These stages are associated to autogenic factors such as changes in wave climate or changes in the position of sediment input points (Rodriguez and Meyer, 2006; Hampson et al., 2008).

The distribution of internal geomorphic features that apparently are not directly related to wave processes (i.e., interstrand marshes from GF2 and their internal fluvial channels) is controlled by the morphology of the strandplain, following the depositional architecture imposed by beach-ridge sets/complexes. Its major effect is the concentration of muddy sediment in strandplain swales parallelly to the strike architectural trend (e.g., Jackson et al., 2010; Berton et al., 2019). Backshore meandering fluvial systems also seem to have small influence on the coast, as their presence is not associated to any changes in geometry or dimension of the strandplain (Fig. 12). Therefore, the Campanian strandplain systems are interpreted as wave-dominated, fluvially-influenced (*sensu* Ainsworth et al., 2011).

7.5.1.2 Forced-regressive deposits in the Eocene interval

The Eocene interval is dominated, as observed in seismic sections, by descending clinoform rollover trajectories that have been previously attributed to long-term forced regressions (Moreira et al., 2001; Berton and Vesely, 2016a). Such conditions result in a low potential of preservation of delta-scale topset clinoforms and associated coastal to shallow marine deposits due to subaerial exposure and erosion (e.g., Posamentier and Morris, 2000; Hampson and Storms, 2003; Steel and Milliken, 2013). Nearshore successions are thus unlikely to be associated with strong descending clinoform rollover trajectories (e.g., Berton and Vesely, 2016a; Patruno and Helland-Hansen, 2018), but might be preserved during shorter-term forced regressions and/or forced regressions associated with relatively low amplitude base level falls. Clear geomorphic elements in horizons associated with descendent trajectories were identified only in slightly descendent, almost flat clinoform rollover trajectories (Fig. 14). Even though, these geomorphic elements are either erosive (GF6) or truncated by erosive features (GF5) (Fig. 11).

GF5 is interpreted as detached shoreline deposits formed in the onset of a regressive trend as indicated by gamma ray log trends (Fig. 15). Its linear strike-parallel geometry is an indirect indicator of wave dominance in the coast, but GF5 occurrence is too local to allow an interpretation of the influence of fluvial and/or tidal processes. Detached shoreline sand bodies such as the ones from GF5 have been previously

associated with forced regressions (Posamentier and Morris, 2000; Catuneanu, 2006; Catuneanu et al., 2011), and the resultant deposits are often compartmentalized by internal incisions and surfaces of marine erosion (e.g., Hampson and Storms, 2003). They are also partially eroded and laterally compartmented by shoreline-transverse incised valleys (GF6) interpreted as the result of shelf erosion during forced regressions (e.g., Peyton et al., 1998; Reynolds, 1999) (Fig. 11), coherently with the descending clinoform rollover trajectories. During subsequent base level rises these valleys were filled and older coastal deposits between them were preserved (e.g., Peyton et al., 1998; Higgs et al., 2012). The meandering elements within the incised valleys indicate fluvial deposition, but the infill patterns of incised valleys between the end of a forced regression and onset of base level rise indicates that tidally-influenced deposition might also be expected (e.g., Mehrabi et al., 2019).

7.5.1.3 Transgressive deposits in the Eocene interval

During transgressions, coastal to shallow marine systems gradually migrate landward following base level rise, while older deposits are subjected to wave erosion (e.g., Heward, 1981; Reynolds, 1999). This results in a relatively low potential of preservation of coastal deposits and higher preservation of backbarrier deposits formed in the end of the transgressive cycle (Heward, 1981). These conditions are favorable for the formation of extensive backbarrier lagoons and flood tidal deltas, while partially-preserved coastal barrier deposits are often truncated by a wave ravinement surface and confined between basal muddy lagoon deposits and upper muddy offshore deposits (e.g., Reynolds, 1999). In Eocene Santos Basin, seismic patterns attributed to nearshore successions were identified only in the uppermost reflectors within a transgressive trend, and were interpreted as spit- and/or barrier island-related sand bodies and associated lagoons (Fig. 17) whose preservation might have been conditioned by allogenic factors in the end of a transgressive trend and onset of a normal regression. The development of linear barrier islands/spits is coherent with wave-dominated conditions on the coast with oblique accretion of the coastal barrier controlled by longshore currents. However, the fan-shaped features composed by distributary channel elements are interpreted as flood tidal deltas that indicate significant tidal influence. The development and preservation of flood tidal deltas are conditioned to the occurrence of tidal processes through channels such as inlets connecting the lagoon with the sea (Heward, 1981). Their presence therefore indicates that this nearshore system was wave-dominated and tidally-influenced.

7.5.2 Implications for Reservoir Quality

The interpretation of short-term stratigraphic cycles from well logs and well correlation is commonly used to predict characteristics such as size, stacking patterns, and architecture of coastal reservoirs (e.g., Jennette and Riley, 1996; Cook et al., 1999; Jackson et al., 2009; Olsen et al., 2017; Niazi et al., 2019), especially when seismic data is not available or have low resolution to image the reservoir (e.g., Ainsworth et al., 2016; Olsen et al., 2017). However, unpredicted reservoir behavior during production stages shows that conceptual models based on well and 2D seismic data might be too simplistic and not able to capture heterogeneities and compartmentalization caused by autogenic controls during deposition (e.g., Hamilton, 1995; Cook et al., 1999; Cross et al., 2015; Phelps et al., 2018). In this sense, seismic-geomorphologic interpretations allow a level of detailing of the reservoir that cannot be reached exclusively from well correlation, resulting in more confidence in the architecture, size and composition of the reservoir, as well as in fewer uncertainties in the distribution of heterogeneities within it (e.g., Dreyer et al., 2005; Jackson et al., 2010; Eluwa et al., 2017).

All coastal sandy deposits interpreted in the study area can potentially configure petroleum reservoirs, but their architecture and compartmentalization differ from each other (Fig. 17). In order to evaluate this compartmentalization, an approach based on the classification of Ainsworth (2010) for scales of reservoir heterogeneity will be used. The inter-parasequence scale of compartmentalization considers the connectivity between short-term stratigraphic units (4^{th} or higher-frequency cycles). These units are internally composed by sand bodies that represent reservoir units. The inter sand-body scale of compartmentalization considers the connectivity between reservoir units in the scale of the GFs described through seismic geomorphology (Element-Complex to Element-Complex Assemblage scales from Vakarelov and Ainsworth, 2013). The intra sand-body scale considers heterogeneities within the reservoir units, seen in the GFs as internal elements in the limit of seismic resolution. This scale also encompasses smaller structures that can only be resolved from analogs or cores.

In terms of reservoir size and homogeneity, strandplain successions formed in highstand conditions have the best potential to configure thick and extensive reservoirs (Reynolds, 1999). The reservoir units would be represented by GF1, characterized by laterally-continuous sandy wedges formed by the

progradation of the coast controlled by longshore currents (Fig. 11). The small ridge elements that mark the surface morphology of GF1 indicate that they are internally composed by beach-face clinoforms (subseismic, only visible in outcrops and high-resolution subsurface data) and other associated subtidal forms (e.g., Hampson et al., 2008; Berton et al., 2019) (Fig. 18). The most expressive heterogeneities in this intra sand-body scale are related to the transition from sandy foreshore to muddy inner shelf deposits within the beach-face clinoforms (Fig. 18). In the inter sand-body scale, the most expressive heterogeneities would be related to concentrations of muddy sediment within interstrand swales (GF2) and truncation surfaces between beach-ridge sets (e.g., Hampson et al., 2008; Jackson et al., 2010; Berton et al., 2019). These surfaces do not represent proper barriers to the flow, but might mark the superposition of reservoir facies (i.e., upper shoreface facies) by non-reservoir facies (i.e., lower shoreface facies).

Inter sand-body heterogeneities are also influenced by the relation of accommodation and supply, as flatter trajectories result in more extensive deposits along dip with better horizontal connectivity. Nearshore successions from ascending trends are not only smaller, but more heterogeneous vertically, as there is more superposition of reservoir by non-reservoir facies (Fig. 18). The inter-parasequence scale of compartmentalization is also strongly influenced by allogenic controls. High frequency stratigraphic cycles (5^{th} order) might result in the formation backbarrier lagoons and/or spit-inlet systems intercalated with the strandplain (e.g., GF4), representing expressive and continuous heterogeneities below seismic resolution (Fig. 18) (e.g., Berton et al., 2019). They can act as barriers to the flow or influence fluid flow circulation patterns within a reservoir unit.

Shoreline deposits formed in forced-regressive conditions such as in the Eocene interval are more discontinuous along dip and strike (Fig. 17). Both detached shoreline deposits (GF5) and incised valley-fill deposits (GF6) can potentially act as reservoirs, with different architecture and heterogeneities. The internal configuration of the forced-regressive nearshore systems (intra sand-body scale of heterogeneity) is of amalgamated sand bodies separated by internal barriers and baffles related to the superposition of different truncation surfaces (Hampson and Storms, 2003; Ainsworth, 2010; Ainsworth et al., 2011; Catuneanu et al., 2011; Steel and Milliken, 2013) (Fig. 12). They are usually disconnected along dip (Steel and Milliken, 2013) and truncated along strike by fluvial incisions, resulting in a very low inter sand-body connectivity. The inter-parasequence connectivity might be enhanced by incised fluvial systems that

vertically connect different reservoir levels (Fig. 18), but this connectivity depends on the composition of the infill sediment trapped in the valleys. The incised valleys itself also have potential as reservoirs if filled by sandy deposits, although they are laterally restrict (Reynolds, 1999). Its internal composition, however, tend to be complex and heterogeneous, with the transition of fluvial basal deposits to tidal upper deposits often resulting in a patchy and complex distribution of inter and intra sand-body heterogeneities (e.g., Jennette and Riley, 1996; Tayyab and Asim, 2017; Mehrabi et al., 2019).

Restrict sand bodies related to transgressive settings, such as spit-inlet or barrier island deposits also have potential as reservoirs, and in the Campanian Jureia Fm. SW of the study area this type of deposit configure reservoirs in the Merluza field (Sombra et al., 1990; Anjos et al., 2003; Chang et al., 2008). These deposits are expected to be relatively heterogeneous, with intra sand-body compartmentalization related to the influence of tidal processes during deposition (e.g., Dreyer et al., 2005; Jackson et al., 2010; Berton et al., 2019) (Fig. 18). The inter sand-body connectivity also tend to be low, as the spit/barrier island successions have restrict distribution along dip and are intersected by tidal channels along strike (Fig. 18). The inter-parasequence compartmentalization is generally related to the inter-bedding of sandy spit/barrier island deposits with muddy lagoonal and offshore deposits (e.g., Hampson and Storms, 2003). Retrograding nearshore successions deposits configure important reservoirs elsewhere (e.g., Dreyer et al., 2005; Olsen et al., 2017; Niazi et al., 2019), but in Eocene Santos Basin they are too small and have little stratigraphic expressiveness to configure potential reservoirs, probably because transgressions represent only short-term trends in a period dominated by regressions (Moreira et al., 2001; Berton and Vesely, 2016a) (Fig. 13).

7.6 Conclusions of the Paper

The three-dimensional seismic interpretation of topset Campanian and Eocene horizons in Santos Basin resulted in the identification of strandplains, incised valleys, detached shoreline deposits, lagoons and spit/barrier island systems in subsurface. The integration of seismic geomorphology with high-resolution stratigraphy from 2D seismic and well log interpretation represents more confidence for reservoir characterization. It leads not only to the definition of allogenic controls on nearshore architecture, but also allows the evaluation of autogenic controls that often result in sub-seismic compartmentalization.

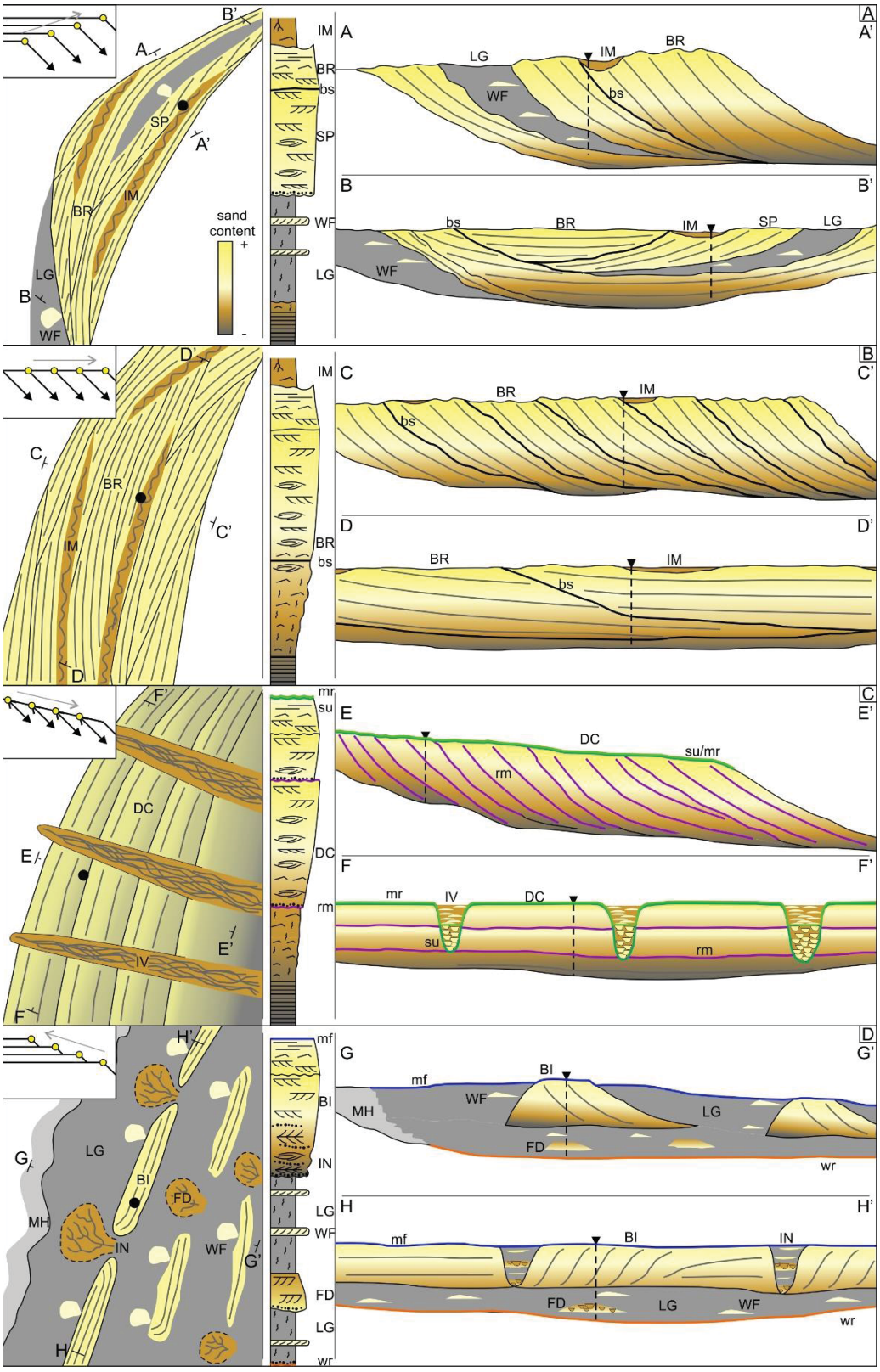

Figure 18: Architecture, sediment distribution, facies and main stratigraphic surfaces in wave-dominated nearshore systems in relation to the trends of delta-scale clinoform rollover trajectories. In (A), a strandplain developed in a normal-regressive period with ascending trend. The strandplain in (B) is also normal-regressive, but associated with a flat clinoform trajectory. In (C), a detached coastal system is cut by incised valleys during a period of descending base level. In (D), a transgressive trend results in the development of barrier-islands and lagoon. BI – barrier island, BR – beach-ridge set, DC – detached coastal deposits, FD – flood tidal delta, IM – interstrand marsh, IN – inlet, IV – incised valleys, LG – lagoon, MH – marsh, SP – spit, WF – wahsover fan; bs – limit between beach-ridge sets, mf – maximum flooding surface, mr – maximum regressive surface, rm – regressive surface of marine erosion, su – subaerial unconformity, wr – wave ravinement surface.

The interpretation of geomorphic features and its internal elements was thus useful to estimate the composition, distribution of heterogeneities and intra-parasequence connectivity of potential reservoirs. These results, compared with modern analogues, can potentially be used as inputs for flow trend maps, for the determination of reservoir draining strategy, and for the estimation of different types of heterogeneities that might affect oil recovery.

All types of coastal systems identified in the Santos Basin subsurface are interpreted as wave-dominated, although tidal and fluvial influences could also be identified. Among these deposits, the strandplain systems associated with flat to slightly ascending trajectories were the ones with best reservoir potential. The regressive conditions with low aggradation result in a homogeneous deposit that is not only elongated along strike, but also extends for several kms along dip. The linear trajectory implies in a good continuity of shallow deposits in the coastal domain, such as sandy upper shoreface to foreshore deposits that are expected to have good sorting and high permo-porosity. Possible heterogeneities from seismic-geomorphologic analysis include the contact between beach-ridge sets and muddy interstrand mashes concentrated in the upper part of the reservoir, both with a strike-elongated distribution that potentially compartmentalize the reservoir along dip. Strandplain systems within ascending trajectories tend to be smaller along dip and more heterogeneous vertically, with the superposition of reservoir units by non-reservoir intervals. Reservoir potential is considerably lower in forced-regressive and transgressive trajectories, resulting in more heterogeneous and compartmented nearshore systems. In Eocene Santos Basin those systems are still wave-dominated, but have a higher influence of fluvial and tidal processes that result in sub-seismic heterogeneities.

8. Quaternary coastal plains as reservoir analogs: wave-dominated sand-body heterogeneity from outcrop and ground-penetrating radar, central Santos Basin, southeast Brazil

8.1 Introduction

Ancient wave-dominated coastal systems are traditional targets for the oil industry, as they often contain sand-rich, laterally-continuous deposits with good reservoir potential (e.g., Howell et al., 1996; Catuneanu, 2006; Rahman et al., 2014; Raef et al., 2015). Subsurface prediction of heterogeneities within these reservoirs is commonly based in Quaternary analogs, using the association between the internal character, geometry, distribution and associations of depositional elements and their evolution through time for the reduction of uncertainties during reservoir modeling (e.g., Corbeanu et al., 2001; Ainsworth et al., 2011; Colombera et al., 2016). Studies on Quaternary coastal successions are traditionally carried out through the analysis of exposures in trenches, cores or, when available, outcrops (e.g., Martin and Suguio, 1975; Hine, 1979; Lessa et al., 2000; Davis Jr et al., 2003; Tamura et al., 2003; Tomazelli and Dillenburg, 2007; Martins et al., 2018). The goal at this analysis is to understand sedimentation processes resulting from complex interactions between sediment balance, base-level oscillations, climate, wave and tidal regimes that act during the construction of a coastal system, and how they affect the depositional architecture through time (Heward, 1981; Niedoroda et al., 1984; Reinson, 1984; Raynal et al., 2009). However, these methods commonly result in local information that may be difficult to correlate with the geometry and architecture of depositional units, a mandatory step for reservoir modeling.

Sedimentological data and non-invasive geophysical methods such as ground-penetrating radar (GPR) can therefore be useful for modern studies on Quaternary coastal successions, as it allows the evaluation and prediction of the internal and external character of sedimentary bodies in the shallow subsurface (e.g., Barboza et al., 2009, 2011, 2013, 2014a, 2018; Clemmensen and Nielsen, 2010; Costas and Fitzgerald, 2011; Dillenburg and Barboza, 2014; Leal et al., 2016; Rockett et al., 2016; Rosa et al., 2016). GPR resolves well dm- to km-scale depositional units and bounding surfaces (Harari, 1996; Corbeanu et al., 2001; Neal, 2004). Field data and facies characteristics, on the other hand, can be used to predict the geological expression and origin of reflector patterns identified in GPR interpretations (Corbeanu et al., 2001; Neal, 2004; Shan et al., 2015; Tamura et al., 2016). This integrated approach leads ultimately to a

multi-scale view of depositional systems, from the internal character of a single lithosome at a mesoscale (10^1–10^2's mm; Dreyer, 1992) to the geometry of depositional elements at a macro to megascale (10^{-1}–10^2's m; Dreyer, 1992; e.g., Corbeanu et al., 2001; Hampson et al., 2008; Liu et al., 2016). Regional correlation of depositional units and bounding surfaces in radargrams ultimately allows assessment of the regional framework of a coastal plain at a megascale (km-scale; Dreyer, 1992), which approximate with the scale detected by conventional seismic data. In addition, classic concepts of seismic stratigraphy can be applied in GPR analysis, providing high-resolution stratigraphic schemes for Quaternary successions to assess relatively high-frequency base-level oscillations (up to 10^5 years; e.g., Hampson et al., 2008; Rosa et al., 2011, 2017; Liu et al., 2016).

The Quaternary succession of central Santos Basin in the Paraná coastal plain (south Brazil) is the object of the present study. These deposits are exposed in sand pits and are very well imaged by GPR surveys, allowing facies in outcrops to be used to help interpret depositional/erosive features and bounding surfaces observed in radargrams. GPR can thus be used as a key tool to understand the architecture of wave-dominated coastal systems in subsurface. The succession is associated with a period of base-level oscillations due to climate changes (Angulo and Suguio, 1995; Angulo and Lessa, 1997; Angulo et al., 2002, 2006), resulting in the formation of strandplains, lagoons, estuaries and spit-inlet systems that imprint a high degree of heterogeneity to the coastal-plain deposits. In subsurface reservoir analogs, such heterogeneities result in an internal compartmentalization that differs from the traditional framework of coastal successions that portrays strike-elongated and relatively homogeneous sand bodies (e.g., Reynolds, 1999; Ainsworth, 2005; Zhuo et al., 2014), being comparable with internally-compartmentalized coastal sand bodies that act as petroleum reservoirs (e.g., Cook et al., 1999; Jackson et al., 2009; Cross et al., 2015).

8.2 Geological Setting

The Santos Basin is located on the southeastern Brazilian continental margin, and is delimited to the north by the Cabo Frio high and to the south by the Florianópolis high (Fig. 19). Basin evolution is associated with the breakup of Gondwana in the early Cretaceous and the consequent opening of the South Atlantic Ocean, with the establishment of open-marine passive-margin conditions from the Albian

to present (Moreira et al., 2007). The studied interval comprises the onshore Quaternary record in the central domain of the basin (Paraná state). This coastal province can be divided into two main geological domains: the Pre-Cambrian igneous/metamorphic basement with Jurassic-Cretaceous intrusions, and the Cenozoic sedimentary cover (Angulo, 1992, 2004) (Fig. 19). The Quaternary sedimentary succession includes continental deposits such as alluvial fans, fluvial and colluvial deposits, and coastal systems such as strandplains and estuarine deposits (Bigarella, 1946; Castro et al., 2008). The coastal plain can be subdivided into Pleistocene and Holocene barriers and paleolagoonal/paleoestuarine deposits, which are associated with two main transgressive-regressive stages during the late Pleistocene and Holocene, respectively (Souza et al., 2012). The Pleistocene succession reflects a period of positive sediment budget and base-level fall that followed the sea-level maximum at 120 ky BP (Marine Isotope Stage 5e), resulting in the sand-rich progradational successions that compose the Pleistocene paleostrandplain (Angulo and Lessa, 1997).

The regressive trend was interrupted after the last glacial maximum, when a transgressive phase took place associated with a maximum sea level achieved around 5 to 6 ky BP (Angulo and Suguio, 1995; Angulo and Lessa, 1997; Angulo et al., 2006). This transgression resulted in the partial erosion of Pleistocene deposits and generation of a regional wave-ravinement surface (Souza, 2005). A second regressive phase was established after the Holocene transgression, forming a highstand to falling stage, progradational, sand-rich Holocene strandplain and, ultimately, the present-day beaches (Lessa et al., 2000; Angulo et al., 2006; Souza et al., 2012). This phase is regarded as a wave-dominated setting strongly influenced by high-energy events such as storms (Souza, 2005; Souza et al., 2012). The Holocene interval is mainly composed of very fine- to fine-grained quartzose sand with subordinate fractions of heavy minerals. Shell fragments, shells, plant debris and wood fragments are common, as are trace fossils of *Ophiomorpha* attributed to *Callichirus major* (Souza, 2005; Souza et al., 2012; Bisi, 2015). The framework of the present-day Paraná coast comprises the barred coastal plain and modern estuarine complexes, composing a predominantly wave-dominated system under a microtidal regime with mean tidal amplitudes of 1.4 m at the open coast and 1.7 m in Paranaguá Bay (Marone and Jamiyanaa, 1997).

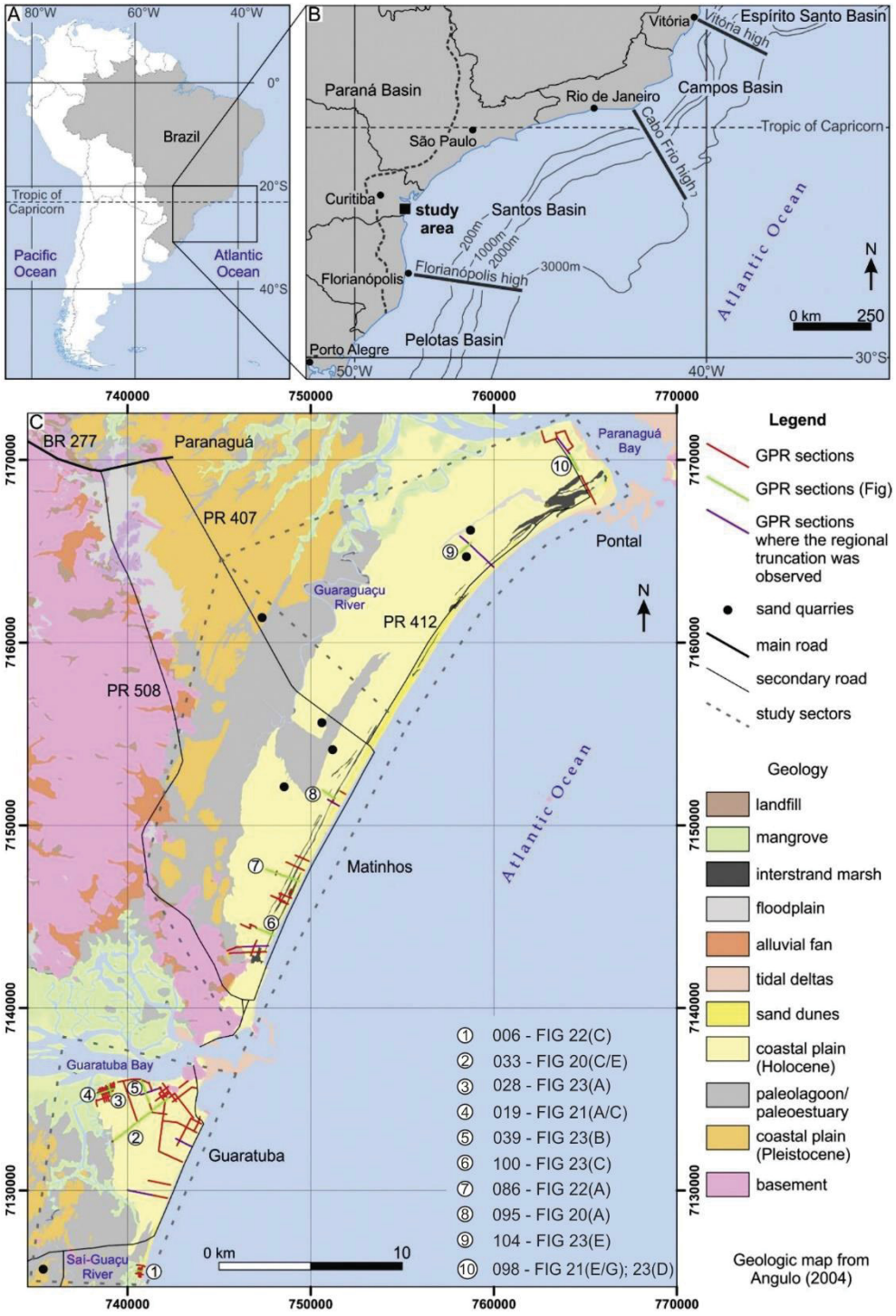

Figure 19: Location of Santos Basin in the Brazilian continental margin (A, B), with (C) geologic map at the Paraná coastal plain (Angulo, 2004). The study area was subdivided in three sectors comprising the Holocene barrier, paleolagoonal/paleoestuarine deposits and part of the Pleistocene barrier, which were studied through the analysis of outcrops in sand quarries (black dots) and GPR sections (red/green lines). The number and location of sections shown in figures are depicted in (C).

8.3 Database and Methods

In order to evaluate the areal distribution of facies and radarfacies, the area was subdivided into three sectors: northern (Pontal), central (Matinhos), and southern (Guaratuba) (Fig. 19). Pleistocene deposits

are exposed in two sand pits (Fig. 19), in outcrops with vertical dimensions reaching 4 m and extent of up to 40 m. They were described through facies analysis, vertical stratigraphic profiles, and photomosaics. The facies were defined with base on descriptive criteria, such as sediment composition, grain size, texture, internal sedimentary structures, body and trace fossils, bed thickness, form and contacts. Previous results from Lessa et al. (2000), Souza (2005), Souza et al. (2012) and Bisi (2015) in exposures of Holocene deposits in Pontal and Matinhos were incorporated here to interpret radar data altogether with the results of the Pleistocene deposits. These include facies description and interpretation in outcrops and cores, vertical profiles and photomosaics.

Radar database includes 108 GPR sections (total length exceeds 77 km) assembled on the Holocene regressive barrier, covering an area of approximately 310 km^2 (Fig. 19). They were acquired with a 200 MHz antenna from Geophysical Survey Systems Inc. (GSSI™ SIR-3000), using the Common Offset method according to Barboza et al. (2014b). During acquisition a dielectric constant of 10 was used, corresponding to an average velocity of 0.085 m/ns (Daniels et al., 1995). This constant was validated by comparison with borehole data from another coastal plain with similar progradational character (Dillenburg et al., 2011). The altimetric precision and the spatial position of the radargrams were assessed by the use of a Trimble® PROXRT GNSS unit with GLONASS option (datum: WGS84) during acquisition. The maximum depth of observation is often up to 15 m, in a few cases <10 m, and exceptionally exceeding 25 m. Depth control in the study area was from the correlation between stratigraphic surfaces interpreted in the sections, core data from previous research (Lessa et al., 2000; Souza, 2005) and exposures in sand quarries. GPR processing using the Radan™ software included background removal, pass band filters (350 MHz for low frequencies and 100 MHz for high frequencies), range gain and topographic correction.

The GPR interpretation routine was based on the recognition of radarfacies (i.e., zones with similar reflection patterns with respect to geometry, continuity, amplitude, and frequency; Neal et al., 2002; Neal, 2004), and on the recognition of reflector termination patterns such as downlap, onlap and truncation and their associated key stratigraphic surfaces. This interpretation allowed the correlation of stratigraphic surfaces and radarfacies between different sections in such a way that a three-dimensional representation of the depositional architecture was possible. The geological interpretation of the reflector patterns and bounding surfaces was based on their geometric characteristics, internal configuration, termination

patterns and stratigraphic position, allowing facies identified in outcrops to be used as a base to predict the internal character of the radarfacies (e.g., Corbeanu et al., 2001; Neal, 2004).

8.4 Results

8.4.1 Radarfacies

Thirteen radarfacies were described in the study area (Table 2). The most common reflector patterns are related to seaward-dipping tangential and sigmoidal clinoforms that are usually observed in the shallower parts of the radargrams (RF2 and RF3) (Figs. 20, 21). The other radar signatures are less common, with variable frequency and distribution. Some of the radarfacies are only differentiable by their external geometry, allowing the definition of different radarfacies with the same internal reflectors patterns (e.g., RF7-RF10) (Figs. 20–22; Table 2). The spatial relations and types of contacts between radarfacies were also taken into account during interpretation, as they support the attribution of geological significance and temporal relations. These aspects were also the base for the definition of three associations of radarfacies.

The first association was identified in all three sectors, and is mainly characterized by the seaward progradation of low-angle clinoforms with internal truncations (RF2) (Fig. 20). The variability of reflectors patterns is relatively high, configuring radarfacies that only occur in the uppermost part of radargrams (RF1/RF2) and radarfacies that only occur below the low-angle clinoforms. RF2 occurs in the uppermost part of radargrams, although it is locally overlapped by wavy reflectors from RF1 (Fig. 20). In some of the dip-oriented radargrams, the external mounded form of RF1 configures ridges between which zones with transparent character (RF8) are confined (Fig. 22). In the bottomset domain of RF2, a wide variety of radarfacies are seen, including small-sized clinoforms (RF4, RF5), hummocky reflectors (RF6), and transparent and chaotic zones with irregular limits (RF7, RF11, respectively) (Fig. 20). In the deeper parts of the sections, radarfacies with well-defined geometries become rarer, and chaotic and transparent patterns prevail.

Table 2: List of radarfacies and their characteristics, specific aspects and associations.

Radarfacies	Code	Reflectors Pattern	External Form	Dimensions	Relative Frequency	Specific Characteristics	Association
Sinuous to wavy	RF1	Sinuous/wavy (dip); sinuous/wavy/tangential clinoforms (strike)	Mounded (elongated NE-SW)	1.5 to 4.0 m thick; 40–150 m dip; up to 200 m strike	Moderate	Always observed in the uppermost part of radargrams	Strandplain; Spit-inlet
Low-angle clinoforms	RF2	Tangential to sigmoidal clinoforms (dip); sub-parallel (strike)	Undefined/wedges separated by truncation surfaces	Up to 4.5 m thick; 10–25 m dip; exceed the size of strike sections	Moderate to high	Dips of 1-6° to SE in dip sections, subhorizontal in strike sections; truncated topsets; internal truncation surfaces separates sets of clinoforms with different angles	Strandplain
High-angle channel-fill clinoforms	RF3	Tangential to sigmoidal clinoforms (dip); sigmoidal clinoforms (strike)	Undefined/wedges in dip sections; channelized in strike sections	Up to 7 m thick; up to 60 m dip; up to 20 m strike	Moderate to high	Dips of up to 15° to SE in dip sections, and up to 20° to SW and NE in strike sections; internal truncation surfaces separates sets of clinoforms with different angles in dip sections; downlap on concave-up, high-amplitude truncation surfaces in strike sections (asymmetric, up to 50 m wide and 9 m deep)	Spit-inlet
Small-sized sigmoidal clinoforms	RF4	Sigmoidal clinoforms (only observed in dip)	Undefined	Up to 1.5 m thick; up to 4 m dip	Moderate	Foreset angles of 5-10° to SE; occurs in the toe of RF2	Strandplain
Small-sized tangential clinoforms	RF5	Tangential clinoforms (dip); wavy to tangential clinoforms (strike)	Lenses limited by truncation surfaces	0.5-1.2 m thick; up to 6 m dip; up to 3 m strike	High	Foreset angles of 5-10° predominantly to NW; lenses with up 45 m in dip and 30 m in strike; locally migrate over the bottomset of RF2; decrease in size updip	Strandplain; Spit-inlet
Hummocky	RF6	Concave-convex reflectors (both dip and strike)	Undefined	Up to 1.5 m thick; up to 10 m (both dip and strike)	Low	Locally truncate underlying reflectors	Strandplain; Spit-inlet
Transparent to semi-transparent (undefined limits)	RF7	Transparent to semi-transparent (chaotic) (both dip and strike)	Undefined	Undefined	-		Strandplain; Spit-inlet
Transparent to semi-transparent (wide channels)	RF8	Transparent to semi-transparent (wavy) (both dip and strike)	Channelized	Up to 4 m thick; up to 40 m dip	-	Confined between ridges from RF1; basal surface truncates RF2	Strandplain
Transparent to semi-transparent (small channels)	RF9	Transparent to semi-transparent (only observed in strike)	Channelized	Up to 3 m thick; up to 15 m strike	-	Basal truncation surface	Spit-inlet
Transparent to semi-transparent (wide zones with basal truncation)	RF10	Transparent to semi-transparent (wavy to chaotic) (only observed in dip)	Undefined	Up to 5 m thick; exceed the size of the sections	-	Basal truncation surface	Lagoon
Chaotic to wavy (undefined)	RF11	Chaotic to wavy (both dip and strike)	Undefined	Undefined	High		Strandplain; Spit-inlet
Chaotic to wavy (mounded)	RF12	Chaotic to wavy (only observed in strike)	Mounded	Up to 1 m thick; up to 5 m strike	Low to moderate	Common in the base of the channels from RF3	Spit-inlet
Moderate-sized clinoforms wedges	RF13	Tangential clinoforms (only observed in dip)	Wedges	Up to 2.5 m thick; up to 15 m dip	Low to moderate	Dips toward NW; progradation from the border of RF10	Lagoon

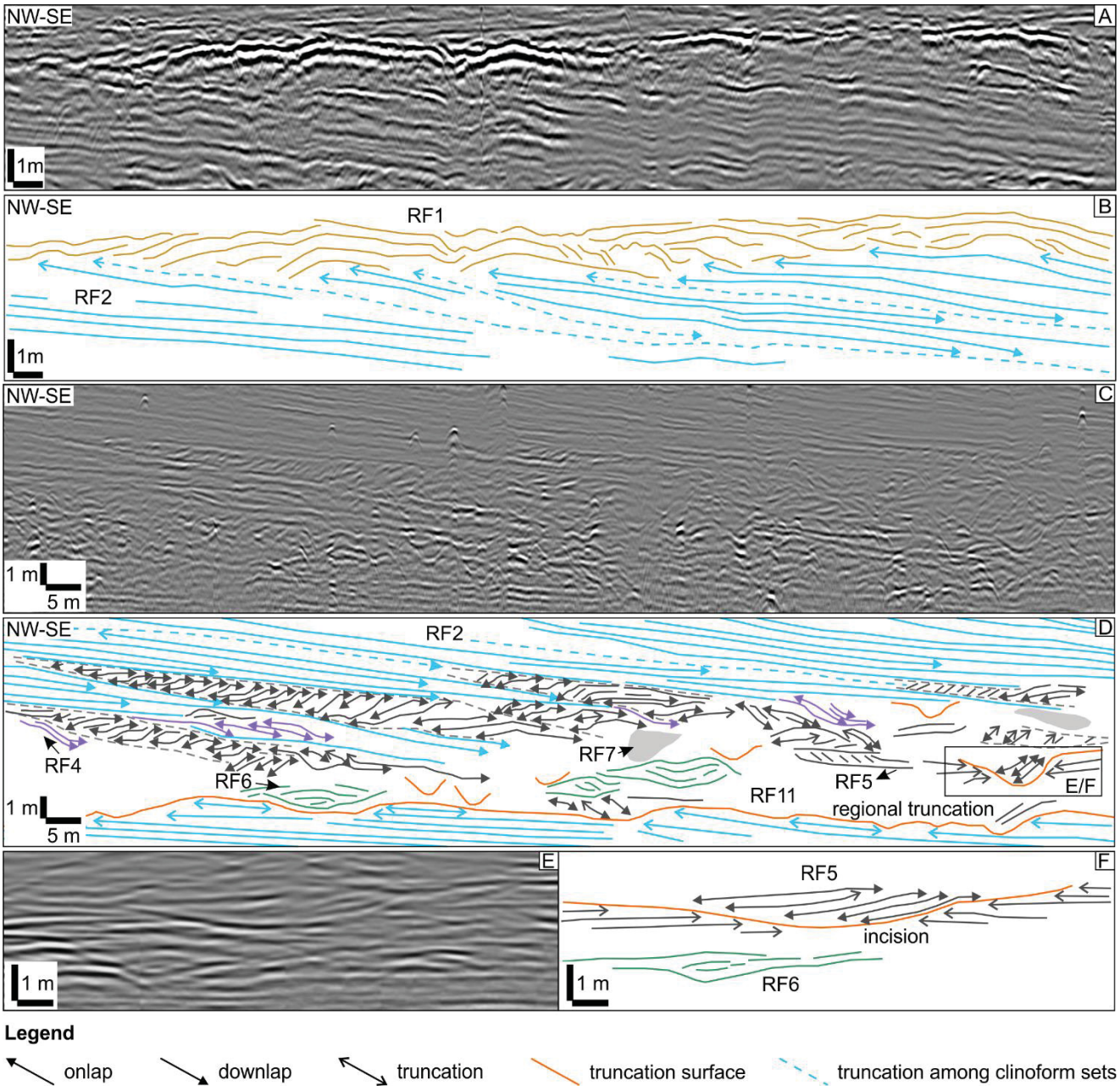

Figure 20: (A, B) Sinuous to wavy reflectors (yellow; RF1) overlay low-angle clinoforms (light blue; RF2) (section 095). (C, D) Low-angle clinoforms (light blue; RF2) overlay lenses of small-sized tangential clinoforms (grey; RF5), conjuncts of small-sized sigmoidal clinoforms (purple; RF4), transparent zones (grey zones; RF7), hummocky reflectors (green; RF6) and chaotic to wavy zones under radar resolution (uninterpreted; RF11) (section 033). Small incisions (erosive base in orange) with internal small-sized clinoforms are also present (detail in E, F). A truncation surface (orange continuous line in C, D) interrupts the uppermost termination of clinoforms in the lower part of the section. This association of radarfacies is attributed to a strandplain context.

The second association was identified in parts of Pontal and Guaratuba sectors. It is represented mainly by high-angle clinoforms (RF3) with seaward-dipping reflectors in dip sections, but also with shore-parallel migration in strike sections (Fig. 21). In dip sections, the radarfacies assemblage at the bottomset of RF3 is similar to the first association, including RF5, RF6, RF7 and RF11. However, in strike sections two different types of radarfacies are observed in association with RF3, including m-scale incisions with internal

transparent character (RF9), and m-scale mounds with internal chaotic character (RF12) onto which RF3 downlaps (Fig. 21).

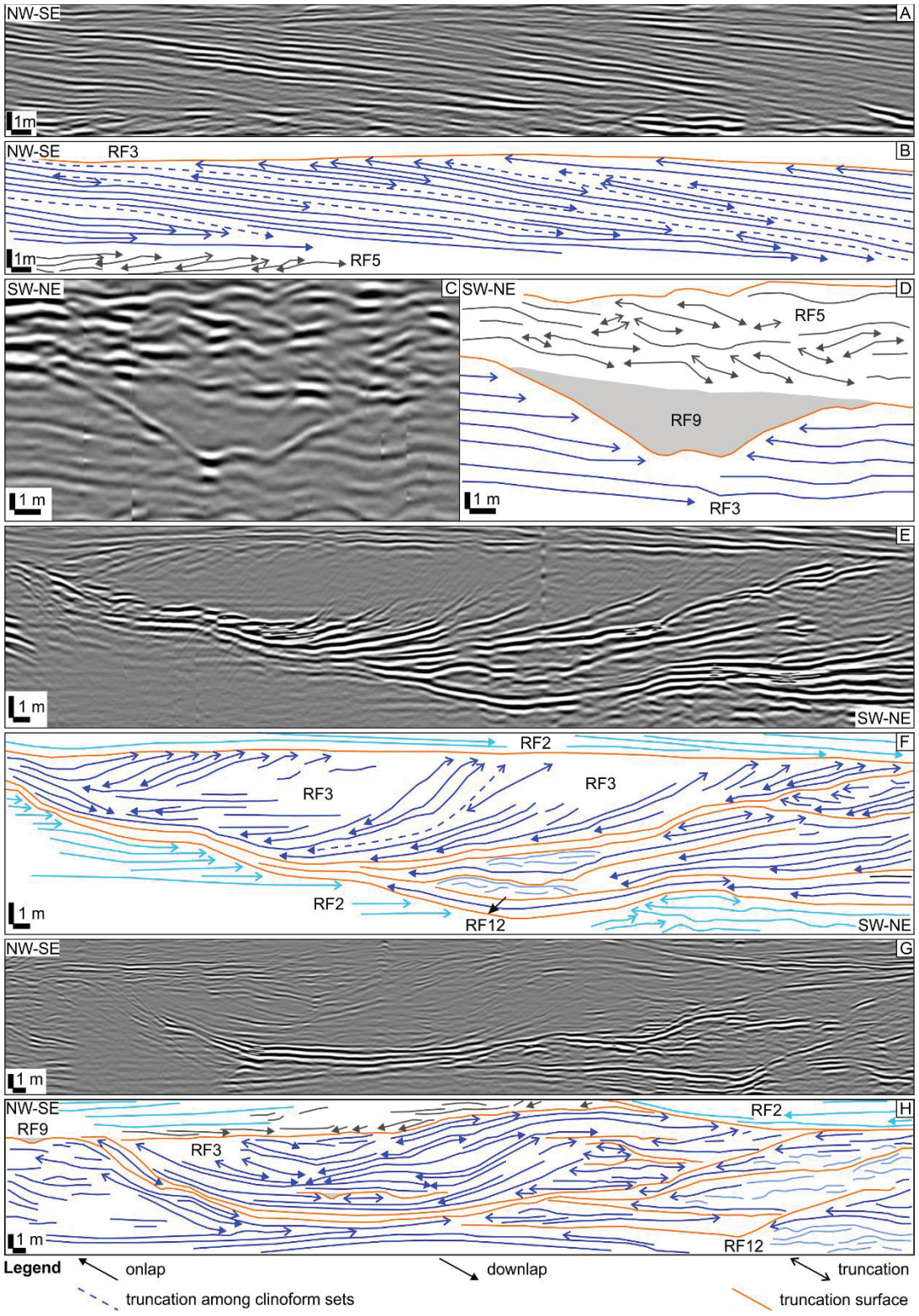

Figure 21: (A, B) High-angle clinoforms (deep blue; RF3) downlap on RF5 in a dip section (section 019). (C, D) Small-sized incisions with internal transparent character (RF9) are associated with larger incisions with internal clinoforms (RF3) (section 019). (E-H) Note the superposition of truncation surfaces that serve as downlap surfaces to high-angle clinoforms (RF3) (section 098). Chaotic to wavy reflectors with a mounded external geometry (pale blue; RF12) may also be present. This association of radarfacies is attributed to a spit-inlet context.

Three types of internal truncations were observed in this association. The first type separates sets of clinoforms in dip-oriented sections, similarly to the ones observed among RF2 clinoforms (Table 2; Fig. 20). The second type is represented by sigmoidal discontinuities that separate and truncate sets of RF3 in strike sections. They are truncated by the third type of truncation surface, a downlap surface for RF3 with channelized geometry up to 50 m wide.

The third radarfacies association was identified in radargrams from Matinhos and Guaratuba, and includes wide areas with internal transparent to chaotic pattern (RF10) and landward-migrating clinoforms (RF13) (Table 2; Fig. 22).

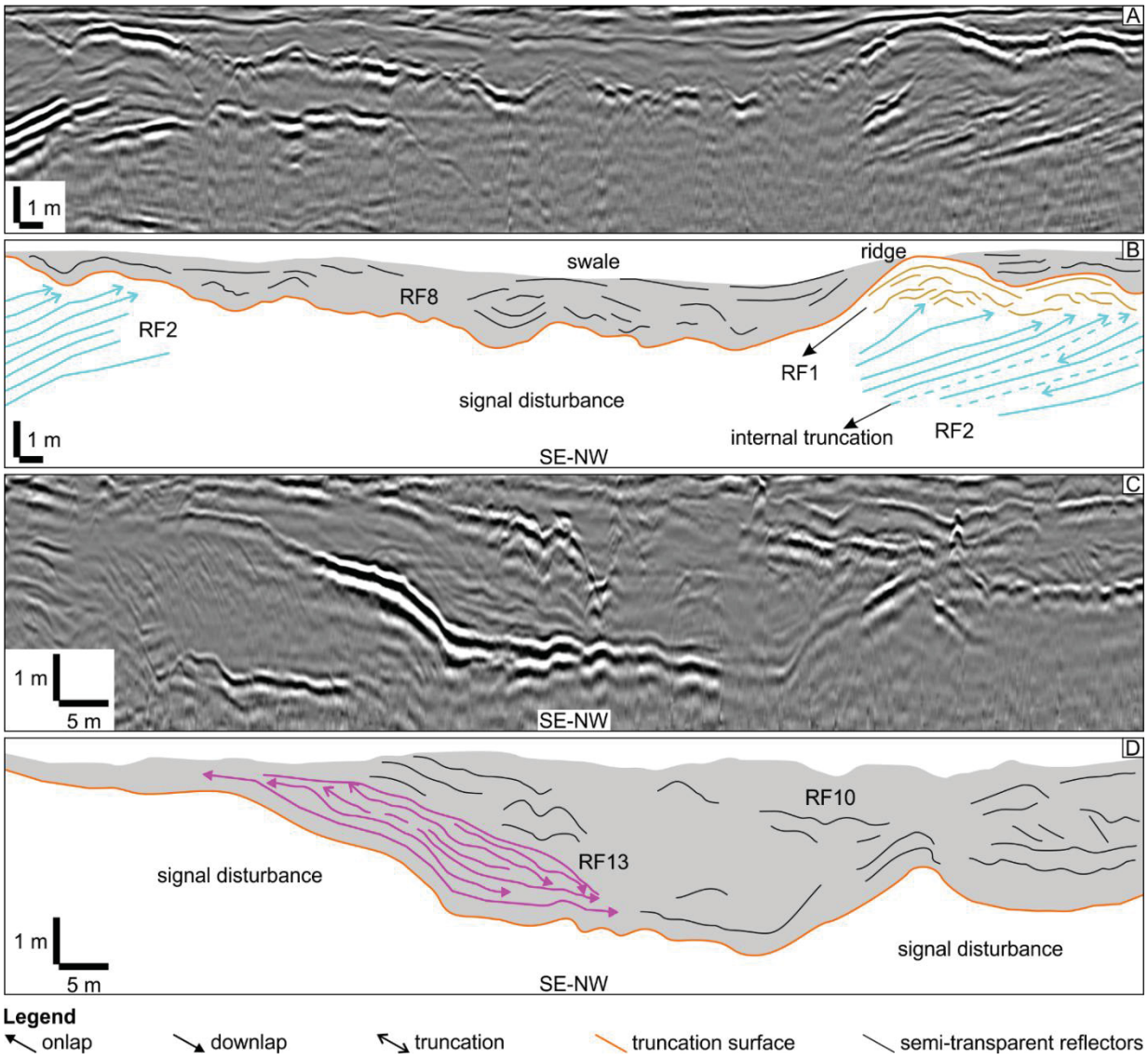

Figure 22: (A, B) The superficial topography of ridge-and-swale of the strandplain is evident in radargrams, and a semi-transparent pattern confined in the swales (gray zone; RF8) is interpreted as the result of the development of wet zones such as interstrand marshes (section 086). (C, D) The semi-transparent pattern (gray zone; RF10) is attributed to paleolagoonal/paleoestuarine deposits, but in this case, a clinoforms wedge (pink; RF13) may be present in the border of the transparent zone (section 006). This association of radarfacies is attributed to a lagoon context.

Radarfacies definition and mapping of reflector terminations, especially RF2 and RF3, lead to the delineation of surfaces of onlap, downlap, and truncation. Most of these surfaces are not mappable regionally, as they are located within sets of clinoforms (e.g., Fig. 20) or at the base of incisions (e.g., Figs. 21, 22), thus representing minor erosional or depositional breaks with no stratigraphic relevance. Only one surface is visible in most sections and therefore has stratigraphic relevance in the study area (Figs. 19, 23), a low-amplitude regional truncation detected at depths of 13 to 9 m. Most of this surface has a wavy character, but locally it can show channel-shaped incisions up to 1 m deep. It separates two major radar-stratigraphic units defined by prograding clinoforms (Fig. 23). The lower unit is represented mostly by seaward-dipping RF2 and/or RF3, whose upper terminations are bounded by the regional truncation (Fig. 23). The upper unit comprises clinoforms from RF2 and RF3 gradually passing downdip into basal radarfacies which, in turn, overlie the truncation surface (Fig. 23). Thus, the regional discontinuity separates two radar stratigraphic units defined by the seaward migration of RF2/RF3, and represents a phase of erosion with regional stratigraphic expression.

8.4.2 Sedimentary facies

The Pleistocene succession is mainly composed of fine- to medium-grained quartz sand with minor amounts of feldspar and/or mafic minerals and laminae with concentration of heavy minerals. Nine facies were described in two sand pits from Matinhos and Guaratuba (Fig. 19), summarized in Table 3. Fig. 24 depicts a photomosaic from a NW-SE cut in the Matinhos sand pit, where a succession of facies representative of the Pleistocene deposits is exposed. The base of the succession depicts massive to poorly-stratified, highly-bioturbated fine- to medium-grained sand with vertical and horizontal *Ophiomorpha* (Fig. 25). Collapse structures, upwardly-convex shell mounds and shell imprints are associated with zones with concentrations of coarser sand. Relicts of trough cross-stratified sand occur locally, with irregular and undefined contacts with the massive sand (Fig. 25). Small-scale muddy intraclasts and highly-disturbed lenses of massive mud also occur locally among the massive sand (Table 3; Fig. 25). Above, this facies is transitionally covered by a zone dominated by cross-stratified sand (Fig. 24).

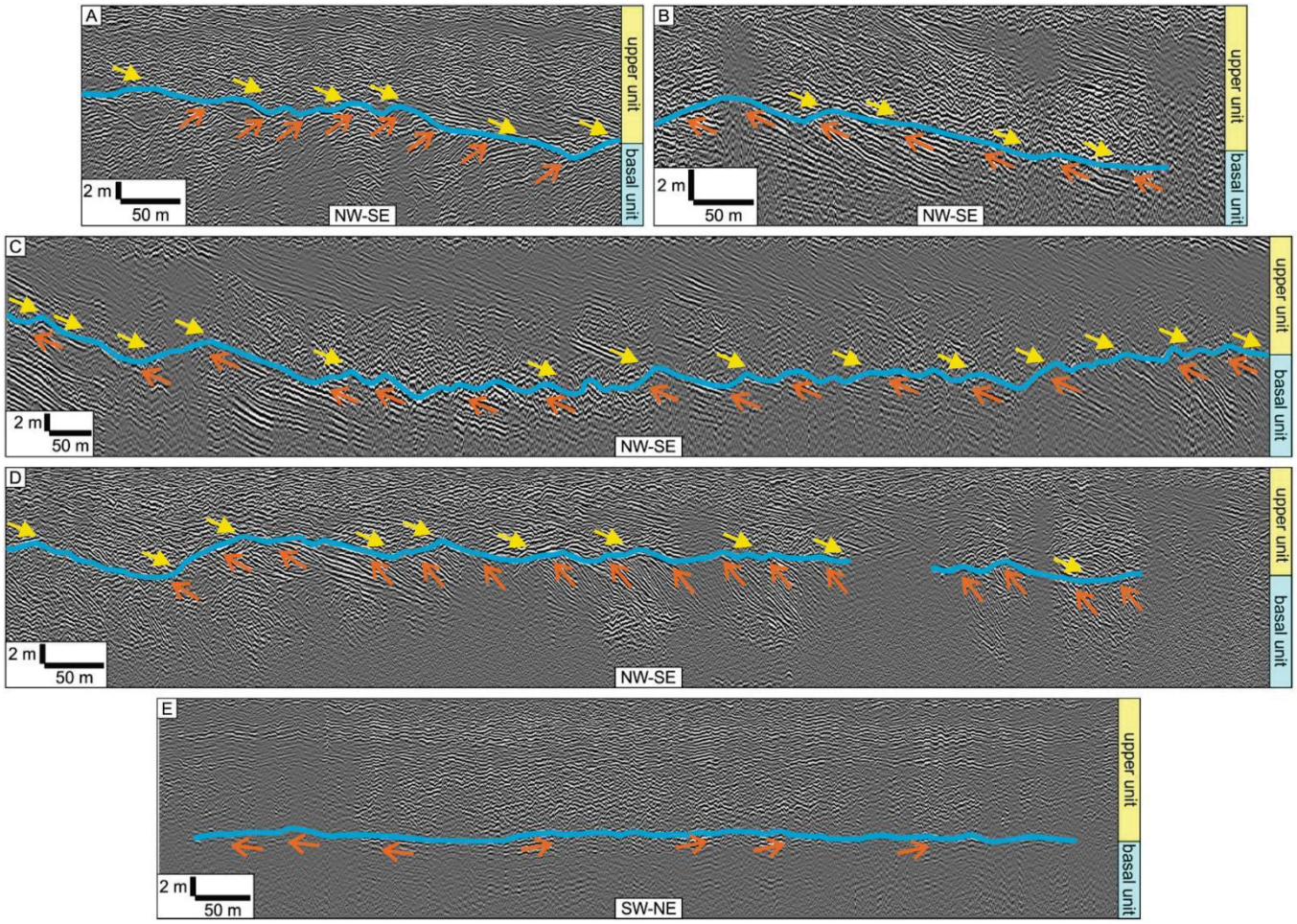

Figure 23: Interpretation of a subtle regional truncation surface (blue line) separating two radar-stratigraphic units defined by prograding clinoforms. Yellow arrows indicate downlap terminations, while orange arrows indicate truncations. (A, B) Dip sections from Guaratuba sector (section 028 in A; 039 in B); (C) dip section from Matinhos sector (section 100); (D) dip section (section 098) and (E) strike section from Pontal sector (section 104).

Fine- to medium-grained trough cross-stratified quartz sand is the most common facies in the Pleistocene deposits, composing cm- to dm-thick lenticular beds bounded by erosive contacts with concentrations of coarse sand (Fig. 26). Paleocurrents have a polymodal distribution, predominantly to NNW (landward) and subordinately to SSE (seaward) and WNW/ESE (longshore) (Table 2; Fig. 24). Fine-grained tabular cross-stratified sand and sigmoidal cross-stratified sand with mud drapes are commonly associated with trough cross-stratified sand (Fig. 26). All these facies are commonly bioturbated by *Ophiomorpha*, especially the basal layers in the deeper parts of the vertical profiles. In dip-oriented exposures (e.g., Fig. 24), the cross-stratified sands are partially bounded by m-scale continuous surfaces. These surfaces are interpreted as macroforms with predominantly S-SE dips (seaward). Above the zone dominated by cross-stratified sands, an abrupt contact marks the limit with the upper zone, dominated by parallel-laminated sands (Fig. 24).

Table 3: List of sedimentary facies described in Pleistocene outcrops, with their characteristics and interpretation of depositional contexts.

Facies	Composition	Grain Size and Sorting	Structures	Paleocurrent	Beding	Bounding Surfaces	Dep. Context
Low-angle parallel-laminated sand	Quartz (100%) ± heavy minerals (trace)	Fine-grained, well-sorted	Low-angle parallel lamination (up to 10°)	S (subordinately N)	Not assessed, up to 1.5 m thick	Transitional contact with subhorizontal parallel-laminated sand below	Upper foreshore
Subhorizontal parallel-laminated sand	Quartz (100%) ± heavy minerals (trace)	Fine-grained, well-sorted	Parallel lamination (<1-4°)	S-SE (subordinately NE)	Tabular, up to 2 m thick and 10's of m long	Transitional contact in the top, abrupt contact in the base	Foreshore
Sigmoidal cross-stratified sand	Quartz (100%) ± heavy minerals (trace)	Fine to very fine-grained sand, well-sorted	Sigmoidal lamination	SE	Wedges, 10-40 cm thick	Transitional with subhorizontal parallel-laminated sand	Foreshore to upper shoreface transition
Fine to medium trough cross-stratified sand	Quartz (95%), feldspar (5%), mafic minerals (trace)	Fine to medium-grained (coarse grains on contacts), well- to moderately- sorted	Trough cross-stratification, cut-and-fill structures, trace fossils (*Ophiomorpha*)	N-NE-NW (subordinately S-SE and WNW-ESE)	Lenses, 5-50 cm thick, locally contained within inclined macroforms	Truncation surfaces with concentration of coarse grains	Upper shoreface
Fine to coarse trough cross-stratified sand	Quartz (80-90%), muscovite (5-10%), biotite (0-5%), feldspar (0-5%), mafic minerals (0-5%), organic matter (trace)	Fine to coarse-grained, poorly-sorted	Trough cross-stratification, trace fossils (*Ophiomorpha*)	N-NE	Lenses, 30-50 cm thick	Truncation surfaces and/or abrupt contacts	Upper shoreface
Tabular cross-stratified sand	Quartz (100%) ± heavy minerals (trace)	Fine-grained sand	Tabular cross-stratification, trace fossils (*Ophiomorpha*)	N-NE	Lenses, 20-40 cm thick	Truncation surfaces and/or abrupt contacts	Upper shoreface
Sigmoidal cross-stratified sand with mud drapes	Quartz (100%) ± heavy minerals (trace)	Fine- to medium-grained, well- to moderately-sorted	Sigmoidal cross-stratification, mud drapes	N-NE	Lenses, 7-20 cm thick	Abrupt contacts	Upper shoreface
Massive sand	Quartz (100%), feldspar (trace)	Fine to medium-grained (locally coarse-grained), well- to moderately- sorted	Massive, relicts of trough cross stratification, trace fossils (*Ophiomorpha* and *Roselia*), collapse structures, upwardly convex shell mounds and shell imprints, mud intraclasts		Undefined, exceed 2 m	Transitional	Upper to medium shoreface
Massive mud		Well-sorted	Massive		Lenses up to 5 cm thick and 2 m long	Abrupt (among massive sand)	Upper to medium shoreface

The upper part of the successions is represented mainly by well-sorted, subhorizontal parallel-laminated quartz sand with predominant seaward dips (S-SE) (Table 2; Fig. 24). This facies locally grades downdip to fine-grained seaward-dipping sigmoidal cross-stratified quartz sand (Table 2; Fig. 26). In the uppermost part of the vertical profiles, subhorizontal parallel-laminated sand (<1 to 4°) is gradually substituted by low-angle parallel-laminated sand (up to 10°) (Fig. 24). This facies consists of fine-grained well-sorted quartz sand with local concentrations of heavy minerals. Laminations dip predominantly to S (seaward) and subordinately to N (landward) (Table 2; Fig. 24).

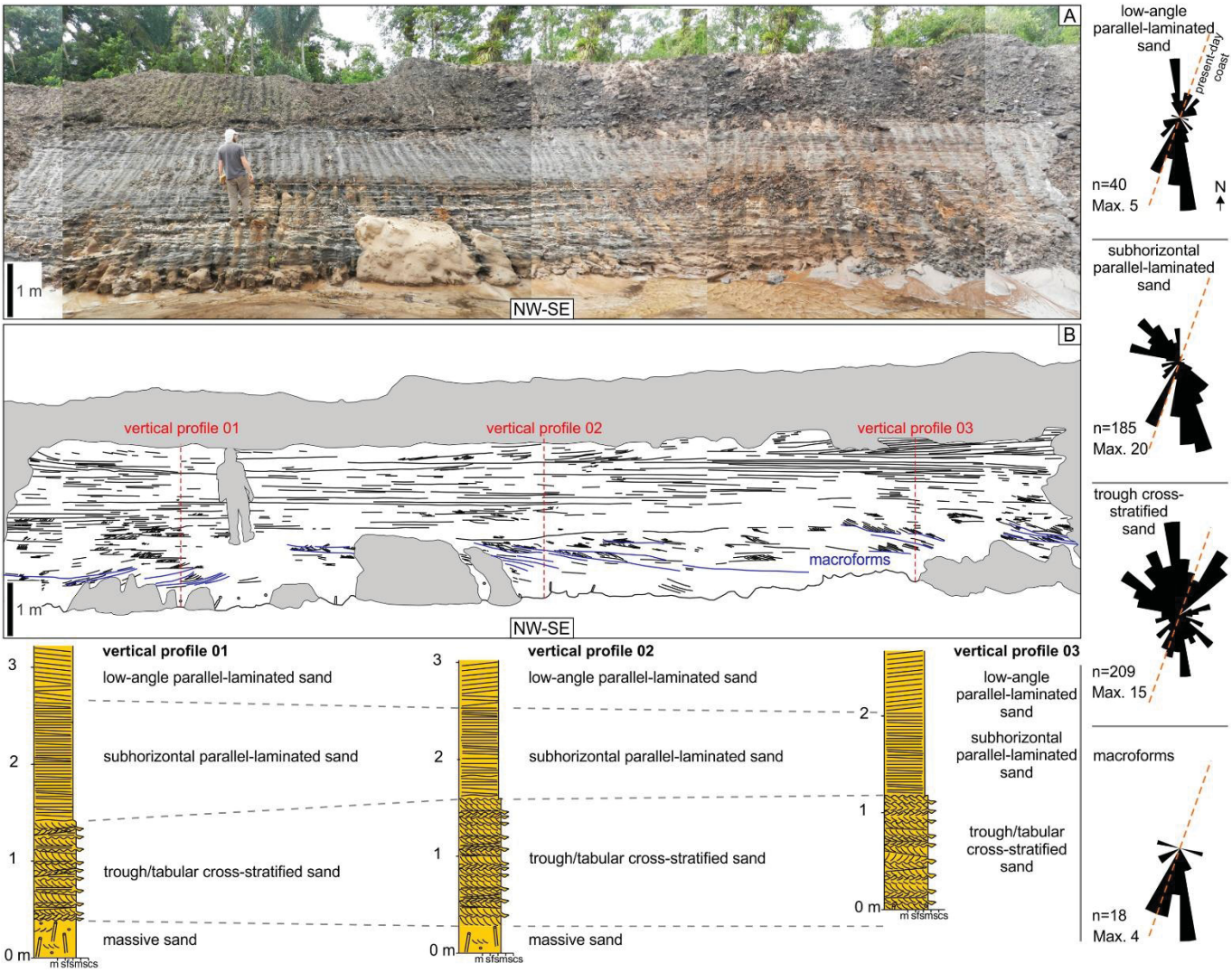

Figure 24: Photomosaic of a Pleistocene outcrop in the Matinhos sector (A), interpreted in (B) through the tracing of surfaces (beds/laminae), vertical profiles, and rosette plots of paleocurrents from facies of low-angle parallel-laminated sand, subhorizontal parallel-laminated sand, trough cross-stratified sand, and macroforms. These facies are interpreted as upper shoreface to foreshore.

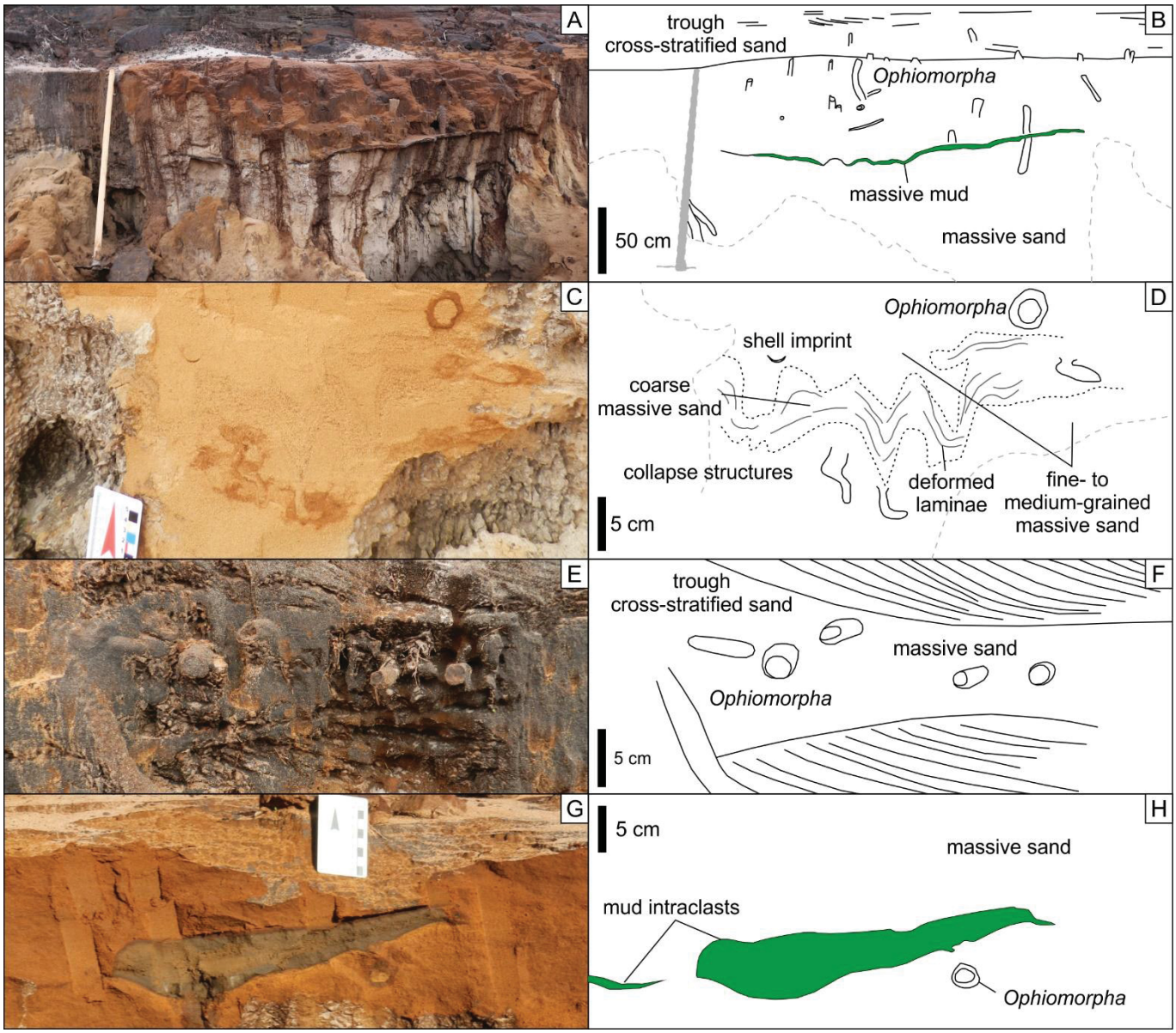

Figure 25: (A, B) Highly-disturbed, bioturbated massive sand and massive mud. (C, D) Detail of horizontal *Ophiomorpha*, convex-upward shell imprint, concentrations of coarse sand and collapse structures within massive sands. (E, F) Relicts of trough cross-stratified sands suggest that this was the dominant structure prior to bioturbation. (G, H) Local occurrences of mud intraclasts among massive sands indicate the influence of high-energy processes during deposition.

8.5 Discussion

8.5.1 Depositional systems

The variability of radarfacies in the study area reflects variable depositional conditions taking place in the buildup of the coastal plain during the late Pleistocene and Holocene. Sedimentary data presented here (Table 3) and in previous studies (e.g., Lessa et al., 2000; Souza, 2005; Souza et al., 2012; Bisi, 2015) are consistent with wave-dominated settings in a microtidal regime and variable energy processes

related to fair weather and storms. These sedimentary descriptions can indirectly serve as a base to predict the internal character of the radarfacies, considering the stratigraphic positions, areal distribution and external geometry, though it must be considered that limitations of radar resolution imply that the limits of the radarfacies do not necessarily coincide with the contacts of sedimentary facies or their associations (Corbeanu et al., 2001). Three main depositional systems corresponding to the radarfacies associations are recognized: (1) strandplain; (2) spits and inlets; and (3) lagoon and/or estuary.

8.5.1.1 Strandplain

In radargrams, the most common radarfacies association is characterized by the superposition of RF2 over RF4, RF5, RF6, RF7 and RF11 (Fig. 20). The seaward migration of RF2, the lateral continuity of reflectors in strike sections and relative low angles allow interpretation as beach-face clinoforms (e.g., Barboza et al., 2009, 2013; Clemmensen and Nielsen, 2010; Costas and Fitzgerald, 2011; Souza et al., 2012; Leal et al., 2016; Dillenburg et al., 2017; Nielsen et al., 2017; Rosa et al., 2017) which, based on the correlation between parallel radargrams, may extend for several km along strike. Internal discontinuities probably correspond to surfaces of truncation between dune/beach-ridge sets (e.g., Rodriguez and Meyer, 2006; Hampson et al., 2008; Takagawa et al., 2008) that may be related to temporal changes in longshore current regime (Hampson et al., 2008) or periodic changes in wave energy regime (e.g., Rodriguez and Meyer, 2006).

RF1 is found above RF2 in the uppermost part of the sections, and its geometry, dimensions, amplitude and stratigraphic position allow interpretation as eolian sand dunes from the backshore (e.g., Harari, 1996; Neal, 2004; Lindhorst et al., 2008; Timmons et al., 2010; Barboza et al., 2013; Leal et al., 2016; Rockett et al., 2016; Dillenburg et al., 2017; Rosa et al., 2017). The short extent along dip and the strike-parallel elongation are coherent with low-mobility vegetated foredunes and blowouts developed in the backshore zone (e.g., Barboza et al., 2011; Guedes et al., 2011). RF1 locally imprints a ridge-and-swale morphology (Figs. 22, 27) with transparent zones (RF8) confined between ridges. RF8 is therefore interpreted as strike-parallel deposits accommodated in swales (e.g., Rocha et al., 2017; Rosa et al., 2017).

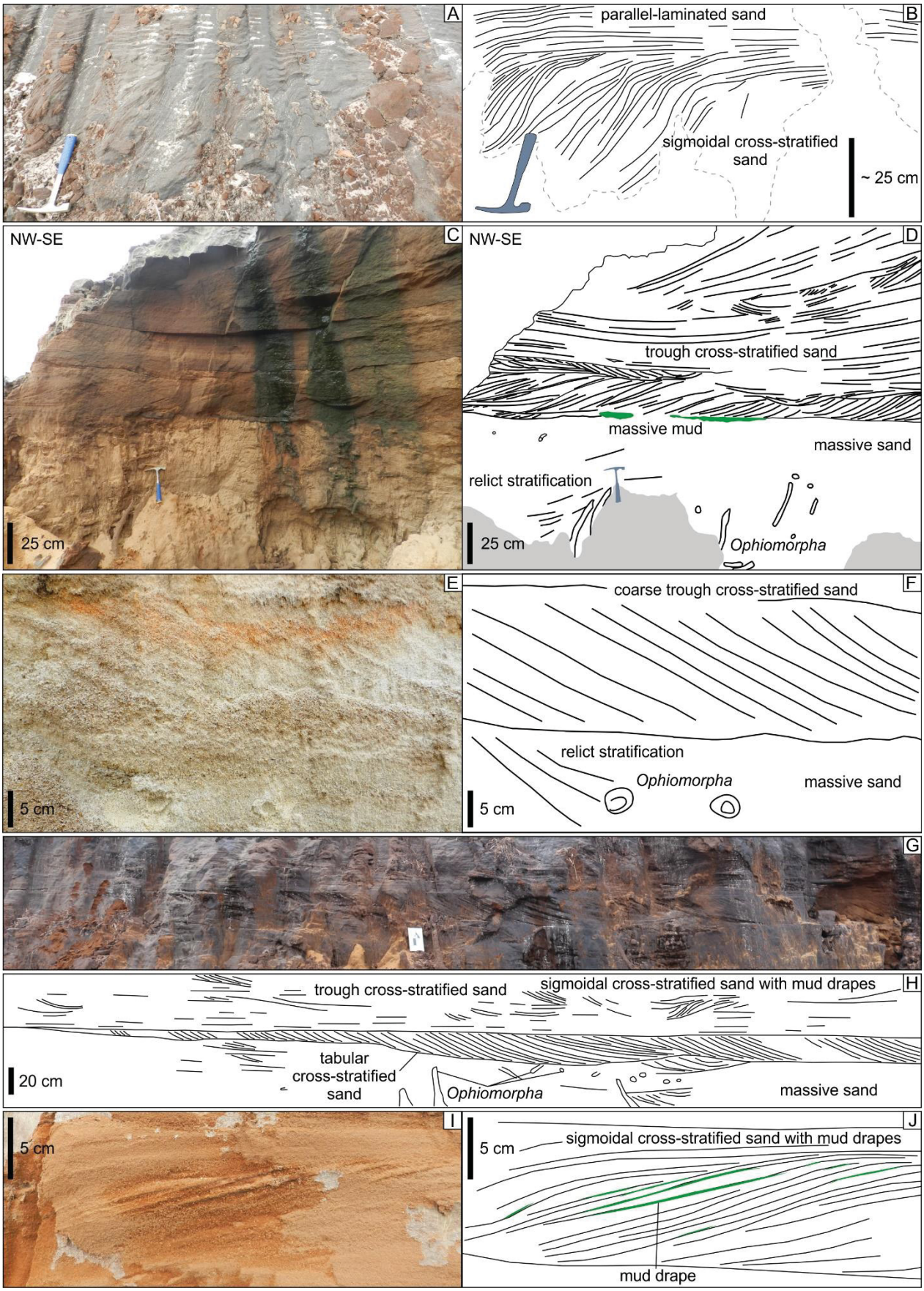

Figure 26: Different types of cross-stratified sands were identified in the study area, including sigmoidal cross-stratified sand (A, B), fine to medium trough cross-stratified sand (C, D), fine to coarse trough cross-stratified sand (E, F), tabular cross-stratified sand (G, H), and sigmoidal cross-stratified sand with mud drapes (I, J). Note the widespread occurrence of bioturbation in the form of *Ophiomorpha* in the base of the cross-stratified sand sets.

Radarfacies identified below RF2 probably correspond to subtidal depositional features. Seaward-migrating sigmoidal clinoforms (RF4) restricted to the toe of RF2 are interpreted as beach steps developed in the upper shoreface (e.g., Hede et al., 2015). The lenticular bodies with small-sized tangential clinoforms (RF5) located in the bottomset of beach-face clinoforms (RF2), can be interpreted as subtidal bars with a predominantly onshore migration due to swash and/or longshore currents (e.g., Houser et al., 2006; Masselink et al., 2006; Houser and Greenwood, 2007; Lindhorst et al., 2008, 2010; Clemmensen and Nielsen, 2010; Costas and Fitzgerald, 2011; Rocha et al., 2017). Similarly, channel-shaped features that occur locally (see detail in Fig. 23E, F) may be related to erosive incisions such as longshore troughs filled due to the migration of subtidal bars (Reinson, 1984). Locally, the lenses with RF5 prograde landward and overlie the bottomset of RF2 (Fig. 20), which may indicate episodic migration.

Hummocky reflectors with m-scale dimensions (RF6) that also occur in the zone below RF2, locally truncating reflectors below (Fig. 20F, G), are interpreted as hummocky and/or swaley cross-stratified deposits (e.g., Souza et al., 2012). The absence of reflectors in RF7 is related to the absence (or quasi-absence) of dielectric contrasts related to structural heterogeneity, possibly as a result of intense bioturbation and consequent obliteration of the original bedding (e.g., Costas and Fitzgerald, 2011). Similarly, the chaotic zones from RF11 cannot be correlated to any specific depositional feature, but their radar expression can be related to the occurrence of small bedforms under radar resolution, subtle grain size variations and/or presence of muddy deposits that are common in the lower shoreface to inner shelf (e.g., Veiga et al., 2004; Hampson et al., 2008; Souza et al., 2012).

Based on reflectors patterns, their relations and geologic interpretation, this radarfacies association is interpreted as wave-dominated strandplain deposits. RF1 is interpreted as backshore dunes, but sedimentary facies compatible with such deposits were not found in the examined exposures. However, Bigarella et al. (1969) described the internal character of present-day foredunes in the Paraná coast as well-sorted, fine-grained quartz sand in dm-scale sets with tabular cross-stratification. The backshore dunes are a typical surface topography of a succession of beach and/or dune ridges and swales (Fig. 22A, B) resulting from seaward migration of the beach system (e.g., Hesp et al., 2005; Hampson et al., 2008; Souza et al., 2012; Gosling and Clemmensen, 2017). The swales may accommodate wetlands or even

small fluvial channels, resulting in shore-parallel interstrand marshes with a predominantly muddy composition (RF8) (Davis Jr and Hayes, 1984; Otvos, 2000, 2012; Jackson et al., 2010).

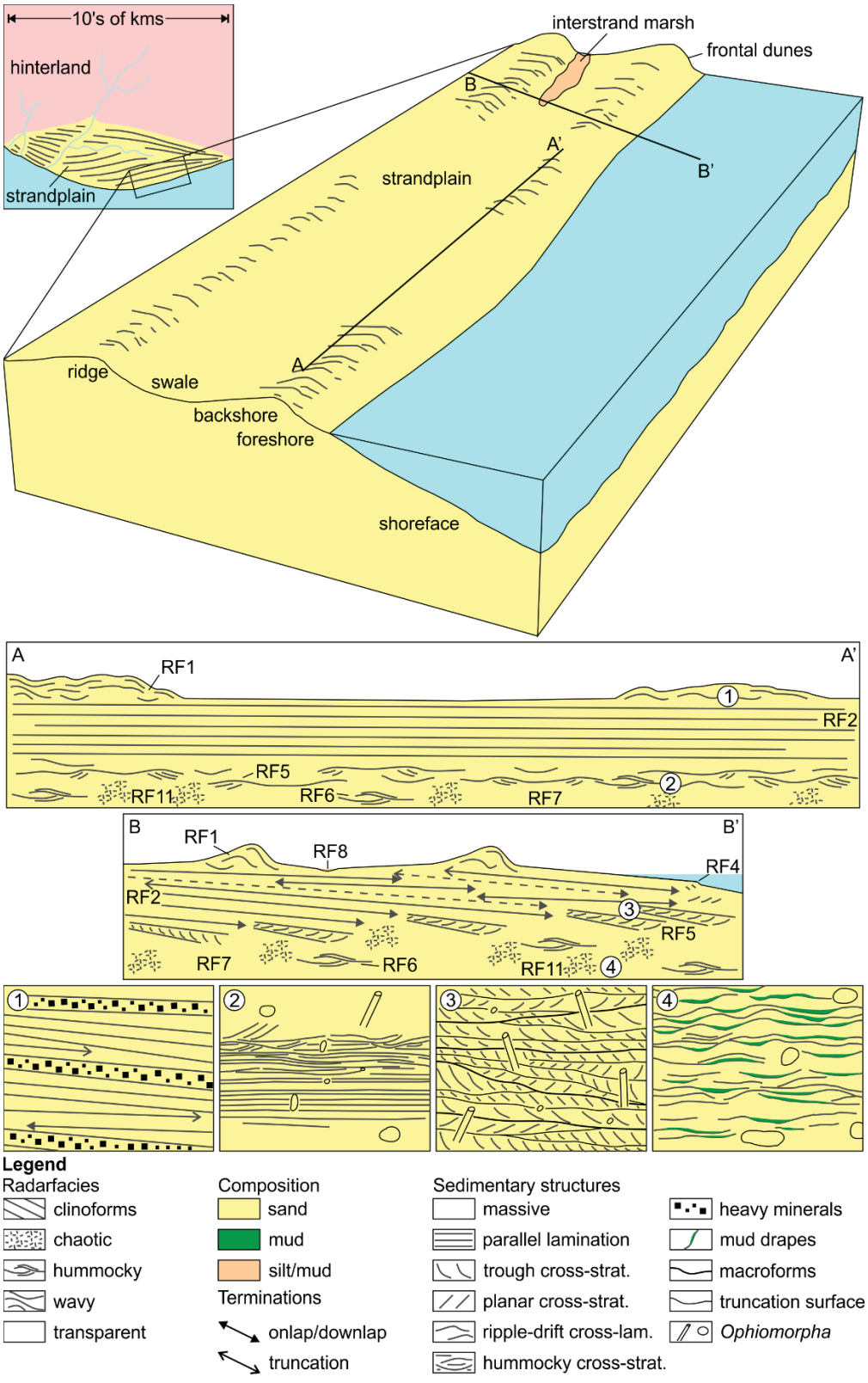

Figure 27: Model of the architecture and internal character of strandplain systems based on the interpretation of GPR and sedimentary facies. Note the km dimensions and lateral continuity of the deposits, as well as the sand-rich composition. The numbers in the cross-sections indicate a more detailed view of the facies that compose these areas, as shown in the correspondent frames below.

Radarfacies attributed to the beach zone composes laterally-continuous clinoform sets with progradation along hundreds of meters (RF2) (Fig. 27), in a configuration typical of strandplain systems (e.g., Rodriguez and Meyer, 2006; Hampson et al., 2008). The most probable internal composition is of well-sorted sand with seaward-dipping sub-horizontal depositional surfaces as the parallel-laminated sands and low-angle cross-stratified sands (e.g., Reinson, 1984; Tomazelli and Dillenburg, 2007; Souza et al., 2012; Vakarelov et al., 2012) (Fig. 24, Table 3), with local occurrences of landward-dipping laminae that may correspond to berm deposits (Hine, 1979; Souza et al., 2012). These structures are related to upper flow conditions that result from wave swash at the beach face. The transition from foreshore to shoreface is well-defined in outcrops, but radarfacies attributed to the beach and to subtidal zones are interfingered in radargrams (Fig. 27).

The subtidal zone is represented by a great variability of radarfacies that occur at the bottomset of RF2 to deeper parts of the sections. The sets of SE-dipping sigmoidal clinoforms (RF4) observed at the toe of RF2 and interpreted as beach steps are probably constituted of sigmoidal cross-stratified sand. They can serve as a proxy to the limit between the swash and surf zones (e.g., Takagawa et al., 2008; Souza et al., 2012; Hede et al., 2015). RF5, interpreted as longshore bars, can be related to an upper shoreface context. Based on sedimentary data, their internal character is probably a combination of structures related to the migration of wave-current-induced subtidal bedforms, such as cross-stratified sands. These structures have cm- to dm-scale dimensions, and are below radar resolution (e.g., Corbeanu et al., 2001). However, m-scale macroforms that occur in association with them might be visible in radargrams, and their dimensions are comparable with the dimensions of clinoforms from RF5.

Hummocky reflectors (RF6) located in the subtidal zone have dimensions and positions comparable to hummocky and/or swaley cross-stratified sands as described by Souza et al. (2012) and Bisi (2015) in Holocene exposures in the Matinhos sector. Sedimentary facies indicate the occurrence of oscillatory currents in the shoreface to inner shelf domain, associated with high-energy episodes (storms) that caused a temporary base-level rise and sediment reworking (Heward, 1981; Dott Jr and Bourgeois, 1982; Eyles and Clark, 1986; Sherman and Greenwood, 1989; Dumas and Arnott, 2006; Howell et al., 2008). RF7 and RF11, interpreted as the result of the absence of dielectric contrasts possibly due to bioturbation, and zones with facies below radar resolution, are common in the lowermost part of sections and probably

associated with the lower shoreface to inner shelf (e.g., Souza et al., 2012). The strandplain systems are therefore sand-rich deposits with km-scale dimensions, elongated along strike, with a succession of clinoform sets (beach- or dune-ridge sets) separated by reactivation surfaces along dip, and with a superficial ridge-and-swale morphology (Fig. 27). Internally, the sedimentary facies reflect variable energy, and locally intense bioturbation. The only expressive concentrations of mud are expected in the interstrand marshes and lower shoreface to inner shelf deposits (Fig. 27).

8.5.1.2 Spits and inlets

Sedimentary facies from the Pleistocene sand pit in the Matinhos sector (Table 3) are predominantly composed of fine to medium sand with local concentrations of mud, and are commonly bioturbated by *Ophiomorpha* attributed to *Callichirus major*, a crustacean that commonly lives in the foreshore to upper shoreface domain (e.g., Weimer and Hoyt, 1964; Barreto et al., 2002; Tomazelli and Dillenburg, 2007; Martins et al., 2018). These deposits are thus interpreted as an upper shoreface to foreshore succession (e.g., Howell et al., 1996), but they are significantly different from equivalent strandplain deposits identified in previous works (e.g. Lessa et al., 2000; Souza et al., 2012; Bisi, 2015). The main differences are the presence of mud-rich facies in the upper shoreface (Fig. 25), concentrations of coarse grains in bounding surfaces (Fig. 26), and a longshore component in paleocurrents, especially the ones associated with subtidal bedforms (Fig. 24). These aspects indirectly indicate deposition in a context where tidal processes played an important role (especially in confined tidal channels), with fine-grained sedimentation taking place in a backbarrier lagoon, and barrier construction driven by longshore currents oblique to the coast, such as in coastal spits (e.g., Hine, 1979).

Spit-inlet systems are identified more directly in radargrams as the second radarfacies association type, especially due to the geometry of RF3 in strike sections (Fig. 21). RF3 can also be attributed to the progradation of beach faces, but their three-dimensional characteristics suggest they are associated with spits with a longshore growth (e.g., Tercier et al., 2000; Jol et al., 2002; Lindhorst et al., 2008, 2010; Costas and Fitzgerald, 2011; Shan et al., 2015). The clinoforms that locally infill wide channels are interpreted as lateral accretion within tidal channels (inlets) that had their axes oriented at high angles with respect to the shoreline (e.g., Tillmann and Wunderlich, 2013) (Fig. 21). While internal truncation surfaces identified in

dip sections probably represent reactivation surfaces between beach-ridge sets (e.g., Rodriguez and Meyer, 2006; Hampson et al., 2008; Takagawa et al., 2008), truncation surfaces in strike sections correspond to partially-eroded to fully-preserved base of channels resulting from the superposition of different episodes of migration of spit-inlet systems (e.g., Reinson, 1984; Parsons et al., 2003; Lindhorst et al., 2010) (Fig. 21).

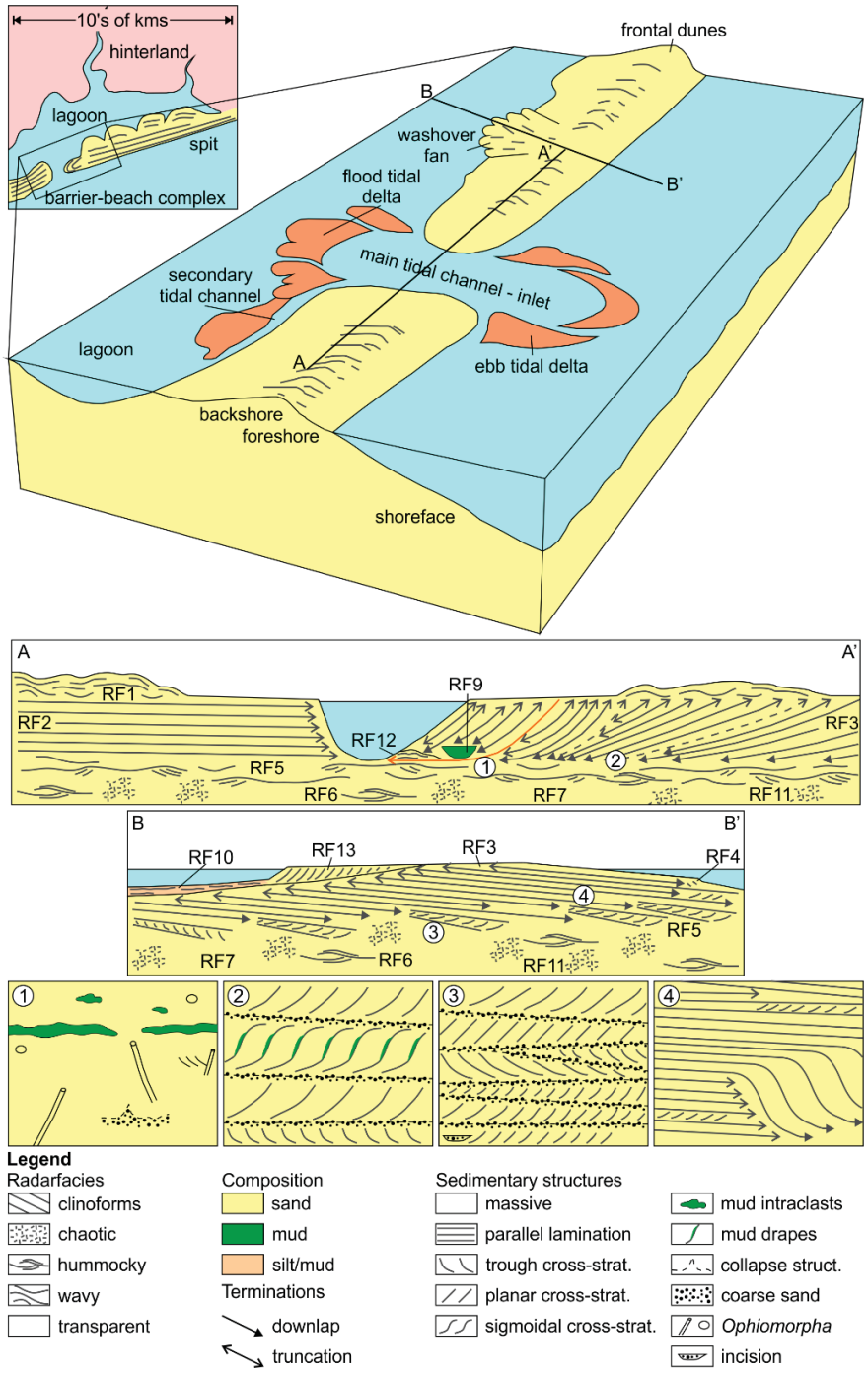

Figure 28: Model of the architecture and internal character of spit-inlet and associated lagoon systems based on the interpretation of GPR and sedimentary facies. The deposits are laterally discontinuous and more heterogeneous than strandplain deposits, with higher proportions of mud. The numbers in the cross-sections indicate a more detailed view of the facies that compose these areas, as shown in the correspondent frames below.

Therefore, RF3 records not only the progradation and longshore migration of a spit, but also the migration of inlets. The high amplitude of channel-base truncations is possibly a consequence of the concentration of coarse sediment (coarse sand to gravel) in lag deposits at the base of the inlets (e.g., Reinson, 1984). The radarfacies assembly at the bottomset of RF3 in dip sections is similar to strandplain systems, including RF5, interpreted as longshore bars expressed as macroforms in outcrop (Fig. 24), RF6, interpreted as hummocky/swaley cross-stratified deposits, RF7, interpreted as massive deposits (Fig. 25), and RF11, interpreted as facies below radar resolution. In strike sections, radarfacies RF9 and RF12 occur in association with RF3 and wide channels interpreted as inlets.

The transparent character of the channelized RF9 is probably a result of a mud-rich composition (e.g., Parsons et al., 2003; Pereira et al., 2003), although equivalent deposits were not identified in outcrop. This facies is interpreted as secondary tidal channels (e.g., Pereira et al., 2003; Maio et al., 2016). RF12, located at the bottomset of RF3, is interpreted based on their external form, dimensions and internal character, as tidal deltas (e.g., Maio et al., 2016). Deposits attributed to tidal deltas were previously interpreted by Lessa et al. (2000) in the Pontal sector as poorly-sorted, dm- to m-thick sandy beds with mud and/or organic laminae and landward-directed tabular cross-stratification. Although a migration pattern was not visible in RF12, from previous outcrop analysis (Lessa et al., 200) it probably corresponds to flood tidal deltas, as ebb tidal deltas have lower preservation potential in wave-dominated contexts (Davis Jr and Hayes, 1984; Reinson, 1984; Murakoshi and Masuda, 1992). It is possible, however, that ebb tidal deltas are also preserved but is not recognizable in the radargrams.

The final configuration of the spit-inlet systems, as seen in radargrams, is of shore-parallel elongated deposits with longshore migration of several km, often filling inlets and downlapping on flood tidal deltas (Hine, 1979; Reinson, 1984; Lindhorst et al., 2010; Costas and Fitzgerald, 2011) (Fig. 28). An internal depositional complexity is expected in these deposits, as a result of the interplay between wave- and tide-related processes and variable depositional energy (e.g., Kumar and Sanders, 1974; Dott Jr and Bourgeois, 1982; Sherman and Greenwood, 1989; Van Heteren and Van de Plassche, 1997). Therefore, the spit-inlet systems have a general sand-rich composition, but with muddy units in the form of restricted bodies at cm- to m-scales (Fig. 28), reflecting deposition in awave-dominated context,with dominance of

tractive depositional processes related to fair-weather wave currents and swash on the beach face, but with influence of tidal and storm-related processes.

8.5.1.3 Lagoons and/or estuaries

The distribution in radargrams of the third type of radarfacies association (RF10, RF13) coincides with areas previously mapped as mud-rich, heterogeneous paleolagoonal/paleoestuarine deposits with variable thicknesses (Angulo, 2004) (Fig. 19). This composition is probably the cause of the transparent to semi-transparent character and irregular distribution of discontinuous reflectors in RF10 (e.g., Pereira et al., 2003; Garrison Jr. et al., 2010; Beni et al., 2013). In this context, the landward-migrating clinoforms from RF13 are interpreted as washover deposits (e.g., Horwitz and Ping, 2005; Costas and Fitzgerald, 2011; Tillmann and Wunderlich, 2013; Rosa et al., 2016, 2017; Zaremba et al., 2016) (Fig. 25C, D). These deposits would be associated with high-energy episodes such as storms (e.g., Heward, 1981; Leatherman and Williams, 1983; Davis Jr and Hayes, 1984; Gosling and Clemmensen, 2017), although such deposits were not identified in previous studies on the Paraná coastal plain, possibly due to their restricted occurrence and/or relatively small dimensions. The absence of expressive backbarrier washover fans in a context with strong influence of storms (e.g., Lessa et al., 2000; Angulo, 2004; Souza et al., 2012; Bisi, 2015) shows that classic depositional models are not fully correlatable to this coastal plain (e.g., Heward, 1981; Davis Jr and Hayes, 1984; Boyd et al., 1992).

8.5.2 The Paraná Coastal Plain as a reservoir analog

Reservoir modeling in coastal deposits commonly uses parasequences as fundamental units for studies of reservoir compartmentalization, due to the compatibility of their dimensions ($10^{1\prime}$ to $10^{2\prime}$ m thick) with the resolution of subsurface-imaging tools such as seismic (e.g., Cook et al., 1999; Reynolds, 1999; Ainsworth, 2005; Cross et al., 2015). Coastal reservoirs are traditionally considered relatively homogeneous, laterally-continuous sand-rich deposits (e.g., Reynolds, 1999; Ainsworth, 2005; Zhuo et al., 2014), but the behavior of pressure and fluids circulation within productive fields attests a sub-seismic internal compartmentalization (e.g., Cook et al., 1999; Jackson et al., 2009; Cross et al., 2015). Results of the present study show that coastal deposits can be internally complex and intersected by a wide variety of heterogeneities of different scales and origins (Figs. 27, 28) and that deposits from different depositional

systems may be in contact (Fig. 29). These heterogeneities are categorized herein according to the classification scheme of Ainsworth (2010) for reservoir heterogeneities on marginal marine reservoirs, considering three orders of internal compartmentalization: inter-parasequence (first order), inter sand-body (second order), and intra sand-body (third order).

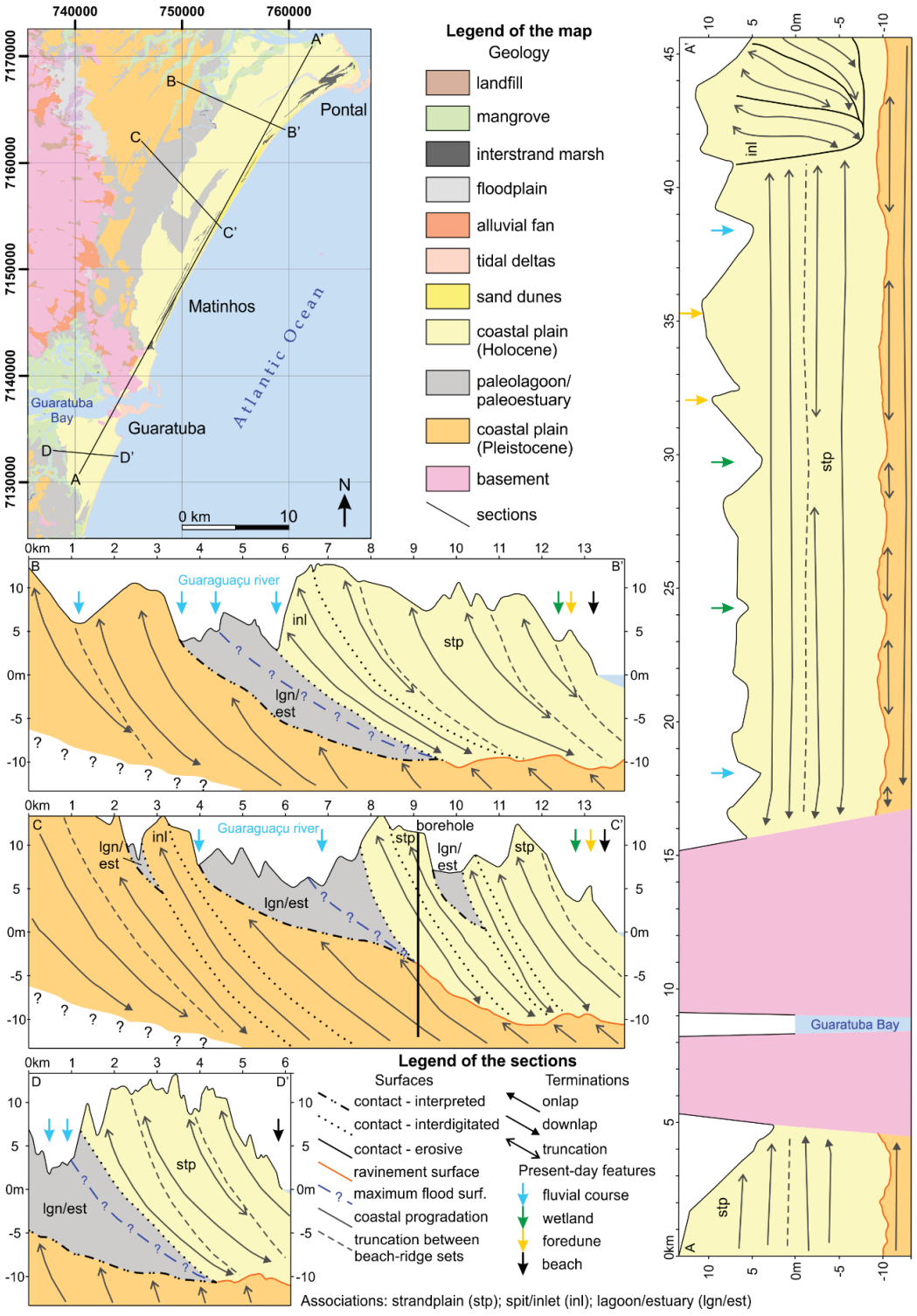

Figure 29: Cross-sections distributed in the Paraná coastal plain with the interpretation of the subsurface framework. Associations of units were determined with base in outcrop and radar interpretations and in previous works by Lessa et al. (2000), Souza (2005), Souza et al. (2012) and Bisi (2015).

The inter-parasequence heterogeneity is related to changes in shoreline trajectory, which in the study area are represented by the superposition of two prograding units (Fig. 26). The first (lower) unit corresponds to the regressive Pleistocene barrier (Lessa et al., 2000; Angulo, 2004; Souza, 2005) (Fig. 29). This succession is partially truncated upward by the regional truncation surface, which is attributed to the Holocene transgression (Souza, 2005) (Fig. 23), and is interpreted thus as a wave ravinement surface (e.g., Boyd et al., 1992; Murakoshi and Masuda, 1992; Parsons et al., 2003; Catuneanu, 2006). The transgression also resulted in the formation of extensive mud-rich paleolagoons/paleoestuaries that locally overlie Pleistocene deposits (Angulo, 2004) (Fig. 29). Following the Holocene transgression, the dominantly regressive trend was established, leading to the construction of the Holocene barrier (Lessa et al., 2000; Souza et al., 2012) (Fig. 29). In radargrams, it is correlated to the upper succession that overlies the Pleistocene unit and the ravinement surface. The regressive successions depicted in Fig. 23 thus represent two coarsening-up parasequences separated by a wave ravinement surface (e.g., Murakoshi and Masuda, 1992; Hampson and Storms, 2003; Tamura et al., 2003; Clifton, 2006). Therefore, the inter-parasequence order of heterogeneities is recorded as the ravinement surface (Fig. 23) and the laterally-extensive seaward-dipping paleolagoonal/paleoestuarine wedges (Fig. 29).

The second order of heterogeneity considers the connectivity between sand bodies that represent individual reservoir units within a single parasequence, in which geometry and distribution are controlled by the dominant depositional process (i.e., waves, tides, fluvial; Reynolds, 1999). In the study area, both Pleistocene and Holocene successions depict the interfingering of spit-inlet deposits among dominant strandplain deposits (Fig. 29). As they have different architectural configurations and facies that imprint variable internal compartmentalization (Figs. 27, 28), spit-inlets and strandplains can be considered as individual sand bodies within the parasequences. Both types of depositional systems are related to wave-dominated conditions that result in laterally-elongated sand bodies overlying mud-bearing deposits from the lower shoreface/inner shelf (Figs. 27, 28). Along dip, they are limited by truncation surfaces that separate individual dune/beach-ridge sets, each with tens to hundreds of m wide. Along strike, dune/beach-ridge sets from strandplain systems have good vertical connectivity (Fig. 27), coherently with a low accommodation/sediment supply (A/S) ratio (Ainsworth, 2010). Sand bodies from spit-inlet systems

are more heterogeneous along strike, as they are commonly truncated by erosive surfaces from the base of tidal inlets (Reinson, 1984) (Fig. 28).

The intra sand-body scale comprises all heterogeneities that act as barriers or baffles for the flow within individual sand bodies, with generation and distribution mainly controlled by depositional processes. In the study area they are represented by a wide variety of surfaces and facies visible in GPR and outcrops, but all of sub-seismic scale (<10 m thick). In dip GPR sections, the most evident discontinuities are individual clinoforms within a single clinoform set (RF2/RF3), representing stages of progradation of the beach, and small-sized clinoforms (macroforms) representing the migration of subtidal bars (RF5) (Figs. 20, 21). This framework changes along strike, as they are laterally-continuous in strandplains, and represented by clinoforms related to longshore accretion in spit-inlets (RF3) (Fig. 21). Mud-rich tidal channels (RF9) and tidal deltas (RF12) also represent intra sandbody heterogeneities within spit-inlet systems, in the form of non-reservoir units. Each intra-parasequence clinoform comprises a variety of interfingered sedimentary facies formed in the backshore/foreshore to the shoreface (e.g., Hampson et al., 2008; Sech et al., 2009). Among these facies, the most expressive as barriers and/or baffles in strandplains are massive sands homogenized by bioturbation and drapes of mud in flaser heterolites. Again, spit-inlet systems are more heterogeneous, as their facies include mud intraclasts, mud beds and drapes in upper shoreface sands, and concentrations of poorly-sorted sand separating beds with well-sorted sand (Fig. 25).

The geometry of the studied coastal successions and their depositional elements, as well as the distribution of facies and stacking patterns, is coherent with subsurface data from petroleum reservoirs in wave-dominated, storm-influenced systems (e.g., Hampson et al., 2008; Zhuo et al., 2014; Klausen et al., 2016). However, the integration of GPR and outcrop interpretations shows that the distribution of heterogeneities within those systems may be more complex than the classic view of homogeneous and laterally-elongated sand bodies (Fig. 30). Spit-inlet systems, for instance, are far more complex than strandplain systems, although their signature in seismic and boreholes would be very similar (strike-parallel negative amplitudes in seismic and shoreface-to-foreshore coarsening-up successions in well logs).

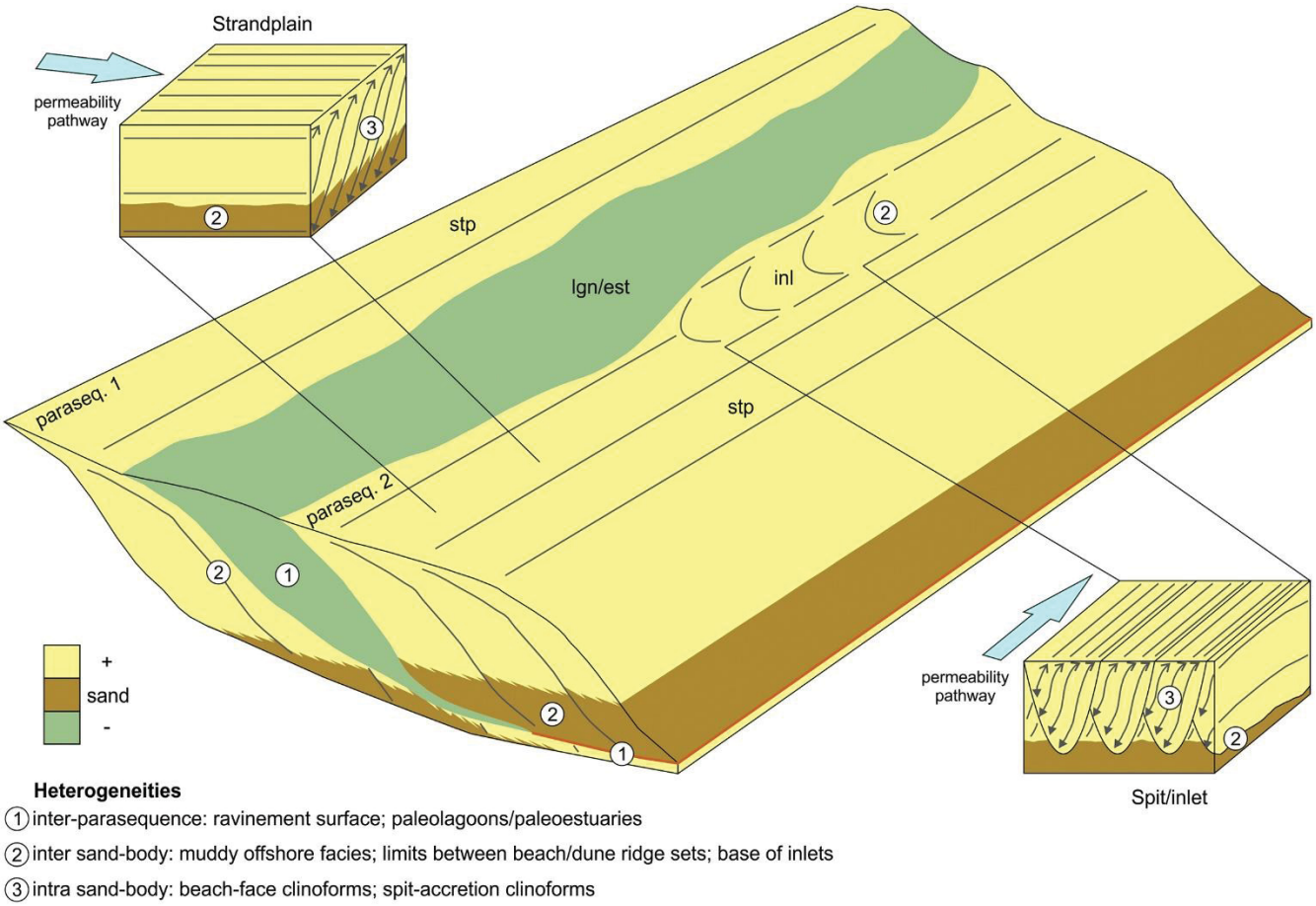

Figure 30: Scales of internal heterogeneities within wave-dominated coastal systems, as seen in the Paraná coastal plain. Inter-parasequence heterogeneities are represented by paleolagoonal/paleoestuarine deposits and wave-ravinement surface. Spit-inlet systems imprint more complex compartmentalization to the reservoirs, in the form of inter and intra sand-body heterogeneities, also controlling the permeability pathways. In strandplain systems, pathways tend to be parallel to the shore, while in spit-inlet systems they are shore-normal.

For example, the tide-influenced shelf facies from the Merluza Field (Santos Basin, Sombra et al., 1990), the presence of tidal deltas in the coastal succession of the Tern Field (North Sea, Jennette and Riley, 1996), and of an intra-parasequence truncation surface with concentration of coarse sediment and mud intraclasts in the Meren Field (Niger Delta, Cook et al., 1999) are indirect indicators of the occurrence of spit-inlet and/or barrier island systems as reservoirs. In the studied area these systems are interfingered with strandplain deposits (Figs. 29, 30), in an arrangement that not only imprints a higher degree of intra-parasequence heterogeneity but also affects the orientation of the permeability pathways in the reservoir units (Fig. 30). Therefore, the coastal plain of Paraná can be used as an analog for highly compartmentalized wave-dominated coastal reservoirs.

8.6 Conclusions of the Paper

The use of GPR in the study of shallow sub-surface led to a different perspective at the architecture and spatial relations of depositional systems that compose the Paraná coastal plain. GPR interpretation is an efficient method for the identification of depositional and erosive elements whose associations allowed the characterization of depositional systems, including strandplain, spit-inlet and lagoon/estuary. Sedimentary facies from similar contexts can be used as a base to interpret the geological expression of reflector patterns in GPR, allowing the prediction of their composition and internal framework. In the study area, facies analysis indicate deposition in a sand-rich, wave-dominated coast within microtidal conditions and variable wave energy, coherently with the geometries identified in radargrams.

The application of methods of seismic stratigraphy on the radar data resulted in a better understanding of the temporal distribution and stratigraphic trends of coastal depositional systems. Strandplain and spit-inlet systems are related with two regressive phases that took place during the late Pleistocene and Holocene respectively, while lagoonal/estuary systems were mostly developed during the Holocene transgression. As a result, the Paraná coastal plain can be divided into two sandy parasequences separated in part by muddy paleolagoonal/paleoestuarine deposits, and in part by a regional wave ravinement surface. As parasequences are commonly used for analog studies in the petroleum industry, GPR can be considered as a potential tool to understand intra-parasequence (or inter sand-body) heterogeneities that are generally too big to be identified in outcrops and too small to be identified in deep subsurface tools.

The interdigitation of strandplain and spit-inlet deposits represents an architectural inter sand-body heterogeneity that would impact the permeability pathways in a reservoir, although their internal sedimentary facies and the expected response in seismic tools would be very similar. The intra sand-body heterogeneities of these two types of deposits would also be different, as in spit-inlet systems the presence of mud is expectedly higher than in strandplain systems, especially in the vicinities of the inlets. Therefore, the coastal plain of Paraná can serve both as an analog of internally-compartmentalized coastal systems, and as an example of the application of GPR for studies of depositional systems at multiple scales.

9. Integrated Discussion

9.1 Evidences of High-Energy Processes in the Quaternary Santos Basin

Facies and radarfacies in the Paraná coastal plain indicate the influence of both 'normal'- and 'abnormal'-energy processes in the coast (*sensu* Miall, 2014), coherently with the concepts from actualism (Gould, 1967) (Table 4). The type of high-energy indicator in the wave-dominated context is controlled by the coastal profile, as the water depth influences on how the current interacts with the sediment (Heward, 1981; Davis Jr and Hayes, 1984; Reinson, 1984). The high-energy processes are predominantly depositional in the lower shoreface to inner shelf, controlling the sand supply to areas of low energy and forming heterolytic facies in the transition to the offshore (e.g., Souza et al., 2012) (Table 4). In shallower sub-zones of the coast high-energy processes are gradually more erosive. From the lower to the upper shoreface these processes form hummocky and swaley cross-stratified facies, facies with intraclasts and shell fragments, facies bounded by truncation surfaces with concentration of coarse grains, and landward-migrating radarfacies in GPR sections (e.g., Souza et al., 2012; Berton et al., 2019) (Table 4). The incidence of storm waves on the foreshore domain erodes fair-weather deposits and impose a higher dip angle on the beach, generating a truncation surface (Table 4).

The high-energy indicators described in the Paraná coastal plain (Lessa et al., 2000; Souza et al., 2012; Bisi, 2015; Berton et al., 2019) can be attributed to episodic processes such as storms acting in the nearshore. Only a part of these indicators is associated with abnormal processes that affected the coastal profile and generated expressive bounding surfaces, and their frequency is too low to consider episodic sedimentation as dominant in the Quaternary stratigraphic record. The most expressive features attributed to episodic processes are landward-prograding clinoforms (RF5) that partially cover low-angle foreshore clinoforms (RF2). The geometric relation between RF5 and RF2 implies in a chronology where (1) RF2 is partially eroded by storm waves, (2) RF5 is formed and migrates updip controlled by strong wave currents striking on the coast, and (3) during fair weather foreshore progradation restores the beach profile, covering the truncation surface and the landward-migrating bar (Fig. 31). Although fair weather deposits are partially eroded in the process, there is no evidence to support the idea that the deposits associated with episodic sedimentation have higher preservation potential than the ones of 'normal' energy (Miall,

2014). An actualistic approach is therefore more realistic to describe and predict facies and heterogeneity distribution in the coastal system, especially when considering that the absence of record represented by erosion and/or non-deposition is also imprinted on the Quaternary deposits.

Table 4: High-energy indicators in the Paraná coastal plain, integrating results and interpretations from Lessa et al. (2000), Souza et al. (2012), Bisi, (2015) and Berton et al. (2019).

Facies	**Sub-zone**	**Type of abnormal-energy indicators**	**High-energy indicators**
Subhorizontal parallel-laminated sand	Foreshore	erosive	Truncation surfaces with up to 4° inclination
Fine to medium trough cross-stratified sand	Upper shoreface	erosive-depositional	Truncation surfaces with concentration of coarse grains
Fine to coarse trough cross-stratified sand	Upper shoreface	erosive-depositional	Fine to coarse-grained, poorly-sorted
Massive sand	Upper shoreface	erosive-depositional	Collapse structures, upwardly convex shell mounds and shell imprints, mud intraclasts
Swaley cross-stratified sand	Upper-mid shoreface	erosive-depositional	Swaley cross-stratification
Hummocky cross-stratified sand	Mid-lower shoreface	erosive-depositional	Hummocky cross-stratification
Heterolytic	Lower shoreface-offshore	depositional	Sand lenses
Radarfacies	**Sub-zone**	**Type of abnormal-energy indicators**	**High-energy indicators**
Moderate-sized clinoforms wedges	Backshore	depositional	Landward-migrating forms within a lagoonal context
Low-angle clinoforms	Foreshore	erosive	Dips up to 6°; internal truncation surfaces separate sets of clinoforms with different angles
High-angle channel-fill clinoforms	Foreshore	erosive	Dips of up to 15°; internal truncation surfaces separates sets of clinoforms with different angles
Small-sized tangential clinoforms	Upper shoreface	erosive-depositional	Lenses that migrate over the bottomset of low-angle clinoforms (episodic deposition)
Hummocky	Shoreface	erosive-depositional	Hummocky reflectors

9.2 Applicability of Modern Analogues

The results from offshore Santos Basin show that seismic geomorphology can cover the gap between the mega and the gigascale of visualization of subsurface (Fig. 6). The architectural features and elements observed in seismic horizons are comparable to depositional and erosive features from modern sedimentary systems, which indirectly lead to estimates about their internal composition and structure. In the Campanian interval, a topset reflector associated with a transgressive trend in a T-R sequence corresponds to a continuous high negative amplitude reflector slightly arched by an underlying salt dome (Fig. 32). A seismic-geomorphological interpretation was carried in the negative amplitude reflector, called HC02, showing a typical strandplain seismic-geomorphologic signature with linear beach-ridge sets

elongated along strike lobate morphology. This strandplain is more than 30 km long in strike direction and reaches 7 km along dip.

Although it is seen as a single reflector in seismic section, these dimensions are coherent with an interval with relative low accommodation and high supply, probably related to flat progradation trajectories (Ainsworth, 2010; Ainsworth et al., 2011). This system is essentially sandy from attribute maps, with potential mud concentrations only within discontinuous GF2 that occur locally. This possible reservoir has therefore high net-gross (e.g., Ainsworth et al., 2011), and expected composition of clean sandstone with low shale volume (e.g., Berton et al., 2019). The inter-parasequence and inter sand-body compartmentalization scales (Ainsworth, 2010) are apparently inexpressive from seismic-geomorphologic interpretations, but the study case in the Quaternary coastal plain indicates that expressive heterogeneities below seismic resolution might be present within a reservoir without impacting its external form or size. This is the case of the coast-parallel paleolagoonal/paleoestuarine muddy deposits that separate two sandy strandplain deposits (Fig. 30). If this system is used as an analog for the strandplain systems in the Campanian interval offshore Santos Basin, the muddy deposits would represent an uncertainty regarding the connectivity between two potential reservoir bodies.

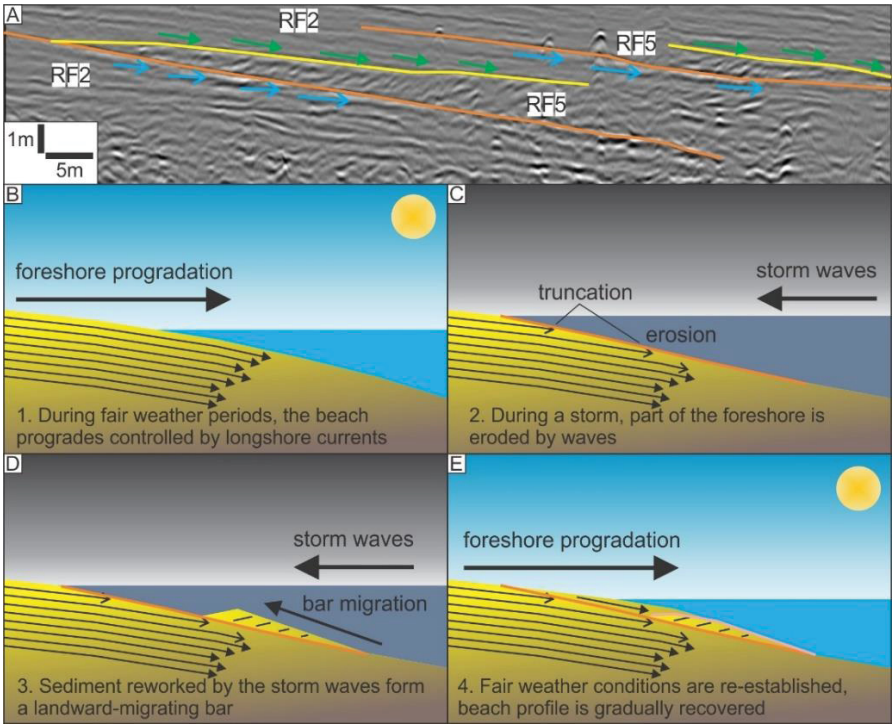

Figure 31: Geometric relation between RF5 and RF2 (A) implies in an evolution with beach progradation under fair weather conditions (B), partial erosion of the coast during a storm (C) and formation and updip migration of a shoreface bar (D), and recovery of the beach profile during fair weather, partially preserving the bar (E).

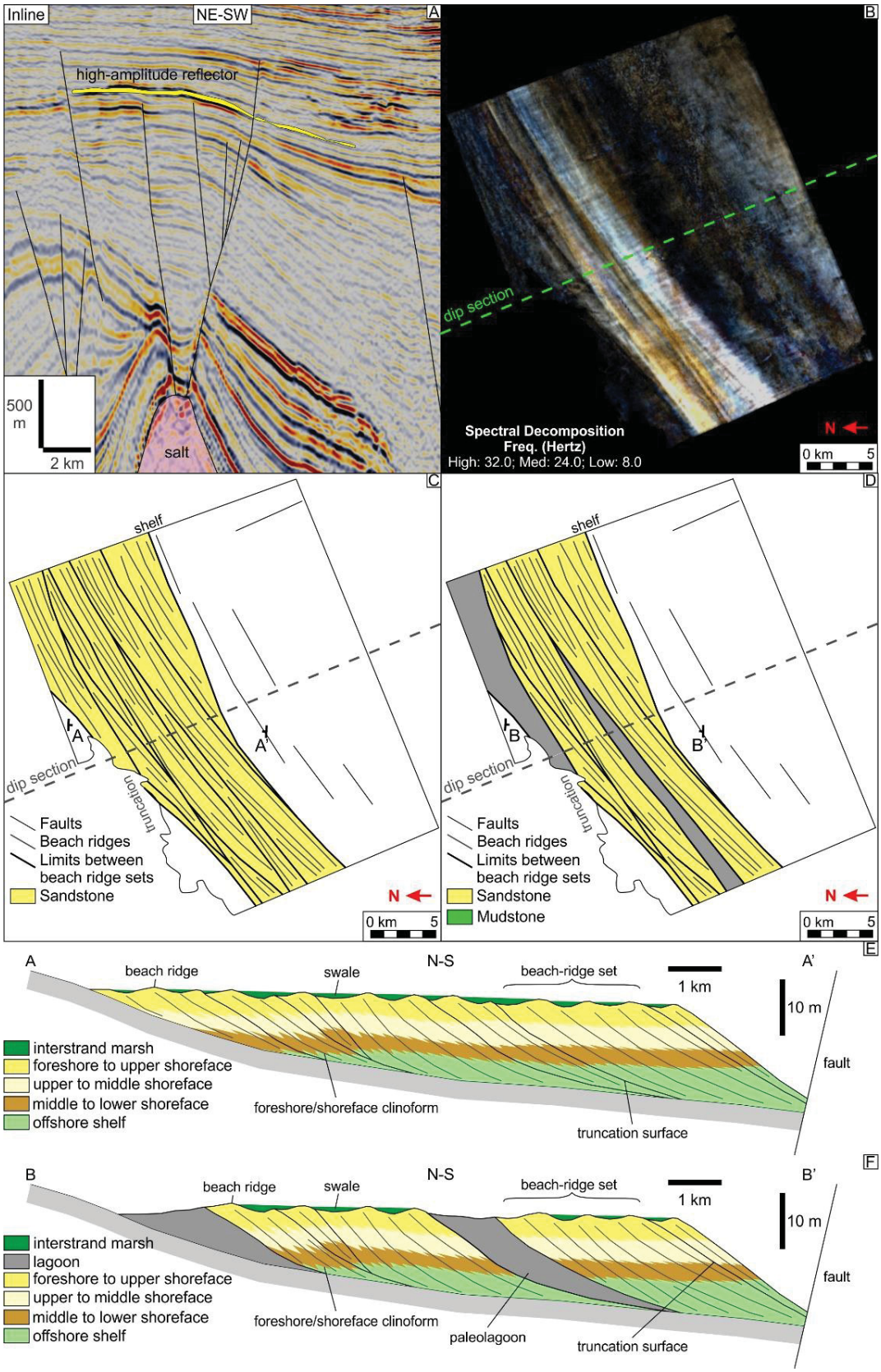

Figure 32: A high-amplitude reflector is a potential reservoir in the Campanian interval, arched by an underlying salt dome (A). In seismic attribute maps it has a laterally-elongated geometry interpreted as a strandplain (B). This system might be sand-rich and homogeneous (C), or present internal muddy lagoonal intervals (D). These two possibilities imply different internal compartmentalization in a reservoir body (E and F).

Heterogeneities internal to the reservoir bodies are also not captured by seismic tools and can only be estimated from well logs if there is enough well density to allow a good correlation. The inter-digitation of strandplain and spit-inlet systems, for instance, can be considered a sub-seismic heterogeneity that impacts fluid-flow trends within a single reservoir body. As the spit develops parallelly to the coast and has a composition similar to a strandplain, its expression in seismic geomorphology would be very subtle. Intra sand-body heterogeneities are even more uncertain, although features associated with variable depositional energy (i.e., surfaces with concentration of coarser grains, mud intraclasts, or hummocky/swaley cross-stratification) can be identified in cores and indicate an internal complexity that differs from classic wave-dominated coastal models. The presence of such features might be hard to identify in well logs if cores are not available, and they can be easily overlooked.

A simple layer-cake structure elongated along strike can therefore be too simplistic and optimistic to serve as input for a reservoir model. The results shown here and in producing oil fields indicate that only a fraction of the information from modern analogues can be included deterministically into a reservoir model without compromising its quality in terms of representativity. Modern analogs should be used only for the assessment of the general geometry of the reservoir, or when it is possible to compare elements identified in wells or seismic geomorphology with the ones from modern systems (e.g., Castellini et al., 2003; Graham et al., 2015). A realistic reservoir model can thus include variations of internal heterogeneities between two end members: an optimistic case considering a layer-cake and homogeneous configuration from classic strandplain systems, and a pessimistic case considering the inter-digitation of different wave-dominated coastal systems and lagoonal deposits, such as the Paraná shore case (Fig. 30).

10. Conclusions

The results from the research show that, far from the classic layer-cake strike-elongated depositional models, coastal systems can be relatively complex due to the interplay of allogenic and autogenic controls through time. Allogenic processes affect the architecture and sand distribution in the systems and control the potential of preservation of the deposits. Even more important for petroleum targets, allogenic controls affect the volume of sand within an interval. Autogenic processes affect the compartmentalization of the

deposits, controlling the distribution of heterogeneities in different scales. Such autogenic products are frequently subseismic, representing great uncertainties for reservoir models.

In subsurface, seismic geomorphology can be the key for the identification of the autogenic controls on deposition and how they affect the quality of a reservoir, decreasing considerably the level of uncertainty in a geological conceptual model. In the seismic scale (or mega to gigascale), this tool can be used to compare geomorphic elements from subsurface with modern analogues from aerial or satellite pictures. This analysis, coupled with classic tools for subsurface studies, result in a more precise picture of a past depositional system. Modern analogues can thus be considered useful for the assessment of the architecture and sediment distribution of buried deposits, at least in the megascale of visualization.

GPR proved to be a useful tool for linking the mesoscale assessed in outcrops and hand samples with the megascale observed in seismic data. Radargrams can cover great areas with a sub-metrical resolution, allowing the interpretation of sedimentary structures and high-frequency stratigraphic cycles. In Quaternary Santos Basin, this tool allowed for the recognition of expressive heterogeneities in a subseismic scale, which could potentially compromise the quality of a reservoir in deep subsurface. Such heterogeneities would not be visible even in the relatively higher-resolution 3D seismic data, and would be difficult to predict from high resolution stratigraphy using wells and 2D seismic. In the other hand, the heterogeneities observed in radargrams can be too big to be recognized in outcrops.

In what refers to the potential of preservation of fair-weather and high-energy facies, results from Quaternary Santos Basin show that both types of sedimentary products can be preserved through time. An actualistic approach is thus recommendable to study the stratigraphic record, using modern systems as analogues, but respecting the variation of energy and the expressiveness of high energy processes in both deposition and erosion. Episodic sedimentation is unquestionably an important part of the sedimentary record, and can be used to describe deposits such as turbidites and mass-transport deposits, but cannot be considered the single type of processes composing the sedimentary record.

References

2017 Atlantic Hurricane Season Fast Facts. (2018, May 31). *CNN Library*. Retrieved from https://edition.cnn.com/2017/05/15/us/2017-atlantic-hurricane-season-fast-facts/index.html. Accessed in July 03, 2018.

Adelu, A.O., Aderemi, A.A., Akanji, A.O., Sanuade, O.A., Kaka, S.I., Afolabi, O., Olugbemiga, S., Oke, R. 2019. Application of 3D static modeling for optimal reservoir characterization. Journal of African Earth Sciences, 152, 184-196.

Ager, D.V. 1993. The nature of the stratigraphical record. Wiley, 3rd ed., 153p.

Ainsworth, R.B. 2005. Sequence stratigraphic-based analysis of reservoir connectivity: influence of depositional architecture – a case study from a marginal marine depositional setting. Petroleum Geoscience, 11, 257-276.

Ainsworth, R.B. 2010. Prediction of stratigraphic compartmentalization in marginal marine reservoirs. In: Jolley, S.J., Fisher, Q.J., Ainsworth, R.B., Vrolijk, P.J., Delisle, S. (eds.). Reservoir Compartmentalization. Geological Society Special Publications, 347, 199-218.

Ainsworth, R.B., Payenberg, T.H.D., Willis, B.J., Sixsmith, P.J., Yeaton, J.W., Sykiotis, N. 2016. Predicting shallow marine reservoir heterogeneity using a high resolution mapping approach, Brigadier Formation, NWS, Australia. Society of Petroleum Engineers, London, SPE Asia Pacific Oil & Gas Conference and Exhibition, ref. SPE182355MS, 1-13.

Ainsworth, R.B., Vakarelov, B.K., Nanson, R.A. 2011. Dynamic spatial and temporal prediction of changes in depositional processes on clastic shorelines: toward improved subsurface uncertainty reduction and management. AAPG Bulletin, 95(2), 267-297.

Angulo, R.J. 1992. Geologia da planície costeira do estado do Paraná. PhD Thesis, Universidade de São Paulo – Instituto de Geociências, 334p.

Angulo, R.J. 2004. Mapa do Cenozóico do litoral do estado do Paraná. Boletim Paranaense de Geociências, 55, 25-42.

Angulo, R.J., Lessa, G.C. 1997. The Brazilian sea-level curves: a critical review with emphasis on the curves from the Paranaguá and Cananéia regions. Marine Geology, 140, 141-166.

Angulo, R.J., Lessa, G.C., Souza, M.C. 2006. A critical review of mid- to late-Holocene sea-level fluctuations on the eastern Brazilian coastline.Quaternary Science Reviews, 25, 486-506.

Angulo, R.J., Pessenda, L.C.R., Souza, M.C. 2002. O significado das datações ao 14C na reconstrução de paleoníveis marinhos e na evolução das barreiras quaternárias do litoral paranaense. Revista Brasileira de Geociências, 32(1), 95-106.

Angulo, R.J., Suguio, K. 1995. Re-evaluation of the Holocene sea-level maxima for the state of Paraná, Brazil. Palaeogeography, Palaeoclimatology, Palaeoecology, 113, 385-393.

Anjos, S.M.C., de Ros, L.F., Silva, C.M.A. 2003. Chlorite authigenesis and porosity preservation in the Upper Cretaceous marine sandstones of the Santos Basin, offshore eastern Brazil. In: Worden, R.H. (ed.). Clay mineral cements in sandstones. International Association of Sedimentologists Special Publication, 34, 291-316.

Asmus, H.E., Ferrari, A.L. 1978. Hipótese sobre a causa do tectonismo cenozóico na região sudeste do Brasil. Série Projeto REMAC – Aspectos estruturais da margem continental leste e sudeste do Brasil, 4, 75-88.

Assine, M.L., Corrêa, F.S., Chang, H.K. 2008. Migração de depocentros na Bacia de Santos: importância na exploração de hidrocarbonetos. Revista Brasileira de Geociências, 38(2), 111-127.

Bailey, R.J., Smith, D.G. 2005. Quantitative evidence for the fractal nature of the stratigraphic record: results and implications. Proceedings of the Geologists' Association, 116, 129-138.

Baker, V.R. 1998. Catastrophism and uniformitarianism: logical roots and current relevance in geology. In: Blundell, D.J., Scott, A.C. (eds.). Lyell: the past is the key to the present. Geological Society Special Publications, 143, 171-182.

Baker, V.R. 2014. Uniformitarianism, earth system science, and geology. Anthropocene, 5, 76-79.

Baker, V.R., Benito, G., Rudoy, A.N. 1993. Paleohydrology of Late Pleistocene superflooding, Altay Mountains, Siberia. Science, 259, 348-350.

Barboza, E.G., Dillenburg, S.R., Rosa, M.L.C.C., Tomazelli, L.J., Hesp, P.A. 2009. Ground-penetrating radar profiles of two Holocene regressive barriers in southern Brazil. Journal of Coastal Research, SI 56, 579-583.

Barboza, E.G., Rosa, M.L.C.C., Dillenburg, S.R., Watanabe, D.S.Z., Esteves, T., Martins, E.M., Gruber, N.L.S. 2018. Diachronic condition between maximum transgressive and maximum eustatic sea-level in Holocene: subsidies for coastal management. Journal of Coastal Research, SI 85, 446-450.

Barboza, E.G., Rosa, M.L.C.C., Caron, F. 2014b. Metodologia de aquisição e processamento em dados de georradar (GPR) nos depósitos quaternários da porção emersa da Bacia de Pelotas. VI Simpósio Brasileiro de Geofísica, 1, 1-6.

Barboza, E.G., Rosa, M.L.C.C., Dillenburg, S.R., Silva, A.B., Tomazelli, L.J. 2014a. Stratigraphic analysis applied on the recognition of the interface between marine and fluvial depositional systems. Journal of Coastal Research, SI 70, 687-692.

Barboza, E.G., Rosa, M.L.C.C., Dillenburg, S.R., Tomazelli, L.J. 2013. Preservation potential of foredunes in the stratigraphic record. Journal of Coastal Research, SI 65, 1265-1270.

Barboza, E.G., Rosa, M.L.C.C., Hesp, P.A., Dillenburg, S.R., Tomazelli, L.J., Ayup-Zouain, R.N. 2011. Evolution of the Holocene coastal barrier of Pelotas Basin (Southern Brazil) – a new approach with GPR data. Journal of Coastal Research, SI 64, 646-650.

Barrell, J. 1917. Rhythms and the measurements of geologic time. Bulletin of the Geological Society of America, 28, 745-904.

Barreto, A.M.F., Bezerra, F.H.R., Suguio, K.,Tatumi, S.H., Yee, M., Paiva, R.P., Munita, C.S. 2002. Late Pleistocene marine terrace deposits in northeastern Brazil: sea-level change and tectonic implications. Palaeogeography, Palaeoclimatology, Palaeoecology, 179, 57-69.

Beni, A.N., Lahijani, H., Harami, R.M., Leroy, S.A.G., Shah-Hosseini, M., Kabiri, K., Tavakoli, V. 2013. Development of spit-lagoon complexes in response to Little Ice Age rapid sea-level changes in the central Guilian coast, south Caspian Sea, Iran. Geomorphology, 187, 11-26.

Berton, F., Guedes, C.C.F., Vesely, F.F., Souza, M.C., Angulo, R.J., Rosa, M.L.C.C., Barboza, E.G. 2019. Quaternary coastal plains as reservoir analogs: wave-dominated sand-body heterogeneity from outcrop and ground-penetrating radar, central Santos Basin, Southeast Brazil. Sedimentary Geology, 379, 97-113.

Berton, F., Vesely, F.F. 2016a. Stratigraphic evolution of Eocene clinoforms from northern Santos Basin, offshore Brazil: evaluating controlling factors on shelf-margin growth and deep-water sedimentation. Marine and Petroleum Geology, 78, 356-372.

Berton, F., Vesely, F.F. 2016b. Seismic expression of depositional elements associated with a strongly progradational shelf margin: northern Santos Basin, southeastern Brazil. Brazilian Journal of Geology, 46(4), 585-603.

Berton, F., Vesely, F.F. 2018. Origin of buried, bottom current-related comet marks and associated submarine bedforms from a Paleogene continental margin, southeastern Brazil. Marine Geology, 395, 347-362.

Bigarella, J.J. 1946. Contribuição ao estudo da planície litorânea do Estado do Paraná. Brazilian Archives of Biology and Technology, 1, 75-111.

Bigarella, J.J., Becker, R.D., Duarte, G.M. 1969. Coastaldunesfrom Paraná (Brazil). Marine Geology, 7, 5-55.

Bisi, F.N. 2015. Arquitetura deposicional da barreira regressiva holocênica de Praia de Leste – Paraná. MSc dissertation, Universidade Federal do Paraná, 84p.

Blackwelder, E. 1909. The valuation of unconformities. The Journal of Geology, 17(3), 289-299.

Bondevik, S., Svendsen, J.I., Mangerud, J. 1997. Tsunami sedimentary facies deposited by the Storegga tsunami in shallow marine basins and coastal lakes, western Norway. Sedimentology, 44, 1115-1131.

Bourget, J., Ainsworth, R.B., Thompson, S. 2014. Seismic stratigraphy and geomorphology of a tide or wave dominated shelf-edge delta (NW Australia): process-based classification from 3D seismic attributes and implications for the prediction of deep-water sands. Marine and Petroleum Geology, 57, 359-384.

Boyd, R., Dalrymple, R., Zaitlin, B.A. 1992. Classification of clastic coastal depositional environments. Sedimentary Geology, 80, 139-150.

Bretz, J.H. 1923. The channeled Scablands of the Columbia Plateau. The Journal of Geology, 8, 617-649.

Bretz, J.H. 1925. The Spokane flood beyond the channeled Scablands. II. The Journal of Geology, 33(3), 236-259.

Bretz, J.H., 1969. The Lake Missoula floods and the channeled Scabland. Journal of Geology, 77, 505-543.

Bretz, J.H., Smith, H.T.U., Neff, G.E. 1956. Channeled Scabland of Washington: new data and interpretations. Bulletin of the Geological Society of America, 67, 967-1049.

Cainelli, C., Mohriak, W.U. 1999. Some remarks on the evolution of sedimentary basins along the eastern Brazilian continental margin. Episodes, 22(3), 206-216.

Calliari, L.J., Speranski, N.S., Torronteguy, M., Oliveira, M. 2000. The mud banks of Cassino Beach, Southern Brazil: characteristics, processes and effects. Journal of Coastal Research, 34, 318-325.

Carneiro, C.D.R., Neves, B.B.B., Amaral, I.A., Bistrichi, C.A. 1994. O atualismo como princípio metodológico em tectônica. Boletim de Geociências da Petrobras, 8(2), 275-293.

Castellini, A., Chawathé, A., Larue, D., Landa, J.L., Jian, F.X., Toldi, J.L., Chien, M.C. 2003. What is relevant to flow? A comprehensive study using a shallow marine reservoir. SPE Reservoir Simulation Symposium #79669.

Castro, L.G., Ferreira, F.J.F., Angulo, R.J. 2008. Modelo gravimétrico-magnético do gráben de Paranaguá – PR, Brasil. Revista Brasileira de Geofísica, 26(3), 273-292.

Catuneanu, O. 2006. Principles of sequence stratigraphy. Elsevier, 373p.

Catuneanu, O., Abreu, V., Bhattacharya, J.P., Blum, M.D., Dalrymple, R.W., Eriksson, P.G., Fielding, C.R., Fisher, W.L., Galloway, W.E., Gibling, M.R., Giles, K.A., Holbrook, J.M., Jordan, R., Kendall, C.G.StC., Macurda, B., Martinsen, O.J., Miall, A.D., Neal, J.E., Nummedal, D., Pomar, L., Posamentier, H.W., Pratt, B.R., Sarg, J.F., Shanley, K.W., Steel, R.J., Strasser, A., Tucker, M.E., Winker, C. 2009. Towards the standardization of sequence stratigraphy. Earth-Science Reviews, 92, 1-33.

Catuneanu, O., Galloway, W.E., Kendall, C.G.StC., Miall, A.D., Posamentier, H.W., Strasser, A., Tucker, M.E. 2011. Sequence stratigraphy: methodology and nomenclature. Newsletters in Stratigraphy, 44/3, 173-245.

Catuneanu, O., Zecchin, M. 2013. High-resolution sequence stratigraphy of clastic shelves II: controls on sequence development. Marine and Petroleum Geology, 39, 26-38.

Chang, H.K., Assine, M.L., Corrêa, F.S., Tinen, J.S., Vidal, A.C., Koike, L. 2008. Sitemas petrolíferos e modelos de acumulação de hidrocarbonetos na Bacia de Santos. Revista Brasileira de Geociências, 38(2), 29-46.

Ciammetti, G., Ringrose, P.S., Good, T.R., Lewis, J.M.L., Sorbie, K.S. 1995. Waterflood recovery and fluid flow upscaling in a shallow marine and fluvial sandstone sequence. Society of Petroleum Engineers, London, Annual Technical Conference and Exhibition, ref. SPE30783, 845-858.

Clemmensen, L.B., Nielsen, L. 2010. Internal architecture of a raised beach ridge system (Anholt, Denmark) resolved by ground-penetrating radar investigations. Sedimentary Geology, 223, 281-290.

Clifton, H.E. 2006. A reexamination of facies models for clastic shorelines. In: Posamentier, H.W., Walker, R.G. (eds.). Facies models revisited. SEPM Special Publication 84, 294-337.

Colombera, L., Mountney, N.P., Hodgson, D.M., McCaffrey, W.D. 2016. The Shallow-Marine Architecture Knowledge Store: a database for the characterization of shallow-marine and paralic depositional systems. Marine and Petroleum Geology, 75, 83-99.

Contreras, J., Zühlke, R., Bowman, S., Bechstädt, T. 2010. Seismic stratigraphy and subsidence analysis of the southern Brazilian margin (Campos, Santos and Pelotas basins). Marine and Petroleum Geology, 27, 1952-1980.

Conybeare, W.D. 1831. An examination of those phoenomena of Geology, which seem to bear most directly on theoretical speculations. Philosophical Magazine Series, 2, 19-23.

Cook, G., Chawathé, A., Larue, D., Legarre, H., Ajayi, E. 1999. Incorporating sequence stratigraphy in reservoir simulation: an integrated study of the Meren E-01/MR-05 sands in the Niger Delta. SPE Reservoir Simulation Symposium #51892.

Corbeanu, R.M., Soegaard, K., Szerbiak, R.B., Thurmond, J.B., McMechan, G.A., Wang, D., Snelgrove, S., Forster, C.B., Menitove, A. 2001. Detailed internal architecture of a fluvial channel sandstone determined from outcrop, cores, and 3-D ground-penetrating radar: example from the middle Cretaceous Ferron Sandstone, east-central Utah. AAPG Bulletin, 85(9), 1583-1608.

Corina, A.N. 2016. Automatic lithology prediction from well logging using Kernel density estimation. Masters degree Dissertation, Norwegian University of Science and Technology, 94 pp.

Costas, S., Fitzgerald, D. 2011. Sedimentary architecture of a spit-end (Salisbury beach, Massachusetts): the imprints of sea-level rise and inlet dynamics. Marine Geology, 284, 203-216.

Cross, N.E., Williams, Z.K., Jamankulov, A., Bostic, C.E., Gayadeen, V.C., Torrealba, H.J., Drayton, E.S. 2015. The dynamic behavior of shallow marine reservoirs: insights from the Pliocene of offshore North Trinidad. AAPG Bulletin, 99(3), 555-583.

Daniels, J., Roberts, R., Vendl, M. 1995. Ground penetrating radar for the detection of liquid contaminants. Journal of Applied Geophysics, 33, 195-207.

Davies, J.A., Posamentier, H.W., Wood, L.J., Cartwright, J.A. (eds.). 2007. Seismic geomorphology: applications to hydrocarbon exploration and production. Geological Society Special Publication, 277, 281p.

Davis, R.A.Jr., Hayes, M.O. 1984. What is a wave-dominated coast? Marine Geology, 60, 313-329.

Davis, R.A.Jr., Yale, K.E., Pekala, J.M., Hamilton, M.V. 2003. Barrier island stratigraphy and Holocene history of west-central Florida. Marine Geology, 200, 103-123.

Davis, W.M. 1926. The value of outrageous geological hypotheses. Science, 63(1636), 463-468.

Dawson, A.G., Shi, S., Dawson, S., Takahashi, T., Shuto, N. 1996. Coastal sedimentation associated with the June 2nd and 3rd, 1994 tsunami in Rajegwesi, Java. Quaternary Science Reviews, 15, 901-912.

Dillenburg, S.R., Barboza, E.G. 2014. The strike-fed sandy coast of southern Brazil. In: Martini, I.P., Wanless, H.R. (eds.). Sedimentary coastal zones from high to low latitudes: similarities and differences. Geological Society Special Publication 388, 333-352.

Dillenburg, S.R., Barboza, E.G., Rosa, M.L.C.C. 2011. Ground penetrating radar (GPR) and Standard penetration test (SPT) records of a regressive barrier in southern Brazil. Journal of Coastal Research, 64, 651-655.

Dillenburg, S.R., Barboza, E.G., Rosa, M.L.C.C., Caron, F., Sawakuchi, A.O. 2017. The complex prograded Cassino barrier in southern Brazil: geological and morphological evolution and records of climatic, oceanographic and sea-level changes in the last 7-6 ka. Marine Geology, 390, 106-119.

Dott, R.H.Jr. 1983. 1982 SEPM presidential address: episodic sedimentation – how normal is average? How rare is rare? Does it matter? Journal of Sedimentary Petrology, 53(1), 5-23.

Dott, R.H.Jr., Bourgeois, J. 1982. Hummocky stratification: significance of its variable bedding sequences. GSA Bulletin, 93, 663-680.

Dreyer, T. 1992. Geometry and facies of large-scale flow units in fluvial-dominated fan-delta-front sequences. In: Ashton, M. (ed.). Advances in Reservoir Geology. Geological Society Special Publications, 69, 135-174.

Dreyer, T., Whitaker, M., Dexter, J., Flesche, H., Larsen, E. 2005. From spit system to tide-dominated delta: integrated reservoir model of the upper Jurassic Sognefjord Formation on the Troll West Field. In: Dorè, A.G., Vining, B.A. (Eds.) Petroleum Geology: North-West Europe and Global Perspectives. Proceedings of the 6th Petroleum Geology Conference, pp. 423–448.

Dumas, S., Arnott, R.W.C. 2006. Origin of hummocky and swaley cross-stratification – the controlling influence of unidirectional current strength and aggradation rate. Geology, 34(12), 1073-1076.

Elsner, J.B., Liu, K.B., Kocher, B. 2000. Spatial variations in major U.S. hurricane activity: statistics and a physical mechanism. Journal of Climate, 13, 2293-2305.

Eluwa, A., Mohrig, D., Ogiesoba, O.C., Ambrose, W.A. 2017. Depositional settings and history of the Lower Miocene Fleming Group, Refugio County, Texas, as defined using seismic geomorphology. Marine and Petroleum Geology, 92, 565-581.

Embry, A.F., Johannessen, E.P. 1992. T-R sequence stratigraphy, facies analysis and reservoir distribution in the uppermost Triassic e lower Jurassic succession, western Sverdrup Basin, Arctic Canada. In: Vorren, T.O., Bergsager, E., Dahl-Stamnes, Ø.A., Holter, E., Johansen, B., Lie, E., Lund, T.B. (Eds.), Arctic Geology and Petroleum Potential, vol. 2. NPF Special Publication, pp. 121-146.

Eyles, N., Clark, B.M. 1986. Significance of hummocky and swaley cross-stratification in late Pleistocene lacustrine sediments of the Ontario basin, Canada. Geology, 14, 679-682.

Frey, R.W., Howard, J.D., Pryor, W.A. 1978. Ophiomorpha: its morphologic, taxonomic, and environmental significance. Palaeogeography, Palaeoclimatology, Palaeoecology, 23, 199-229.

Fuck, R.A., Trein, E., Muratori, A., Rivereau, J.C. 1969. Mapa geológico preliminar do litoral, da Serra do Mar, e parte do Primeiro Planalto do Estado do Paraná. Boletim Paranaense de Geociências, 27, 123-152.

Galloway, W.E., Hobday, D.K. 1996. Terrigenous clastic depositional systems. Springer, 489p.

Garrison Jr., J.R., Williams, J., Miller, S.P., Weber II, E.T., McMechan, G., Zeng, X. 2010. Ground-penetrating radar study of North Padre Island: implications for barrier island internal architecture, model for growth of progradational microtidal barrier islands, and Gulf of Mexico sea-level cyclicity. Journal of Sedimentary Research, 80, 305–319.

Gosling, J., Clemmensen, L.B. 2017. Proxy records of Holocene storm events in coastal barrier systems: storm-wave induced markers. Quaternary Science Reviews, 174, 80-119.

Gould, S.J. 1967. Is uniformitarianism useful? In: Cloud, P. (ed.). Adventures in Earth history. Freeman, 51-53.

Graham, G.H., Jackson, M.D., Hampson, G.J. 2015. Three-dimensional modeling of clinoforms in shallow-marine reservoirs: part 1. Concepts and application. AAPG Bulletin, 99(6), 1013-1047.

Grammer, G.M., Harris, P.M., Eberli, G.P. 2004. Integration of outcrop and modern analogs in reservoir modeling: overview with examples from the Bahamas. In: Grammer, G.M., Harris, P.M., Eberli, G.P. (eds.). Integration of outcrop and modern analogs in reservoir modeling. AAPG Memoir, 80, 1-22.

Griffin, S., Pippett, T. 2002. Ground penetrating radar. In: Papp, É. (ed.). Geophysical and remote sensing methods for regolith exploration. CRCLEME Open File Report, 144, 80-89.

Guedes, C.C.F., Giannini, P.C.F., Sawakuchi, A.O., DeWitt, R., Nascimento Jr., D.R., Aguiar, V.A.P., Rossi, M.G. 2011. Determination of controls on Holocene barrier progradation through application of OSL dating: the Ilha Comprida Barrier example, southeastern Brazil. Marine Geology, 285, 1-16.

Hamilton, D.S. 1995. Approaches to identifying reservoir heterogeneity in barrier/strandplain reservoirs and the opportunities for increased oil recovery: an example from the prolific oil-producing Jackson-Yegua trend, south Texas. Marine and Petroleum Geology, 12(3), 273-290.

Hampson, G.J., Rodriguez, A.B., Storms, J.E.A., Johnson, H.D., Meyer, C.T. 2008. Geomorphology and high-resolution stratigraphy of progradational wave-dominated shoreline deposits: impact on reservoir-scale facies and architecture. SEPM Special Publication, 90, 117-142.

Hampson, G.J., Storms, J.E.A. 2003. Geomorphological and sequence stratigraphic variability in wave-dominated, shoreface-shelf parasequences. Sedimentology, 50, 667-701.

Harari, Z. 1996. Ground-penetrating radar (GPR) for imaging stratigraphic features and groundwater in sand dunes. Journal of Applied Geophysics, 36, 43-52.

Hede, M.U., Sander, L., Clemmensen, L.B., Kroon, A., Pejrup, M., Nielsen, L. 2015. Changes in Holocene relative sea-level and coastal morphology: a study of a raised beach ridge system on Samsø, southwest Scandinavia. The Holocene, 25, 1402-1414.

Helland-Hansen, W., Hampson, G.J. 2009. Trajectory analysis: concepts and applications. Basin Research, 21, 454-583.

Henriksen, S., Helland-Hansen, W., Bullimore, S. 2011. Relationships between shelf-edge trajectories and sediment dispersal along depositional dip and strike: a different approach to sequence stratigraphy. Basin Research, 23, 3-21.

Hesp, P.A., Dillenburg, S.R., Barboza, E.G., Tomazelli, L.J., Ayup-Zouain, R.N., Esteves, L.S., Gruber, N.L.S., Toldo-Jr., E.E., Tabajara, L.L.C.A., Clerot, L.C.P. 2005. Beach ridges, foredunes or transgressive dunefields? Definitions and an examination of the Torres to Tramandaí barrier system, southern Brazil. Anais da Academia Brasileira de Ciências, 77(3), 493-508.

Heward, A.P. 1981. A review of wave-dominated clastic shoreline deposits. Earth-Science Reviews, 17, 223-276.

Higgs, K.E., Arnot, M.J., Browne, G.H., Kennedy, E.M. 2010. Reservoir potential of Late Cretaceous terrestrial to shallow marine sandstones, Taranaki Basin, New Zealand. Marine and Petroleum Geology, 27, 1849-1871.

Hine, A.C. 1979. Mechanisms of berm development and resulting beach growth along a barrier spit complex. Sedimentology, 26, 333-351.

Hooykaas, R. 1970. Catastrophism in geology, its scientific character in relation to actualism and uniformitarianism. North-Holland Publishing Company, 50p.

Horwitz, M., Ping, W. 2005. Sedimentological characteristics and internal architecture of two overwash fans from hurricanes Ivan and Jeanne. Gulf Coast Association of Geological Societies Transactions, 55, 342-352.

Houser, C., Greenwood, B. 2007.Onshore migration of a swash bar during a storm. Journal of Coastal Research, 23(1), 1-14.

Houser, C., Greenwood, B., Aagaard, T. 2006.Divergent response of an intertidal swash bar. Earth Surface Processes and Landforms, 31, 1775-1791.

Howell, J.A., Flint, S.S., Hunt, C. 1996. Sedimentological aspects of the Humber Group (Upper Jurassic) of the South Central Graben, UK North Sea. Sedimentology, 43, 89-114.

Howell, J.A., Skorstad, A., MacDonald, A., Fordham, A., Flint, S., Fjellvoll, B., Manzocchi, T. 2008. Sedimentological parametrization of shallow-marine reservoirs. Petroleum Geoscience, 14, 17-34.

Hsü, K.J. 1983. Actualistic catastrophism. Address of the retiring president of the International Association of Sedimentologists. Sedimentology, 30, 3-9.

Hughes, T.McK. 1872. Lyell's principles of Geology. Nature, 6, 165-168.

Hutton, J. 1788. Theory of the Earth; or an investigation of the laws observable in the composition, dissolution, and restoration of land upon the globe. Transactions of the Royal Society of Edinbugh, 1(2), 209-304.

Jackson, C.A.-L., Grunhagen, H., Howell, J.A., Larsen, A.L., Andersson, A., Boen, F., Groth, A. 2010. 3D seismic imaging of lower delta-plain beach ridges: lower Brent Group, northern North Sea. Journal of the Geological Society, 167, 1225-1236.

Jackson, M.D., Hampson, G.J., Sech, R.P. 2009. Three-dimensional modeling of a shoreface-shelf parasequence reservoir analog: part 2. Geologic controls on fluid flow and hydrocarbon recovery. AAPG Bulletin, 93(9), 1183-1208.

Jennette, D.C., Riley, C.O. 1996. Influence of relative sea-level on facies and reservoir geometry of the Middle Jurassic lower Brent Group, UK North Viking Graben. In: Howell, J.A., Aitken, J.F. (eds.). High Resolution Sequence Stratigraphy: Innovations and Applications. Geological Society Special Publications, 104, 87-113.

Jol, H.M., Lawton, D.C., Smith, D.G. 2002. Ground penetrating radar: 2-D and 3-D subsurface imaging of a coastal barrier spit, Long Beach, WA, USA. Geomorphology, 53, 165-181.

Kjønsvik, D., Doyle, J., Jacobsen, T., Jones, A. 1994. The effects of sedimentary heterogeneities on production from a shallow marine reservoir – what really matters? Society of Petroleum Engineers, London, European Petroleum Conference, ref. SPE28445, 27-40.

Klausen, T.G., Ryseth, A., Helland-Hansen, W., Gjelberg, H.K. 2016. Progradational and backstepping shoreface deposits in the Ladinian to Early Norian Snadd Formation of the Barents Sea. Sedimentology, 63, 893-916.

Kumar, N., Sanders, J.E. 1974. Inlet sequence: a vertical succession of sedimentary structures and textures created by the lateral migration of tidal inlets. Sedimentology, 21, 491-532.

Leal, R.A., Barboza, E.G., Bitencourt, V.J.B., Silva, A.B. 2016. Geological and stratigraphic characteristics of a Holocene regressive barrier in southern Brazil: GIS and GPR applied for evolution analysis. Journal of Coastal Research, SI 75, 750-754.

Leatherman, S.P., Williams, A.T. 1983. Vertical sedimentation units in a barrier island washover fan. Earth Surface Processes and Landforms, 8(2), 141-150.

Lessa, G.C., Angulo, R.J., Giannini, P.C., Araújo, A.D. 2000. Stratigraphy and Holocene evolution of a regressive barrier in south Brazil. Marine Geology, 165, 87-108.

Lindhorst, S., Betzler, C., Hass, H.C. 2008. The sedimentary architecture of a Holocene barrier spit (Sylt, German Bight): swash-bar accretion and storm erosion. Sedimentary Geology, 206, 2-16.

Lindhorst, S., Fürstenau, J., Hass, H.C., Betzler, C. 2010. Anatomy and sedimentary model of a hooked spit (Sylt, southern North Sea). Sedimentology, 57(4), 935-955.

Liu, Y., Huang, H., Qi, Y., Liu, X., Yang, X. 2016. Holocene coastal morphologies and shoreline reconstruction for the southwestern coast of the Bohai Sea, China. Quaternary Research, 86, 144-161.

Lyell, C. 1835. Principles of Geology: an inquiry how far the former changes of the Earth's surface are referable to causes now in operation. John Murray, 4th ed., vol. 1, 406p.

Macedo, J.M. 1989. Evolução tectônica da Bacia de Santos e áreas continentais adjacentes. Boletim de Geociências da Petrobras, 3(3), 159-173.

Maio, C.V., Gontz, A.M., Sullivan, R.M., Madsen, S.M., Weidman, C.R., Donelly, J.P. 2016. Subsurface evidence of storm-driven breaching along a transgressing barrier system, Cape Cod, U.S.A. Journal of Coastal Research, 32(2), 264-279.

Malaizé, B., Bertran, P., Carbonel, P., Bonissent, D., Charlier, K., Galop, D., Imbert, D., Serrand, N., Stouvenot, C., Pujol, C. 2011. Hurricanes and climate in the Caribbean during the past 3700 years BP. The Holocene, 21(6), 911-924.

Marone, E., Jamiyanaa, D. 1997. Tidal characteristics and a variable boundary numerical model for the M2 tide for the estuarine complex of the Bay of Paranaguá, PR, Brazil. Nerítica, 11(1), 95-107.

Martin, L., Suguio, K. 1975. The state of São Paulo coastal marine Quaternary geology. Anais da Academia Brasileira de Ciências, 249-263.

Martins, D.C., Cancelli, R.R., Lopes, R.P., Hadler, P., Testa, E.H., Barboza, E.G. 2018. Occurrence of Ophiomorpha nodosa in Pleistocene sediments of Coastal Plain of Pinheira, Santa Catarina, Brazil. Revista Brasileira de Paleontologia, 21(1), 79-86.

Martinius, A.W., van den Berg, J.H. 2014. Holocene sediments of the Rhine-Meuse-Scheldt estuaries as aids to interpret tidal and fluvial-tidal deposits in outcrop and core. AAPG Search and Discovery Article #50950.

Masselink, G., Kroon, A., Davidson-Arnott, R.G.D. 2006. Morphodynamics of intertidal bars in wave-dominated coastal settings – a review. Geomorphology, 73, 33-49.

McCubbin, D.G. 1982. Barrier-island and strand-plain facies. In: Clifton, H.E. (ed.). Sandstone depositional environments. AAPG Memoir, 58, 247-279.

Mehrabi, H., Esrafili-Dizaji, B., Hajikazemi, E., Noori, B., Mohammad-Rezaei, H. 2019. Reservoir characterization of the Burgan Formation in northwestern Persian Gulf. Journal of Petroleum Science and Engineering, 174, 328-350.

Miall, A.D. 2000. Principles of sedimentary basin analysis. Springer-Verlag, 616p.

Miall, A.D. 2012. The nature of the sedimentary record. AAPG Search and Discovery Article #90174.

Miall, A.D. 2014. Updating uniformitarianism: stratigraphy as just a set of 'frozen accidents'. In: Smith, D.G., Bailey, R.J., Burgess, P.M., Fraser, A.J. (eds.). Strata and Time: probing the gaps in our understanding. Geological Society Special Publications, 404.

Miall, A.D. 2016. The valuation of unconformities. Earth-Science Reviews, 163, 22-71.

Modica, C.J., Brush, E.R. 2004. Postrift sequence stratigraphy, paleogeography, and fill history of the deep-water Santos Basin, offshore southeast Brazil. AAPG Bulletin, 88(7), 923-945.

Mohriak, W.U. 2012. Bacias de Santos, Campos e Espírito Santo. In: Hasui, Y., Carneiro, C.D.R., Almeida, F.F.M., Bartorelli, A. (orgs.). Geologia do Brasil, Beca, 481-496.

Mohriak, W.U., Magalhães, J.M. 1993. Estratigrafia e evolução estrutural da área norte da Bacia de Santos. Atas do III Simpósio de Geologia do Sudeste, 1, 19-26.

Moreira, J.L.P., Madeira, C.V., Gil, J.A., Machado, M.A.P. 2007. Bacia de Santos. Boletim de Geociências da Petrobras, 15(2), 531-549.

Moreira, J.L.P., Nalpas, T., Joseph, P., Guillocheau, F. 2001. Stratigraphie sismique de La Marge éocène du nord du Bassin de Santos (Brésil): relations plate-forme/systèmes turbiditiques; distorsion des séquences de dépôt. Earth and Planetary Sciences, 332, 491-498.

Murakoshi, N., Masuda, F. 1992. Estuarine, barrier-island to strand-plain sequence and related ravinement surface developed during the last interglacial in the Paleo-Tokyo Bay, Japan. Sedimentary Geology, 80, 167-184.

Neal, A. 2004. Ground-penetrating radar and its use in sedimentology: principles, problems and progress. Earth-Science Reviews, 66, 261-330.

Neal, A., Pontee, N.I., Pye, K., Richards, J. 2002. Internal structure of mixed-sand-and-gravel beach deposits revealed using ground-penetrating radar. Sedimentology, 49, 789-804.

Niazi, A.M.K., Jahren, J., Mahmood, I., Javaid, H. 2019. Reservoir quality in the Jurassic sandstone reservoirs located in the Central Graben, North Sea. Marine and Petroleum Geology, 102, 439-454.

Nichols, G. 2009. Sedimentology and stratigraphy. Wiley-Blackwell, 2nd ed., 419p.

Niedoroda, A.W., Swift, D.J.P., Hopkins, T.S., Ma, C.-M. 1984. Shoreface morphodynamics on wave-dominated coasts. Marine Geology, 60, 331-354.

Nielsen, J.K., Hansen, K.S., Simonsen, L. 1996. Sedimentology and ichnology of the Robbedale Formation (Lower Cretaceous), Bornholm, Denmark. Bulletin of the Geological Society of Denmark, 43, 115-131.

Nielsen, L., Bendixen, M., Kroon, A., Hede, M.U., Clemmensen, L.B., Weβling, R., Elberling, B. 2017. Sea-level proxies in Holocene raised beach ridge deposits (Greenland) revealed by ground-penetrating radar. Nature Scientific Reports, 7(46460), 1-8.

Nyberg, B., Howell, J.A. 2016. Global distribution of modern shallow marine shorelines. Implications for exploration and reservoir analogue studies. Marine and Petroleum Geology, 71, 83-104.

O'Byrne, C.J., Flint, S. 1993. High-resolution sequence stratigraphy of Cretaceous shallow marine sandstones, Book Cliffs outcrops, Utah, USA – application to reservoir modeling. First Break, 11(10), 445-459.

Olsen, H., Briedis, N.A., Renshaw, D. 2017. Sedimentological analysis and reservoir characterization of a multi-darcy, billion barrel oil field – the Upper Jurassic shallow marine sandstones of the Johan Sverdrup field, North Sea, Norway. Marine and Petroleum Geology, 84, 102-134.

Otvos, E.G. 2000. Beach ridges – definitions and significance. Geomorphology, 32, 83-108.

Otvos, E.G. 2012. Coastal barriers – nomenclature, processes, and classification issues. Geomorphology, 139-140, 39-52.

Paris, R., Lavigne, F., Wassmer, P., Sartohadi, J. 2007. Coastal sedimentation associated with the December 26, 2004 tsunami in Lhok Nga, west Banda Aceh (Sumatra, Indonesia). Marine Geology, 238, 93-106.

Parsons, B., Swift, D.J.P., Williams, K. 2003. Quaternary facies assemblages and their bounding surfaces, Chesapeake Bay mouth: an approach to mesoscale stratigraphic analysis. Journal of Sedimentary Research, 73(5), 672-690.

Partyka, G., Gridley, J., Lopez, J. 1999. Interpretational applications of spectral decomposition in reservoir characterization. The Leading Edge, 18(3), 353-360.

Passega, R. 1962. Problem of comparing ancient with recent sedimentary deposit. AAPG Bulletin, 48(1), 114-124.

Patruno, S., Helland-Hansen, W. 2018. Clinoforms and clinoform systems: review and dynamic classification scheme for shorelines, subaqueous deltas, shelf edges and continental margins. Earth-Science Reviews, 185, 202-233.

Pereira, A.J., Gambôa, L.A.P., Silva, M.A.M., Rodrigues, A.R., Costa, A. 2003. A utilização do ground penetrating radar (GPR) em estudos de estratigrafia na praia de Itaipuaçú – Maricá (RJ). Revista Brasileira de Geofísica, 21(2), 163-172.

Pereira, M.J., Barbosa, C.M., Agra, J., Gomes, J.B., Aranha, L.G.F., Saito, M., Ramos, M.A., Carvalho, M.D., Stamato, M., Bagni, O. 1986. Estratigrafia da Bacia de Santos: análise das sequências, sistemas deposicionais e revisão litoestratigráfica. Anais do XXXIV Congresso Brasileiro de Geologia, 1, 65-71.

Pereira, M.J., Macedo, J.M. 1990. A Bacia de Santos: perspectivas de uma nova província petrolífera na plataforma continental sudeste brasileira. Boletim de Geociências da Petrobras, 4(1), 3-11.

Pereira, P.S., Calliari, L.J. 2005. Variação morfodinâmica diária da Praia do Cassino, RS, durante os verões de 2002/2003 no setor do terminal turístico. Brazilian Journal of Aquatic Science and Technology, 9(1), 7-11.

Peyton, L., Bottjer, R., Partyka, G. 1998. Interpretation of incised valleys using new 3-D seismic techiniques: a case history using spectral decomposition and coherency. The Leading Edge, 17, 1294-1298.

Phelps, A.S., Hofmann, M.H., Hart, B.S. 2018. Facies and stratigraphic architecture of the Upper Devonian-Lower Mississippian Sappington Formation, southwestern Montana: a potential outcrop analog for the Bakken Formation. AAPG Bulletin, 102(5), 793-815.

Posamentier, H.W., Davies, R.J., Cartwright, J.A., Wood, L. 2007. Seismic geomorphology – an overview. In: Davies, R.J., Posamentier, H.W., Wood, L.J., Cartwright, J.A. (eds.). Seismic geomorphology: applications to hydrocarbon exploration and production. Geological Society Special Publication, 277, 1-14.

Posamentier, H.W., Kolla, V. 2003. Seismic geomorphology and stratigraphy of depositional elements in deep-water settings. Journal of Sedimentary Research, 73(3), 367-388.

Posamentier, H.W., Morris, W. 2000. Aspects of the stratal architecture of forced regressive deposits. In: Hunt, D., Gawthorpe, R.L. (Eds.), Sedimentary Responses to Forced Regressions, vol. 172. Geological Society Special Publication, pp. 19-46.

Prather, B.E., Deptuck, M.E., Mohrig, D., van Hoorn, B., Wynn, R.B. 2012. Application of the principles of seismic geomorphology to continental-slope and base-of-slope systems: case studies from seafloor and near-seafloor analogues. SEPM Special Publication, 99, 5-9.

Raef, A.E., Mattern, F., Philip, C., Totten, M.W. 2015. 3D seismic attributes and well-log facies analysis for prospect identification and evaluation: interpreted paleoshoreline implications, Weirman field, Kansas, USA. Journal of Petroleum Science and Engineering, 133, 40-51.

Rahman, A.H.A., Menier, D., Mansor, Md.Y. 2014. Sequence stratigraphic modelling and reservoir architecture of the shallow marine successions of Baram field, West Baram Delta, offshore Sarawak, East Malaysia. Marine and Petroleum Geology, 58, 687-703.

Raynal, O., Bouchette, F., Certain, R., Séranne, M., Dezileau, L., Sabatier, P., Lofi, J., Hy, A.B.X., Briqueu, L., Pezard, P., Tessier, B. 2009. Control of alongshore-oriented sand spits on the dynamics of a wave-dominated coastal system (Holocene deposits, northern Gulf of Lions, France). Marine Geology, 264, 242-257.

Reinson, G.E. 1984. Barrier-island and associated strand-plain systems. In: Walker, R.G. (ed.). Facies Models. Geoscience Canada, 2nd edition, 119-140.

Reynolds, A.D. 1999. Dimensions of paralic sandstone bodies. AAPG Bulletin, 83(2), 211-229.

Riccomini, C. 1989. O rift continental do sudeste do Brasil. PhD thesis, Universidade de São Paulo, 256p.

Rider, M. 1996. The geological interpretation of well logs. Whittles Publishing, Glasgow, 280p.

Rider, M., Kennedy, M. 2011. The geological interpretation of well logs. Rider-French, Glasgow, 432p.

Rocha, T.B., Fernandez, G.B., Rodrigues, A. 2017. Registros de erosão e progradação revelados por radar de penetração do solo (GPR) na barreira regressiva pleistocênica do complexo deltaico do Rio Paraíba do Sul (RJ). Quaternary and Environmental Geosciences, 8(1), 24-37.

Rockett, G., Barboza, E.G., Rosa, M.L.C.C. 2016. Ground penetrating radar applied to the characterization of the Itapeva dune field, Torres, Brazil. Journal of Coastal Research, SI 75, 323-327.

Rodriguez, A.B., Meyer, C.T. 2006. Sea-level variation during the Holocene deduced from the morphologic and stratigraphic evolution of Morgan Peninsula, Alabama, U.S.A. Journal of Sedimentary Research, 76, 257-269.

Romano, M. 2015. Reviewing the term uniformitarianism in modern Earth sciences. Earth-Science Reviews, 148, 65-76.

Rosa, M.L.C.C., Barboza, E.G., Abreu, V.S., Tomazelli, L.J., Dillenburg, S.R. 2017. High-frequency sequences in the Quaternary of Pelotas Basin (coastal plain): a record of degradational stacking as a function of longer-term base-level fall. Brazilian Journal of Geology, 47(2), 183-207.

Rosa, M.L.C.C., Barboza, E.G., Dillenburg, S.R., Tomazelli, L.J., Ayup-Zouain, R.N. 2011. The Rio Grande doSul (southern Brazil) shoreline behavior during the Quaternary: a cyclostratigraphic analysis. Journal of Coastal Research, 64, 686-690.

Rosa, M.L.C.C., Hoyal, D.C., Barboza, E.G., Fedele, J., Abreu, V.S. 2016. River-dominated deltas: upscaling autogenic and allogenic processes observed in laboratory experiments to field examples of

small deltas in southern Brazil. In: Budd, D.A., Hajek, E.A., Purkis, S.J. (eds.). Autogenic dynamics and self-organization in sedimentary systems. SEPM Special Publication 106, 176-197.

Rudwick, M.J.S. 1967. A critique of uniformitarian Geology: a letter from W.D. Conybeare to Charles Lyell, 1841. Proceedings of the American Philosophical Society, 111(5), 272-287.

Sadler, P.M. 1981. Sediment accumulation rates and the completeness of stratigraphic section. The Journal of Geology, 89(5), 569-584.

Sadler, P.M. 1999. The influence of hiatuses on sediment accumulation rates. Geo Research Forum, 5, 15-40.

Sech, R.P., Jackson, M.D., Hampson G.J. 2009. Three-dimensional modeling of a shoreface-shelf parasequence reservoir analog: part 1. Surface-based modeling to capture high-resolution facies architecture. AAPG Bulletin, 93(9), 1155-1181.

Shan, X., Yu, X., Clift, P.D., Tan, C., Jin, L., Li, M., Li, W. 2015. The ground penetrating radar facies and architecture of a paleo-spit from Huangqihai Lake, north China: implications for genesis and evolution. Sedimentary Geology, 323, 1-14.

Sherman, D.J., Greenwood, B. 1989. Hummocky cross-stratification and post-vortex ripples: length scales and hydraulic analysis. Sedimentology, 36, 981-986.

Slatt, R.M. 2006. Stratigraphic reservoir characterization for petroleum geologists, geophysicists and engineers. Elsevier, 6, 478p.

Sloss, L.L. 1963. Sequences in the cratonic interior of North America. GSA Bulletin, 74, 93-114.

Smith, D.G., Bailey, R.J., Burgess, P.M., Fraser, A.J. 2015. Strata and Time: probing the gaps in our understanding. In: Smith, D.G., Bailey, R.J., Burgess, P.M., Fraser, A.J. (eds.). Strata and Time: probing the gaps in our understanding. Geological Society Special Publications, 404.

Sombra, C.L., Arienti, L.M., Pereira, M.J., Macedo, J.M. 1990. Parameters controlling porosity and permeability in clastic reservoirs of the Merluza deep Field, Santos Basin, Brazil. Boletim de Geociências da Petrobras, 4(4), 451-466.

Sommerfield, C.K. 2006. On sediment accumulation rates and stratigraphic completeness: lessons from Holocene ocean margins. Continental Shelf Research, 26, 2225-2240.

Souza, M.C. 2005. Estratigrafia e evolução das barreiras holocências paranaenses, sul do Brasil. PhD Thesis, Universidade Federal do Paraná, 99p.

Souza, M.C., Angulo, R.J., Assine, M.L., Castro, D.L. 2012. Sequences of facies at a Holocene storm-dominated regressive barrier at Praia de Leste, southern Brazil. Marine Geology, 291-294, 49-62.

Steel, R.J., Caravajal, C., Petter, A., Uroza, C. 2008. Shelf and shelf-margin growth in scenarios of rising and falling sea level. In: Hampson, G.J., Steel, R.J., Burgess, P.M., Dalrymple, R.W. (Eds.), Recent advances in models of siliciclastic shallow-marine stratigraphy. SEPM Special Paper, 90, 47-71.

Steel, R.J., Milliken, K.L. 2013. Major advances in siliciclastic sedimentary geology, 1960-2012. In: Bickford, M.E. (Ed.), The Web of Geological Sciences: Advances, Impacts, and Interactions. Geological Society of America Special Paper, 500, 121-167.

Steel, R., Olsen, T. 2002. Clinoforms, clinoform trajectories and deepwater sands. 22nd Annual Gulf Coast Section SEPM Foundation Bob F. Perkins Research Conference, 367-380.

Sundal, A., Nystuen, J.P., Rørvik, K.-L., Dypvik, H., Aagaard, P. 2016. The Lower Jurassic Johansen Formation, northern North Sea – depositional model and reservoir characterization for CO2 storage. Marine and Petroleum Geology, 77, 1376-1401.

Takagawa, T., Fukase, Y., Liu, H., Sato, S. 2008. Coastal erosion surfaces detected by ground penetrating radar and coring survey: a case study in coastal area around the Tenryu river mouth. Fourth International Conference on Scour and Erosion, B-14, 336-339.

Tamura, L.N., Almeida, R.P., Taioli, F., Marconato, A., Janikian, L. 2016. Ground penetrating radar investigation of depositional architecture: the São Sebastião and Marizal formations in the Cretaceous Tucano Basin (northeastern Brazil). Brazilian Journal of Geology, 46(1), 15-27.

Tamura, T., Masuda, F., Sakai, T., Fujiwara, O. 2003. Temporal development of prograding beach-shoreface deposits: the Holocene of Kujukuri coastal plain, eastern Japan. Marine Geology, 198, 191-207.

Tayyab, M.N., Asim, S. 2017. Application of spectral decomposition for the detection of fluvial sand reservoirs, Indus Basin, SW Pakistan. Geosciences Journal, 21(4), 595-605.

Tercier, P., Knight, R., Jol, H. 2000. A comparison of the correlation structure in GPR images of deltaic and barrier-spit depositional environments. Geophysics, 66(4), 1142-1153.

Tillmann, T., Wunderlich, J. 2013. Barrier rollover and spit accretion due to the combined action of storm surge induced washover events and progradation: insights from ground-penetrating radar surveys and sedimentological data. Journal of Coastal Research, 65, 600-605.

Timmons, E.A., Rodriguez, A.B., Mattheus, C.R., DeWitt, R. 2010. Transition of a regressive to a transgressive barrier island due to back-barrier erosion, increased storminess, and low sediment supply: Bogue Banks, North Carolina, USA. Marine Geology, 278, 100-114.

Tomazelli, L.J., Dillenburg, S.R. 2007. Sedimentary facies and stratigraphy of a last interglacial coastal barrier in south Brazil. Marine Geology, 1, 33-45.

Vail, P.R., Mitchum, R.M., Thompson, S. 1977. Seismic stratigraphy and global changes of sea level: part 4. Global cycles and relative changes of sea level. In: Payton, C.E. (ed.). Seismic stratigraphy and application to hydrocarbon exploration, AAPG Memoir, 26, 83-98.

Vakarelov, B.K., Ainsworth, R.B. 2013. A hierarchical approach to architectural classification in marginal-marine systems: bridging the gap between sedimentology and sequence stratigraphy. AAPG Bulletin, 97(7), 1121-1161.

Vakarelov, B.K., Ainsworth, R.B., MacEachern J.A. 2012. Recognition of wave-dominated, tide-influenced shoreline systems in the rock record: variations from a microtidal shoreline model. Sedimentary Geology, 279, 23-41.

Van Heteren, S., de Plassche, O.V. 1997. Influence of relative sea-level change and tidal-inlet development on barrier-spit stratigraphy, Sandy Neck, Massachusetts. Journal of Sedimentary Research, 67(2), 350-363.

Van Wagoner, J.C., Mitchum, R.M., Campion, K.M., Rahmanian, V.D. 1990. Siliciclastic sequence stratigraphy in well logs, cores, and outcrops: concepts for high-resolution correlation of time and facies. AAPG Methods in Exploration Series, 7, 1-55.

Van Wagoner, J.C., Posamentier, H.W., Mitchum, R.M., Vail, P.R., Sarg, J.F., Loutit, T.S., Hardenbol, J. 1988. In: C. K. Wilgus, B. S. Hastings, C.G. St. C. Kendall, H. W. Posamentier, C. A. Ross and J. C. Van Wagoner (Eds.), Sea Level Changes – An Integrated Approach, SEPM Special Publication, vol. 42, pp. 39–45.

Veiga, F.A., Angulo, R.J., Sá, F., Odreski, L.L.R., Lamour, M.R., Disaró, S.T. 2004. Origin of mud deposits in a wave dominated shallow inner continental shelf of the state of Paraná coast, southern Brazil. Journal of Coastal Research, SI 39, 262-265.

Weimer, J.K.T., Hoyt, J.H. 1964. Burrows of Callianassa major say, geologic indicators of littoral and shallow neritic environments. Journal of Paleontology, 38, 761–767.

Williams, B.G., Hubbard, R.J. 1984. Seismic stratigraphic framework and depositional sequences in the Santos Basin, Brazil. Marine and Petroleum Geology, 1, 90-104.

Woolsey, J.R., Henry, V.J., Hunt, J.L. 1975. Backshore heavy-mineral concentration on Sapelo Island, Georgia. Journal of Sedimentary Petrology, 45(1), 280-284.

Zachos, J., Pagani, M., Thomas, E., Billups, K. 2001. Trends, rhythms, and aberrations in global climate 65 Ma to present. Science, 292, 686-693.

Zalán, P.V., Oliveira, J.A.B. 2005. Origem e evolução do Sistema de Riftes Cenozóicos do sudeste do Brasil. Boletim de Geociências da Petrobras, 13(2), 269-300.

Zaremba, N.J., Smith, C.G., Bernier, J.C., Forde, A.S. 2016. Application of ground penetrating radar for identification of washover deposits and other stratigraphic features: Assateague Island, MD. Journal of Environmental and Engineering Geophysics, 21(4), 173-186.

Zecchin, M., Catuneanu, O. 2013. High-resolution sequence stratigraphy of clastic shelves I: units and bounding surfaces. Marine and Petroleum Geology, 39, 1-25.

Zhu, X., Zeng, H., Li, S., Dong, Y., Zhu, S., Zhao, D., Huang, W. 2017. Sedimentary characteristics and seismic geomorphologic responses of a shallow-water delta in the Qingshankou Formation from the Songliao Basin, China. Marine and Petroleum Geology, 79, 131-148.

Zhuo, H., Wang, Y., Shi, H., Zhu, M., He, M., Chen, W., Li, H. 2014. Seismic geomorphology, architecture and genesis of Miocene shelf sand ridges in the Pearl River Mouth Basin, northern South China Sea. Marine and Petroleum Geology, 54, 106-122.